L-Selectin and ADAM17 in Activation of Virus Specific T-Cells

Abdullah Saad A Alanazi

Thesis presented for the award of PhD (Doctor of Philosophy) at Cardiff University

Division of Infection and Immunity, School of Medicine,
Cardiff University

December 2022

Acknowledgments

I am deeply grateful to Ann Ager and Vera Knäuper for their invaluable guidance, support, and encouragement throughout my PhD journey. Their expertise and insights have greatly contributed to the development and success of this research. Thanks to all the great members of the Ager lab, and Knäuper lab, especially Frank Antwi.

I would like to express my sincere gratitude to my sponsorship Saudi Arabia Government for their generous support and sponsorship of my research. Their financial assistance has allowed me to focus on my work and has played a crucial role in the successful completion of this project. Thank you for believing in me and my research and for providing the resources that have allowed me to thrive. I am deeply grateful for your support, and I am honored to have been a recipient of your sponsorship.

I am grateful to my parents for their love, support, and constant encouragement. Without their belief in me, I would not have been able to reach this point in my academic career.

I would also like to express my sincere appreciation to my lovely wife Rawan for her unwavering love and support. Her encouragement and understanding have been a constant source of strength and motivation for me.

I would like to thank my daughters Reema (left) and Mohra (right) for their understanding and patience during the many late nights and weekends I spent working on this thesis. Their presence in my life has been a constant source of joy and inspiration.

I am also grateful to my siblings, especially brothers Mohammed and Salman, for their love and support throughout my academic journey. Their encouragement and belief in me have meant the world to me.

Finally, I would like to extend my heartfelt thanks to my friends Stefan Milutinovic, Ruban Peter Durairaj, Jake Scott, Abdullah Alghamdi, Mohammed Mudhhi, Faya Algahtani, Mohammed Alhazmi and Tareq Alanazi for their support and encouragement throughout this process. Their friendship has been a constant source of comfort and inspiration.

Thank you all for being a part of my journey.

Abstract

L-selectin (CD62L) is a homing molecule expressed by leukocytes and is involved in the multistep adhesion cascade of leucocyte recruitment from the bloodstream into tissues. It was previously shown that L-selectin is re-expressed and maintained on primed virus-specific CD8+ T-cells and is required for recruitment to virus infected organs and for protective immunity. Understanding how L-selectin re-expression is regulated may have important implications for endogenous responses as well as clinical implications in adoptive T-cell therapies for viral infection treatment and cancer. It is known that ectodomain proteolytic shedding of L-selectin is regulated by ADAM17. Using an *in vitro* model of B-cell based peptide-MHC presentation to T-cells expressing a SLY-specific TCR revealed that L-selectin and ADAM17 expression can be detected by flow cytometry and western blotting before and after SLY engagement. Pulldown experiments revealed that L-selectin and ADAM17 are not present in a preformed complex in the cell lysate before activation and were not detectable in a complex after TCR engagement. It is therefore still unclear how ADAM17 comes to cleave L-selectin. Following SLY engagement, the released tail of L-selectin was shown to be degraded by either the proteasome or γ-secretase using specific inhibitors of both pathways. This is consistent with previous work which used the same inhibitors but different modes of T-cell activation (anti-CD3/CD28 and PMA). Furthermore, this is in-line with previous work which showed that cleavable L-selectin drives CD25 expression and clonal T-cell expansion during virus infection. The proteolysis product of the L-selectin membrane retained fragment and its function in driving T-cell expansion remains to be determined in future experiments.

Table of Contents

Table of Contents

List of Tables

List of Figures

Table of Abbreviation

aa	Amino acid
ACE2	Angiotensin converting enzyme 2
ADAMs	A disintegrin and metalloproteinases
ADCC	Antibody-dependent cellular cytotoxicity
ADCC	Antibody dependent cell cytotoxicity
AEC	3-amino-9-ethylcarbazole
AMC	Antibody-mediated clustering
AP-1	Adaptor protein complex 1
APC	Antigen presenting cell
AREG	Amphiregulin
CAMs	Cell adhesion molecules
CANDIS	Conserved Adam seventeeN Dynamic Interaction Sequence
CC	Chemokine
CCL2	Chemokine ligand 2
CCL21	Chemokine ligand 21
CCL7	Chemokine ligand 7
CCR2	Chemokine receptor 2
CCR5	Chemokine receptor 5
CCR7	Chemokine receptor 7
CCR7^{hi}	Chemokine receptor 7 high
CCR7^{lo}	Chemokine receptor 7 low
CD62L	L-selectin
CD62L^{hi}	L-selectin high
CD62L^{lo}	L-selectin low
CTLD	C-type Lectin domain
DCs	Dendritic cells
EGF	Epidermal growth factor
EGFR	Epidermal Growth Factor Receptor
EL4	Eukaryota lymphoblast 4
ER	Endoplasmic reticulum
ERM	Ezrin-Radixin-Moesin
Ets1	External Transcribed Spacer Region
FOXO1	Forkhead box protein O1
FoxP3	Forkhead box protein 3
GPCRs	G protein coupled receptors
HB-EGF	Heparin binding - Epidermal growth factor
HB-EGFR	Heparin binding - Epidermal growth factor receptor
Her2	Human epidermal growth factor receptor 2
HEV	High endothelial venule
HIV	Human immunodeficiency virus
IAV	Influenza A virus

ICAM-1	Intercellular adhesion molecule 1
ICAM-2	Intercellular adhesion molecule 2
IFN-γ	Interferon gamma
Ig	Immunoglobulin
IK7	Ikaros 7
IL-1RII	Interleukin 1 receptor, type II
IL-2	Interleukin 2
IL6R	Interleukin 6 receptor
Irf1	Interferon Regulatory Factor 1
IRHD	Intact iRhom homology domain
kDa	Kilodalton
KLF2	Krüppel-like Factor 2
L-selectin-v1	L-selectin variants 1
L-selectin-v2	L-selectin variants 2
LAG-3	Lymphocyte activation gene 3
LAM-1	Leukocyte adhesion molecule 1
LDL	Low-Density Lipoprotein
LDLR	Low-Density Lipoprotein receptor
LFA-1	Lymphocyte function associated antigen 1
Ly6C^{lo}	Lymphocyte antigen 6 complex low
MAC-1	Macrophage antigen 1
MAdCAM-1	Mucosal vascular addressin cell adhesion molecule 1
MAPK	Mitogen-activated protein kinase
MCP-1	Monocyte chemoattractant protein 1
MHC	Major histocompatibility complex
MMP	Matrix metalloproteinases
MPD	Membrane-proximal domain
MRF	Membrane retained fragment
mRNA	Messenger Ribonucleic acid
Mzf1	Myeloid zinc finger 1
NETosis	Program for formation of neutrophil extracellular traps
NK	Natural killer cell
PACS2	Phosphofurin acidic cluster sorting protein 2
PAMPs	Pathogen associated molecular patterns
PDI	Protein disulfide isomerase
PI3Kδ	Phosphoinositide 3-kinase
PKCs	protein kinase catalytic
PMA	Phorbol myristate acetate
PPME	Phosphomannan polysaccharide
PRRs	pattern recognition receptors
PS	Phosphatidylserine
RIP	Regulated Intramembrane Proteolysis

SARS-CoV2	Severe acute respiratory syndrome coronavirus 2
SCR	Sequence consensus repeats
SEM	Standard error of the mean
sLe^x	Sialyl Lewis x
sL-selectin	Soluble L-selectin
SorLA	Sorting protein-related receptor containing LDLR class A repeats
Sp1	Specificity protein 1
TACE	Tumor necrosis factor-α-converting enzyme
T_{CM}	Central memory T-cells
TCR	Thymus cell receptor
TEM	Transendothelial migration
T_{EM}	Effector memory T-cells
TGFα	Transforming growth factor alpha
T_H	T helper cells (also known as effector T-cells)
TIMP3	Tissue inhibitor of metalloproteinases 3
TLRs	Toll-like receptors
TNF-α	Tumor necrosis factor alpha
TNFR1	Tumor necrosis factor receptor 1
Tregs	Regulatory T-cells
Vpu	Viral protein u

1 Introduction

1.1 The immune response to pathogens

The vertebrate host responds to bacterial, viral, fungal, and protozoan pathogens by eliciting immune responses in both the innate as well as adaptive arms of the immune system. The host utilizes leukocytic immune surveillance and the activity of tissue resident immune cells to eliminate these invading pathogens and mount a stronger immune response by utilizing the preserved memory cells that recognize the same pathogen upon reinfection later in lifetime. Both immune surveillance and immune response to a pathogen challenge requires the leukocyte migration and recruitment to secondary lymphoid tissues. The leukocytes in circulation migrate differentially in and out of various tissues due to specific interactions between cell adhesion receptors and tissue specific ligand that enable immune cell homing to these organs. This step is pivotal in both immune cell monitoring of the host against foreign threats as well as mounting of an efficacious immune response in response to an invasion by a pathogen.

1.2 Role of L-selectin in inflammatory immune response

Sentinel cells in tissue play a critical role in inducing the expression of L-selectin ligands on the luminal surface of vessels. Sentinel cells such as dendritic cells play an important role in inducing the expression of L-selectin ligands such as PNAd and are essential for maintaining constitutive PNAd expression in LN HEVs. In particular, CD11c+ CD11b+ CD103+ DCs which mobilize from the gut lamina propria in response to microbial colonization, have been shown to drive the vascular switch from mucosal to peripheral addressin (PNAd) expression by HEVs (Zhang et al. 2016). CD11c+ cells have also been shown to maintain functional HEVs via LTβR dependent signalling in high endothelial cells (HECs) (Moussion and Girard 2011; Onder et al. 2013).

1.3 Leukocyte adhesion and migration cascade

Immune surveillance mechanism of the host involves constant monitoring to detect pathogen infected or diseased tissue by the circulating leukocytes. The process enables the recruitment and extravasation of leukocytes to the site of tissue injury or invasion to

eliminate the threat and begin the healing process to restore the tissue function. Leukocytic adhesion is a multi-step complex cascade that recruits various immune cells, causes localized accumulation of chemokines, immunogenic peptides, pro-inflammatory cytokines, and many acute-phase proteins at the inflamed site thereby preventing the tissue damage and ultimately completing the restoration of the tissue function (Figure 1.1). The inflammatory process that involves cellular interactions between leukocytes and endothelial cells facilitated by cell adhesion molecules (CAMs) and chemokine receptor-ligand interactions causes dilation of blood vessels, increasing vascular permeability. This causes immune cells to migrate to the inflamed tissue by the process known as extravasation (Kuby 2015).

Entry of Immune cells through High Endothelial Venules (HEVs)

The paracortical region of a lymph node is characterized by the existence of specialized structures called high endothelial venules (HEVs) recognized by their appearance of plump cells that protrude into the vascular lumen (Murphy et al. 2022)

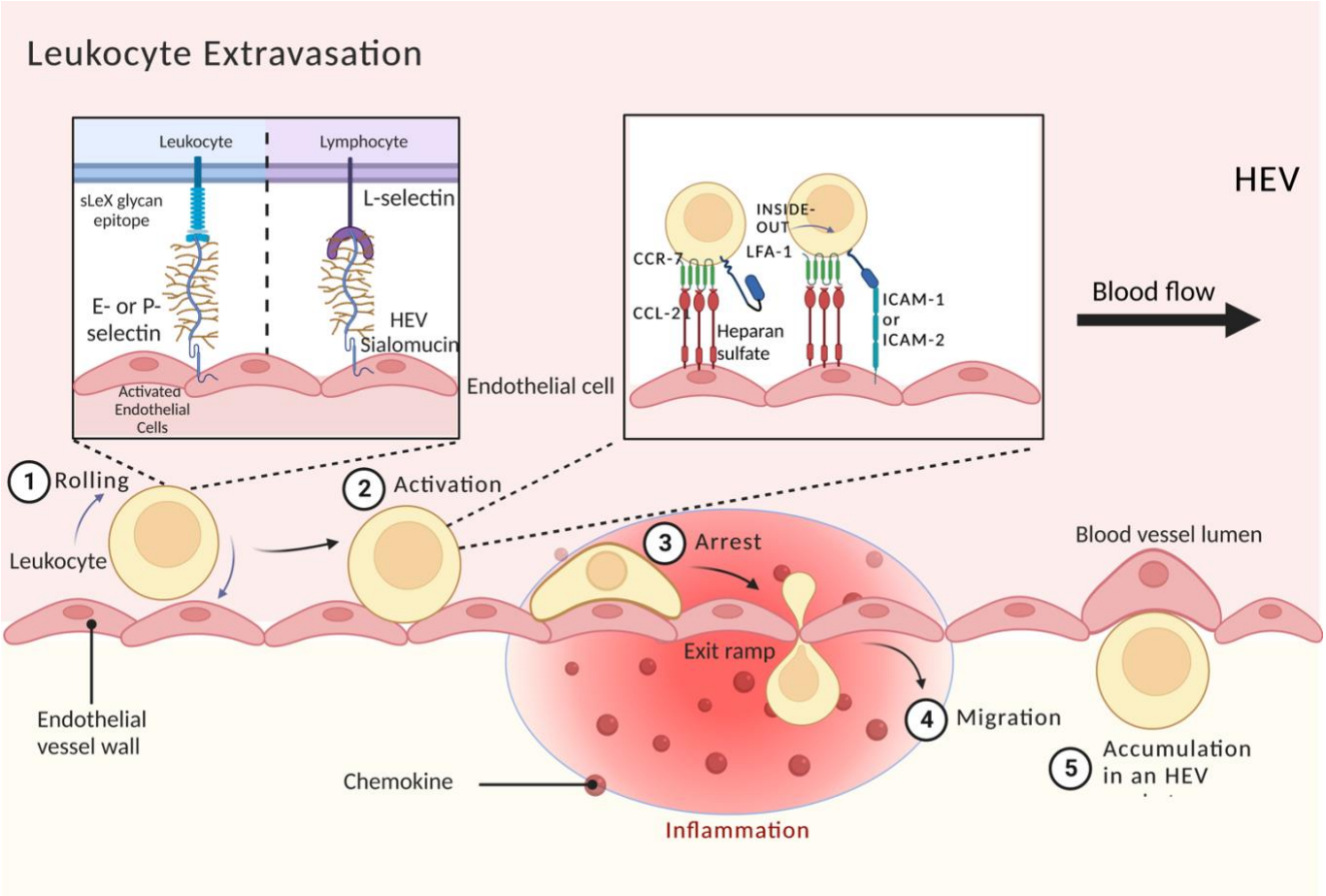

Figure 1.1 Multistep cascade of leukocytic recruitment. Multistep adhesion and migration cascade involves the rolling, sticking, crawling and transmigration of naïve lymphocytes into the inflamed site. The interaction between L-selectin on circulating lymphocytes and sialylated mucin glycoproteins also known as addressins on HEVs leads to tethering and rolling of lymphocytes along the walls of HEVs. Activated endothelial cells under inflamed conditions express E- or P-selectin which can bind sLeX glycan expressed by leukocytes. (Figure created using Biorender.com).

Naïve but mature T and B lymphocyte, enter the regional lymph nodes at HEVs through the process of extravasation or diapedesis. A multitude of cell adhesion molecules, chemokine receptors, and integrins are involved in this multistep adhesion and migration

cascade that involves rolling, sticking, crawling and transmigration of naïve lymphocytes into the inflamed site. The unique ability of HEVs to capture several circulating lymphocytes is due to the expression of sialomucins that recognize the molecules on the surface of naïve lymphocytes. The primary stage of adhesion involves interaction between the CD62L (L-selectin or lymphocyte homing receptor) of naïve circulating lymphocytes and sialylated mucin glycoproteins also known as addressins on endothelial cells of HEVs leads to tethering and rolling of lymphocytes along the walls of HEVs (Girard and Springer 1995; Butcher and Picker 1996; von Andrian and Mempel 2003; Mitoma et al. 2007). This is followed by chemokine mediated activation of rolling lymphocytes. HEVs express heparan sulfate bound CC-Chemokine ligand 21 (CCL21) which mediates binding to CC-Chemokine receptor 7 on lymphocytes coupled with shear blood flow induces conformational change in integrin- lymphocyte function associated antigen (LFA-1) through an inside-out unfolding mechanism (Shamri et al. 2005). Activated LFA-1 on the lymphocytes binds to intercellular adhesion molecule (ICAM-1) and ICAM-2 on endothelium causing the arrest of B and T lymphocytes in the peripheral lymph nodes whereas binding of integrin α4β7 to mucosal addressin cell adhesion molecule 1 (MAdCAM-1) expression in HEVs regulates recruitment into gut-associated lymphoid tissues such as mesenteric lymph nodes and Peyer's patches (Miyasaka and Tanaka 2004; Shamri et al. 2005). B lymphocytes also express the CXCR5 chemokine receptor which binds to CXCL13 presented on HEVs (Shamri et al. 2005).

Following the firm arrest of lymphocytes along the walls of HEVs, naïve lymphocytes crawl along the surface of HEVs finding the perfect region for transendothelial migration (TEM). The naïve lymphocytes crawl at an average speed of 10 μm per minute and exit through discrete sites also known as 'exit ramps' (Boscacci et al. 2010; Park et al. 2010). A transient accumulation of lymphocytes in pockets underneath the endothelial cells may contribute to 'highness' or plumpness of HEVs (Mionnet et al. 2011). In addition to naïve lymphocytes, central memory T-cells, and FoxP3 expressing regulatory T-cells that express CD62L and CCR7 have also been shown to undergo transendothelial migration through HEVs and accumulate into the paracortical region of lymph node during homeostasis (Ueha et al. 2007; Förster et al. 2008). Furthermore, migration of NK cells in lymph nodes has also been shown to be CD62L dependent (Chen et al. 2005).

1.4 Innate immunity to infection

The first line of host defense against pathogens is the innate immune system. A multitude of innate cells participate in providing protection to the host. These cells express pattern recognition receptors (PRRs) that recognize and bind pathogen associated molecular patterns (PAMPs). These cells include:

Neutrophils- Neutrophils are the first leukocytes to respond to infection or inflammation. Following the generation from the myeloid progenitors in the bone marrow, neutrophils migrate to the blood stream. Upon pathogen challenge, neutrophils migrate to the site of inflammation where they mount a proinflammatory response to eliminate the pathogen. N-formylated bacterial peptides or leukotrienes in the inflamed tissue cause the activation of neutrophils (Kuby 2015). In murine models of Influenza A virus (IAV) infection, neutrophils produce proinflammatory cytokines that recruit CD8+ lymphocytes in addition to neutrophil mediated NETosis of infected cells. L-selectin expression on neutrophils has been shown to contribute to rolling, tethering as well as transendothelial migration to the site of infection (Rahman et al. 2021). In mice infected with *S. aureus,* neutrophils recruitment to peripheral lymph nodes was shown to be L- and P-selectin mediated (Bogoslowski et al. 2018) whereas LFA-1 and MAC-1 are significant in adhesion to the endothelial cell membrane (Kuby 2015).

Monocytes- Inflammatory monocytes are also generated from myeloid precursors in the bone marrow and are $Ly6C^{lo}$ in mice. Upon pathogen challenge or an injury, the recruitment of monocytes occurs to the site of inflammation via adhesion and trafficking where they differentiate into macrophages or dendritic cells. This process of monocytic recruitment involves rolling, adhesion and transmigration and is dependent on the expression of cell adhesion molecules and chemokine receptors. Infection with viruses such as Vaccinia Virus, West Nile Virus and Herpes Simplex Virus demonstrated delayed clearance in the absence of CC Chemokine receptor 2 (CCR2) suggesting the role of CCR2- mediated recruitment and differentiation of $Ly6^{hi}$ monocytes in the clearance of viral infections (Shi and Pamer 2011). CCL2 and CCL7 ligands facilitate the recruitment of CCR2 expressing monocytes at the site of inflammation (Tsou et al. 2007). $LY6C^{hi}$ monocytes in mice have also been shown to express cell adhesion molecule, L-selectin (also known as CD62L). L-selectin also well known as a homing receptor

facilitates the transendothelial migration of monocytes at HEVs by regulating the tethering and rolling of monocytes (Ivetic et al. 2019; Reed and Ager 2022). Under inflammatory conditions, chemokine monocyte chemoattractant protein (MCP-1) in inflamed skin was also shown to cause integrin mediated recruitment of blood borne monocytes to lymph nodes via HEVs (Palframan et al. 2001). Due to its expression on early progenitor cells in the bone marrow, L-selectin plays a significant role in trafficking of monocytes to the peripheral lymphoid organs and hence clearance of viral pathogens. Consistently, in peripheral blood of SARS-CoV2 positive patients, a higher percentage of CD62L expressing monocytes was observed (Rutkowska et al. 2022).

Natural Killer Cells (NK cells) - NK cells were identified in 1975 as cells that recognize viral or tumor antigens without the need for antigen presenting cell (APC) mediated antigen presentation or prior sensitization with the antigens (Kiessling et al. 1975). The role of NK cells in antiviral immunity has been studied through animal models as well as human patients. NK cells offer immune protection through production of proinflammatory cytokines or cytotoxic effects on virus infected cells in many viral infections. Consistent with this, IAV infection leads to increased accumulation of NK cells in the lungs in mice (Carlin et al. 2018). Studies in animal models of viral infections have suggested the role of CCR5 in NK cell homing to infected tissues in acute infections while there is lack of sufficient data on NK cell homing in viral infections in humans (Björkström et al. 2022). A role for L-selectin in the migration and recruitment of NK cells has been shown in mice during the generation of an anti-tumor response (Sobolev et al. 2009), however the significance of L-selectin in homing of NK cells in anti-viral immunity is yet unclear.

1.5 Adaptive Immunity to infection

The adaptive branch of the immune system comprises of T- and B- lymphocytes that generate pathogen specific responses due to the presence of antigen-specific receptors on the surface of lymphocytes that recognize and bind antigens on the antigen presenting cells (APCs). The adaptive immune system response develops after 5-6 days of the initial breach and is also dependent upon the activity of innate immune system (Kuby 2015).

A myriad of factors determines the type, duration, and quality of adaptive immune response to the pathogen challenge. Of these, the type of pathogen plays a significant role in determining the initial adaptive response. In the presence of extracellular pathogens such as bacteria and fungi, pathogen specific naïve or memory B- cells upon activation by helper T-cells, complement proteins or cells of innate immune system secrete antibodies that can penetrate the extracellular spaces easily and neutralize the pathogens. In case of viruses that are obligate intracellular parasites and spend most of their lifecycle within the host utilizing host cell resources and machinery for their own replication and maintenance, a more sophisticated and robust mechanism of removal is required. The immune response to viruses is initiated by the innate immune system and followed by the generation of a long-lasting adaptive immunity mediated by an interplay of CD4+, CD8+ cytotoxic T lymphocytes and antibody generating B-cells both locally and systemically.

The specific immune response to viruses by lymphocytes is mediated by antigen specific receptors on B and T-cells that recognize antigenic peptides presented by APCs expressing specialized class of proteins expressed by the genes of major histocompatibility complex (MHC). Two types of MHC proteins are expressed in vertebrates; Class I MHC is expressed in nucleated cells of vertebrates and presents antigenic peptides to CD8+ Cytotoxic T-cells (Janeway et al. 2011) and Class II MHC molecules that are expressed on immune cells such as mature dendritic cells (DCs) or activated macrophages (Banchereau et al. 2000; Paul A. and Kazuyuki 2015) and present antigenic peptides to CD4+ T-cells. However, some viruses such as Herpes Simplex Virus and Measles Virus can compromise the function of APC by inhibiting DC maturation.

B-cell responses to a viral infection occur in lymphoid tissues and are mediated by antibody production whereby antibody coating of the viral particle or virally infected cells may either lead to neutralization or antibody dependent cell cytotoxicity (ADCC). This may prevent the infection or entry of new cells by virus. In some viruses such as HIV or Dengue, this is used to facilitate reentry into the cells (Takada and Kawaoka 2003) thereby increasing the extent of damage to the host cells.

T-cells originate from hematopoietic precursors in the bone marrow and develop in thymus before entering into the bloodstream as naïve T-cells. Similar to B-cell responses, T-cell responses against various pathogens also commence in the secondary lymphoid tissues like lymph nodes that sample the antigen from the pathogen in antigen presenting cells. The response that follows then varies according to the type of the immune cell activated. Class I MHC restricted naïve CD8+ T-cells that are $CD62L^{hi}CCR7^{hi}$ upon activation, undergo proliferation and differentiation into effector cytotoxic CD8+ T-cells that are $CD62L^{lo}CCR7^{lo}$. The activated CD8+ T-cells produce IFN-γ and TNF-α, both of which have antimicrobial and anti-tumor effect. Class II MHC restricted naïve, helper T-cells (T_H) or CD4+ T-cells undergo activation to proliferate as central memory and effector cells that produce T_H1 cytokines such as IFN-γ, IL-2 or T_H17 cytokines such as IL-17, IFN-γ or IL-22 (Sarin et al. 2011). Central memory T-cells acquire $CD62L^{hi}CCR7^{hi}CD28^{hi}$ phenotype and circulate until they get challenged by the same antigen upon reinfection.

The generation of a timely adaptive immune response is critically dependent on the expression of chemokines, chemokine receptors, and cell adhesion molecules. These enable the migration of lymphocytes to the infected or inflamed tissue prior to and after immune response like innate immune cells. Cell adhesion molecules (CAMs) such as integrins and selectins enable the adherence of naïve or memory cells to endothelial cell membranes, enable diapedesis and extravasation to the draining lymph nodes through HEVs (Ager and May 2015; Reed and Ager 2022). Effector T-cells CD4 and CD8 are recruited from post-capillary venules that are not HEV in infected or diseases tissues and also use the multistep adhesion cascade (Ager and May 2015). Cell adhesion molecules CAMs are also pivotal in strengthening the T_H-APC (Monks et al. 1998), T_H- B-cells (Dustin and Dustin 2001) and T_{cyt} to target cell interactions (Jenkins and Griffiths 2010).

A particular subset of CD4+ T helper cells termed Tregs, have the capacity to control the activity of other immune cells. T cell-mediated immunosuppression was discovered shortly after the identification of the thymus as an essential component of the immune system. Initial research by Nishizuka and Sakakura demonstrated that removing the thymus of neonatal mice on day 3 resulted in autoimmunity, while removal on day 7 did

not, suggesting that suppressive cells are released from the thymus after conventional T cells. In 1995, Sakaguchi and colleagues showed that CD4+ suppressive cells, which migrate from the thymus after day 3, express the IL-2 receptor CD25. Removing CD4+ CD25+ cells from mice led to the production of autoantibodies and the development of inflammatory lesions, similar to those observed in human autoimmune diseases (Nishizuka and Sakakura 1969; Taguchi et al. 1980).

Reintroducing CD4+ CD25+ cells prevented autoimmune disease and could also transfer tolerance to other mice, indicating that these cells are critical for controlling self-reactive T cells and maintaining peripheral tolerance. The discovery of the CD25 marker coincided with the identification of a population of Tregs that prevented the development of colitis upon transfer. However, subsequent studies demonstrated that most regulatory activity within the CD45RBlo group was confined to CD25+ cells, validating CD25 as a reliable marker for suppressive T cells. Due to their ability to suppress immune responses to both self and foreign antigens, these CD4+ CD25+ suppressive cells, now known as Tregs, have been implicated in autoimmune disease, as well as tolerance, allergy, and anti-tumor immunity (Sakaguchi et al. 1995; Asano et al. 1996).

Tregs are characterized and subdivided based on surface expression levels of CD62L (Ivetic, 2019). Interestingly, Tregs expressing high levels of CD62L have been shown to have superior immunosuppressive roles in several murine disease models (Gallatin et al. 1983; Fu et al. 2004; Ermann et al. 2005; Lange et al. 2011). Furthermore, whilst the immunosuppressive function of CD62L+ and CD62L- Tregs was shown to be comparable in-vitro, the ability of CD62L+ Tregs to home to LNs and to express higher CCR7 levels was linked to superior immunosuppressive activity in-vivo (Szanya et al. 2002; Fu et al. 2004) thereby linking the importance of L-selectin expression on Tregs, homing to SLOs and immunosuppressive function (Szanya et al. 2002; Ivetic, 2019).

The specific locations where regulatory T cells (Tregs) most effectively suppress the immune response have been the subject of various studies, with differing results. Studies which involved blocking the function of CD62L (L-selectin), found that the migration of Tregs to lymph nodes was crucial for their induction and allograft tolerance. In concordance with this speculation, previous studies have shown that the LN-homing

CD62L+ Treg population expressed high levels of CCR7 and exerted suppressive function far better than did the CD62L tissue-homing population, despite the 2 subpopulations demonstrated equivalent suppressive functions in vitro (Szanya et al. 2002).

1.6 Cell Adhesion Molecules

Immune cells mediate inflammation following their recruitment to sites of infection or injury. The migration of naïve lymphocytes to the secondary lymphoid organs through the HEVs is achieved by adhesion of circulating leukocytes via selectin-and-integrin-mediated interactions (Ley 2003). The trafficking of naïve cells to lymph nodes via HEVs during steady state conditions or to the inflamed endothelial vessels requires immune cell receptor and tissue ligand interactions for cell adhesion. This naïve immune cell homing to the lymph node or migration of lymphocytes to the site of inflammation thus leads to the exposure of naïve cells in the lymph nodes to antigenic peptide bearing antigen presenting cells enabling the generation of effector cells that respond immediately and memory cells that reenter circulation to respond to antigenic threat later during their lifetime. Several cell adhesion molecules that belong to one of the four families mediate the process of cell recruitment and migration. These belong to 1. Mucin-like family 2. Selectin family 3. Integrins 4. Ig Superfamily and play a role in cellular adhesion process prior to the extravasation of lymphocytes to the site of inflammation. These aid in increasing the strength of cellular interaction between immune cells as well their target cells.

Selectins are a family of calcium-dependent transmembrane carbohydrate-binding adhesion receptors found on the surface of leukocytes, platelets and endothelial cells. Selectins mediate the initial stages of low affinity rolling adhesion of circulating leukocytes leading to firmer adhesion by integrins followed by leukocyte transmigration across endothelial cells lining blood vessels in peripheral lymph nodes and inflamed tissues under shear forces of the blood flow during inflammation (Imhof 1995).

1.7 L-Selectin Structure and Function

L-selectin also known as CD62L, leukocyte adhesion molecule 1 (LAM-1), leukocyte surface antigen (Leu-8), TQ1 (Ley 2003) is expressed by the majority leukocytes including neutrophils, monocytes, naïve T-cells, B-cells and memory cells It comprises: a calcium-dependent lectin domain (C-type Lectin domain, CTLD), an epidermal growth factor (EGF) like domain, two sequence consensus repeats (SCR) of the complement-regulatory protein domains, membrane proximal extracellular cleavage site, transmembrane helix and a calmodulin regulated intracellular cytoplasmic tail comprising 17 amino acids **(Figure 1.2: Structure of L-selectin)** (Ivetic 2004).

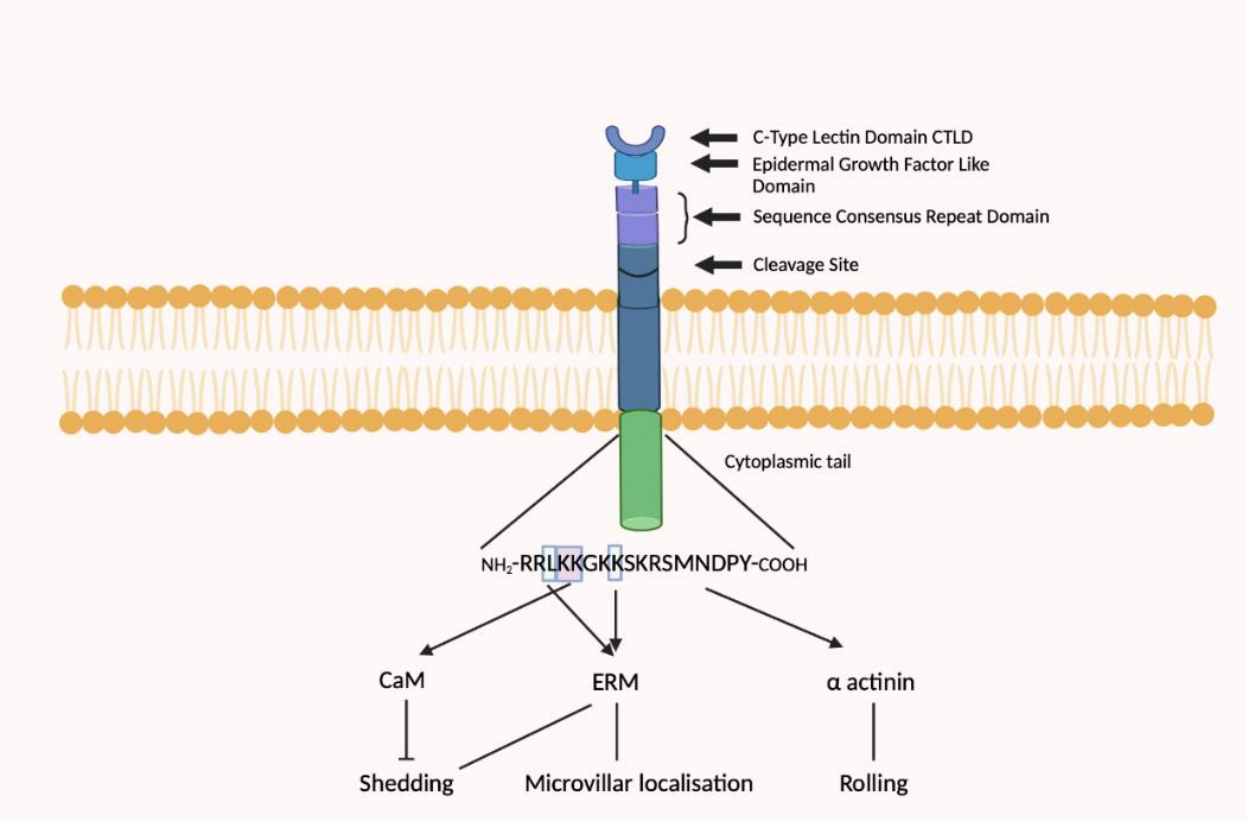

Figure 1.2: Structure of L-selectin: L- selectin is a transmembrane multicellular domain protein with C-Type Lectin domain that recognizes binds to various glycans found attached to proteins and lipids on cell surfaces of other cells, Epidermal Growth factor like domain, Sequence consensus repeat domain, a cleavage site for ectodomain shedding, a short transmembrane region, a cytoplasmic tail that binds calmodulin CaM, Ezrin-Radixin-Moeisin (ERM) and α-actinin protein. Figure created using Biorender.com

The L-selectin gene SELL is located on long arm of human chromosome 1 (1q24.2) and on murine chromosome 1 near E- and P-selectin genes in both species. The close association of these genes and sequence homology of selectin genes (40–60% at the nucleotide level) suggest a common ancestral origin. Alternative splicing of SELL and post translational modification of the protein contribute to the functional diversity of L-selectin (Furukawa et al. 2008). The murine SELL gene comprises of 9 exons that are spliced to generate two variants (L-selectin-v1 and L-selectin-v2) whereas the human L-selectin gene has ten exons that are spliced to form a mature mRNA that when translated forms a ~30 kDa product. However, molecular weight of L-selectin isolated from lymphocytes and neutrophils varies owing to the cell type specific glycosylation ranging between 65 kDa in lymphocytes to 100 kDa in neutrophils (Schleiffenbaum et al. 1992; Wedepohl et al. 2010).

L-selectin is widely recognized as the tethering and rolling receptor for circulating immune cells. The migration and trafficking of cells in both the adaptive and innate arms of the immune system is significantly decreased due to aberrant or absent L-selectin expression. The studies by Jutila et al (1989) and Kishimoto et al (1989) showed the significance of L-selectin mediated neutrophil migration to the inflamed sites. Neutrophil recruitment in L-selectin-null mice was also shown to be significantly reduced in a model of thioglycollate-induced peritonitis (Arbones et al. 1994). Human monocyte recruitment to activated endothelium was also demonstrated to be L-selectin mediated (Spertini et al. 1992). Antibodies targeting L-selectin have been shown to block the homing of lymphocytes into lymph nodes from HEV blood vessels in mice. Consistent with this, lymphocytic homing, rolling and migration to lymph nodes was shown to be impaired in L-selectin null mice (Ley 2008). In addition to recruitment function in lymphocytes, L-selectin clustering is also associated with enhanced T-cell receptor signaling (Nishijima et al. 2005). Furthermore, in human tumor antigen primed CD8+T_{CM} cells, enhanced tumor lysis was correlated with increased L-selectin shedding (Yang et al. 2011). However, the exact mechanism of this L-selectin mediated tumor lysis by T-cells remains unknown. Shedding of L-selectin was also shown to control proliferation of naïve CD8 T-cells following TCR engagement (Mohammed et al. 2019). The examples point to non-homing roles for L-selectin.

1.8 Regulation of L-selectin expression in immune cell subsets

The identification of L-selectin expressing early hematopoietic stem cells $CD62L^{+}CD10^{-}lin^{-}CD34^{+}$ lymphoid primed population in human bone marrow suggests the role of L-selectin in trafficking and differentiation of lymphocytes and myeloid cells prior to their commitment to either B or T-cells as well as a role in cell adhesion in the bone marrow microenvironment (Kohn et al. 2012). The activation state of the leukocyte significantly regulates L-selectin expression as highest level of expression of L-selectin is observed in naïve and, not activated, effector, or central memory T-cells. The expression of L-selectin on memory cells is, however, debatable with several studies also reporting tissue specific expression of L-selectin on memory cells (Masayuki 1998). Furthermore, the age of the immune cells also has been shown to affect the expression of L-selectin. For instance, aging neutrophils have decreased levels of L-selectin compared to central memory T-cells that live longer (6 weeks) than neutrophils (~3 days) (Hengel et al. 2003; Pillay et al. 2010; Zhang et al. 2015). Using disease models, Foxp3 expressing regulatory T-cells (Tregs) were shown to demonstrate better immunosuppressive function when they express L-selectin (Fu et al. 2004), however whether L-selectin mediated trafficking contributes to this increased immunosuppression remains unclear.

1.8.1 Transcriptional regulation of L-selectin mRNA expression

Most of our current knowledge on the transcriptional regulation of SELL gene expression is through studies on human lymphocytes ex vivo, murine lymphocytic cell lines in vitro or in vivo murine models of lymphocytic trafficking and migration. It is now understood that the expression of L-selectin occurs in triphasic (cyclical) pattern in T-cells after TCR stimulation: an initial decrease, transiently boosted expression and then loss of expression. Short term in vitro studies using mitogen or IL-2 stimulated human T-cells have shown that transient upregulation of L-selectin mRNA expression precedes the downregulation from the cell surface (Chao et al. 1997). However, the long-term activation of lymphocytes indefinitely downregulated the expression of L-selectin via transcriptional suppression (Venturi et al. 2007).

Specific transcription factors that regulate the expression of genes coding for L-selectin are not fully elucidated yet in humans. In murine EL4 T lymphoblast cell line, the transcription factors Mzf1, KLF2, Sp1, Ets1, and Irf1 were shown to bind to and activate the mouse SELL promoter (Dang et al. 2009). According to Christopherson and colleagues (2001), Ikaros family member specifically, IK7 was shown to regulate L-selectin mRNA expression in a T-cell line. The immunomodulatory cytokine interferon-alpha is proposed to upregulate the L-selectin surface expression by resulting in an increase in the mRNA steady state levels (Evans et al. 1993). Recently, transcription factor FOXO1 was shown to upregulate human L-selectin expression by binding to the FOXO1 consensus in a dose-dependent manner (Lou et al. 2012). A recent study determined the significance of Krüppel-like factor2 KLF2 in activation of CD62L promoter thereby affecting T-cell homeostasis (Bai et al. 2007). Furthermore, previous work (Mohammed et al. 2016) defined a pattern of cyclical expression of L-selectin in influenza A virus primed CD8+ T-cells in murine model of IAV infection. Following the primary regulation by ectodomain shedding due to proteolytic activity of ADAM17, the molecular receptor expression underwent secondary downregulation by silencing the transcriptional factor KLF2 that binds to the SELL gene promoter element (Mohammed et al. 2016). The importance of this finding is that L-selectin shedding and re-expression occurred in lymph nodes where T-cells are activated and silencing occurs when activated T-cells relocate to infected lungs in IAV infection.

1.8.2 Regulation of L-selectin surface expression

Circulating leukocytes constitutively express L-selectin on finger like projections called microvilli (Stein et al. 1999) that undergoes turnover due to shedding of external domain. A plethora of physiological or artificial agonists of cell activation can induce ectodomain shedding of L- selectin and regulate the migration of leukocytes to secondary lymphoid organs and peripheral tissues.

L-selectin shedding- The surface levels of L-selectin expression upon activation are downregulated mainly through the L-selectin shedding process. The shedding process has been demonstrated in neutrophils and lymphocytes (Smalley and Ley 2005; Klinger et al. 2009; Buscher et al. 2010) and is completed within a short duration of initiation (Jung and Dailey 1990; Jutila et al. 1991). Activation of the cell leads to rapid shedding of L-selectin by protelolytic enzymes or sheddases, a distintegrin and metalloproteinase 17 (ADAM17), ADAM10 and ADAM8 (Long et al. 2010) in the cells allowing for other integrin based stronger receptor-ligand interactions (Condon et al. 2001). Shedding of L-selectin can be induced after activation of the cell by phorbol esters, IL-8, or activation via the T-cell receptor by superantigens (Fors et al. 2001). Cross-linking of L-selectin itself, without further activation of the cell (Drost and MacNee 2002), also leads to cleavage of the molecule. The shedding of membrane proximal extracellular region requires interaction between the highly basic cytoplasmic tail of L-selectin and at least three other proteins: alpha- actinin, Calmodulin (CaM) and members of the ERM (ezrin/radixin/moesin) family of cytoskeletal proteins (Ivetic 2004). Intracellular events that cause disruption of CaM and L-selectin binding due to protein kinase C activation are known to cause rapid shedding by ADAM17 as CaM binding is removed. ERM proteins on the other hand, unlike CaM, enhance shedding by regulating L-selectin interaction with cytoskeletal actin (Ivetic 2004). The polarization of monocytes undergoing transendothelial migration in murine model was demonstrated to require serine phosphorylation sequentially at positions 364 and 367 in the cytoplasmic tail of L-selectin thereby also regulating ezrin-radixin-moesin adaptors required for outside-in clustering of L-selectin (Newe et al. 2019). The exchange of ezrin for moesin in the cytoplasmic tail is pro-shedding event to limit protrusion. (Walcheck et al. 2003) also reported the presence of ADAM17 independent metalloprotease shedding in L-selectin using ADAM17 deficient

mouse fibroblast cell line. The authors proposed that while ADAM17 dependent shedding might be an inducible process, the independent process may contribute to the basal turnover of the L-selectin physiologically (Walcheck et al. 2003; Mohammed et al. 2019).

The triggers for ectodomain shedding are not fully understood. Ligand-mediated clustering of L-selectins, CD18 integrin clustering, contact with oxidized LDL, osmotic stress and the exposure to several pro-inflammatory cytokines have been implicated in L-selectin shedding. Recently, Mohammad et al (2016) have shown that peptide-MHC activation of TCR stimulates ADAM17 dependent shedding in T-cells although the mechanism of activation of ADAM17 by TCR remains unknown. The final effect of ectodomain shedding is instantaneous cessation in the function of L-selectin, adhesion to endothelium and signaling events dependent on intact full-length L-selectin. However, the membrane retained fragment (MRF) or cleaved cytoplasmic tail could still signal in activated T-cells (Mohammed et al. 2019). The surface expression of L-selectin and subsequent shedding varies with cell subset and/or in response to the pathogen challenge. For example, L-selectin receptor has been identified as a receptor of HIV entry in naïve T-cells. HIV encoded proteins Nef and Viral protein u (Vpu) can decrease cell surface expression of L-selectin by sequestration (Stolp et al. 2012; Vassena et al. 2015). This mechanism of regulation of the shedding of L-selectin leads to increased viremia as HIV infected cells are redirected back into the circulation. Furthermore, senescent neutrophils express low levels of L-selectin, i.e., most of their L-selectin has been cleaved, while on the other hand, bone marrow homing receptors are upregulated (for shifting the migration of aged neutrophils to the bone marrow for elimination and clearance by bone marrow resident macrophages) (Ivetic 2018). The cyclical expression, with internalization of membrane retained fragment of L-selectin may be further regulated by µ1-A, a 45kDa protein of clathrin coated AP-1 complex (Dib et al. 2017). Additionally, Ager et al. have showed the presence of cyclical pattern of L-selectin expression on antigen specific CD8+ T-cells during influenza A virus infection (Mohammed et al. 2016) in which L-selectin shedding is understood to be the primary regulatory mechanism.

The rate of L-selectin shedding also varies with the activation state and cell subtype. When neutrophils are activated, L-selectin shedding occurs rapidly mostly completing within 5 minutes. This consistent phenomenon is used in vitro to assess the

functional state of neutrophils. L-selectin shedding releases the ectodomain in the extracellular space. The cleaved soluble ectodomain retains the ability to bind ligands in the vasculature and indirectly acts as a potent competitive inhibitor to L-selectins expressed on the cell surface. In healthy individuals, the average concentration of plasma soluble L-selectin is 0.7 to 1.5 µg/mL. For example, studies have found that in systemic lupus erythematosus or in Sjogren syndrome, the levels of soluble L-selectin > 2 µg/mL. (Font et al. 2000). Interestingly, the soluble form of L-selectin has been associated with negatively regulating inflammation and lymphocytic migration to the peripheral lymph nodes with levels as low as 0.9 µg/mL reducing the migration by 30% (Smalley and Ley 2005).

L-selectin shedding gives rise to a membrane-retained 6 kD fragment which is a fragment of L-selectin that is retained in the membrane after cleavage by a membrane metalloprotease. The MRF is subject to further degradation by γ-secretase leading to the formation of an intracellular fragment (ICD) with signaling potential (Ivetic et al. 2013).

1.8.3 Regulation of L-selectin binding to ligands

In addition to the above, L-selectin ligand binding is also regulated by post-translational modifications. Activation of T lymphocytes by cross-linking the T-cell receptor leads to changes in the affinity of L-selectin on the cell surface. This was tested using phosphomannan polysaccharide (PPME), a phospho-mannan that resembles the carbohydrate structure of the natural ligand of L-selectin (Yoshida et al. 1994) (Kraal and Mebius 1997).

The C-type lectin domain (CTLD) binds to various glycans found attached to proteins and lipids on cell surfaces of other cells. The minimal structural requirement for binding to L-selectin is a branched tetrasaccharide, called sialyl Lewis ^{x} (sLe^{x}), made of sialic acid, galactose, fucose and N-acetyl glucosamine. Overexpression of mouse splice variants of L-selectin, L-selectin-v1 and L-selectin-v2 in cells lacking L-selectin have revealed altered capacities in adhesion to sLe^{x} under flow, ectodomain shedding in response to cellular activation, and signaling to p38 MAPK following antibody-mediated clustering (AMC) (Furukawa et al. 2008)

Post translational glycosylation in any of the seven N-glycosylation sites of human L-selectin yields different molecular isoforms that are differentially expressed in various leukocyte subsets: 75 kDa in lymphocytes, 95–105 kDa in neutrophils and 110 kDa in monocytes (Masayuki 1998). Appropriate post translational glycosylation in the ligands is also an important determinant in the ability of endothelial cells to bind to L-selectin. The ligands for L-selectin are sialomucins on endothelial cells, whose expression depends on cytokine signals. These mucin -like glycoproteins are serine/threonine rich and undergo sialylation, fucosylation and sulfation during post translational modification that allows increased trans endothelial migration (Mcever et al. 1995). L-selectin recognizes sialylated Lewis^{x} and sialylated Lewis^{a} moieties and binds to sulfatides and sulfated polysaccharides such as fucoidan and heparin. The most studied L-selectin binding determinant on endothelial cells' sialomucins is O-glycosylated form, sialyl 6-sulfo Lewis ^{X} (Ley 2003). Using a function-blocking monoclonal antibody MECA 79, several distinct L-selectin specific ligands have been identified in mouse including podocalyxin, nepmucin, endomucin as well as CD34 and glycam-1 (Streeter et al. 1988; Imai et al. 1991; Hemmerich et al. 1994). These glycoproteins are associated with HEVs and exhibit high affinity for L-selectin at the site of inflammation. These include a specific glycosylated form of membrane bound CD34 and a secreted GlyCAM-1 glycoform at the sites of inflammation. Additionally, MAdCAM-1 is found in the mesenteric lymph nodes HEV of mice as an L-selectin specific glycoform. Finally, a fourth HEV- associated Sgp200 ligand is also observed but remains to be identified at the molecular level.

1.8.4 Ligands binding to the L-selectin tail

Alpha-actinin: Kansas et al. (1993) showed that 11 amino acids cytoplasmic tail in the COOH terminus of L-selectin regulate the rolling of leukocytes to the inflamed endothelium. Injection of cytoplasmic tail abrogated deletion mutants of L-selectin in the physiological circulation of rats caused severe reduction in the rolling efficiency (Kansas et al. 1993) (Figure 1.3). Furthermore, an in vitro study showed that this interaction of C-terminus was mediated by its interaction with classic actin filament cross linking protein alpha-actinin using microfilament disrupting agent, cytochalasin B (Pavalko et al. 1995). This implicated the role of cytoskeletal filaments in the function of L-selectin in leukocytes.

Calmodulin (CaM): Calmodulin is a calcium binding regulatory 18kDa protein that remains bound to the membrane proximal region of L-selectin in resting naïve cells. Upon appropriate stimuli, CaM is released from the L-selectin inducing conformational allosteric change leading to neutrophil rolling and adhesion of lymphocytes to HEVs of peripheral lymph nodes (Rzeniewicz et al. 2015). Furthermore, calmodulin inhibitors induce proteolytic shedding of L-selectin thereby disrupting adhesion (Rzeniewicz et al. 2015).

Ezrin-Radixin-Moesin Proteins (ERM): These proteins act as cytoskeletal linkers to L-selectin facilitating receptor clustering and tethering under flow conditions. ERM proteins are also essential for the microvilli formation (Bretscher 1983; Bretscher et al. 1997).

Protein Kinase C and Serine-364 Phosphorylation of the L-selectin cytoplasmic tail: Two isoforms of Protein Kinase C (α and δ) readily phosphorylate the serine-364 in the cytoplasmic tail of L-selectin causing CaM dissociation (Rzeniewicz et al. 2015)

(Figure 1.3). However, whether the process occurs during or after shedding remains unclear.

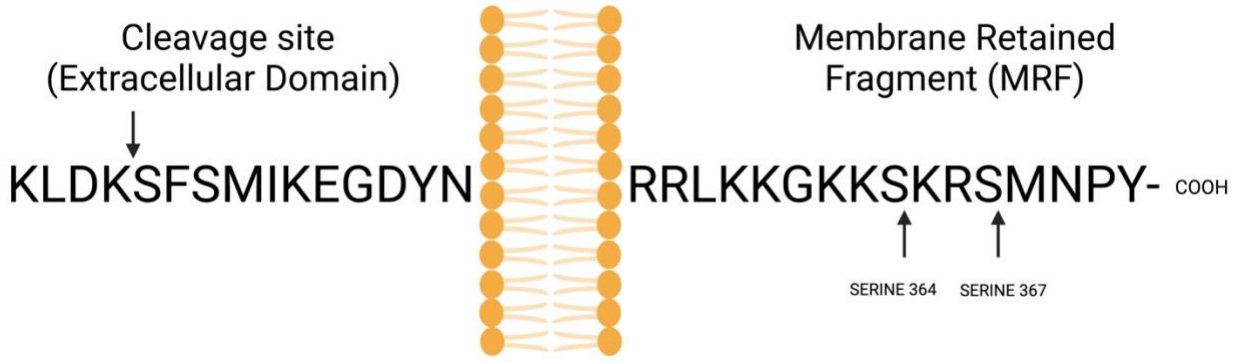

Figure 1.3: Amino acid sequence of the L-selectin cleavage site and the cytoplasmic tail with serine residues. Cleavage site is in the ectodomain region close to the cytoplasmic membrane. Serine residues in the cytoplasmic tail undergo phosphorylation causing the recruitment of ERM-proteins following detachment of calmodulin initiating process of shedding. Figure created using Biorender.com.

1.8.5 Clinical significance of L-selectin

L-selectin being a widely and constitutively expressed leukocyte cell adhesion protein bears therapeutic relevance in many diseases and clinical disorders. Due to its role in adhesion cascade, migration of leukocytes and homing of lymphocytes to HEVs and inflamed endothelium, it has been investigated in variety of diseases including cancer, viral infections and autoimmune disorders. Watson et al (2019) and Mohammed et al (2016) recently demonstrated that maintenance of L-selectin expression on tumor specific and virus-specfic T-cells following activation was advantageous in mouse models of immunotherapy. In another study, higher expression of L-selectin expressing SELL gene was associated with better survival outcome in basal, Her2 + and luminal B subtypes of breast cancer (Kumari et al. 2021).

In Type-I diabetes, sL-selectin was a late marker of autoimmune destruction of islets (Kretowski et al. 2000). A study of 38 women and 2 men showed an association between higher concentrations of circulating sL-selectin in the sera of patients with primary Sjogren's syndrome and the presence of Raynaud's phenomenon, autoimmune thyroiditis and rheumatoid factor (Carrasco et al. 2000).

Targeting L-selectin may have therapeutic potential in the management of thyroid nodules, as it could potentially prevent the development of cancer or stop the spread of cancerous cells. L-selectin may be a useful diagnostic marker for thyroid nodules, as its expression levels have been shown to correlate with the aggressiveness of the nodules. Overall, the potential clinical implications of targeting L-selectin in the management of thyroid nodules, both as a therapeutic target and a diagnostic marker. However, further research is needed to fully understand the role of L-selectin in thyroid nodules and to develop effective therapies targeting this adhesion molecule (Rabi et al. 2023).

Measuring the levels of soluble L-selectin (sL-selectin) in the serum of T1DM patients could potentially serve as a marker for disease activity. sL-selectin notably is elevated in T1DM patients compared to healthy controls and that this elevation may reflect the increased immune cell trafficking and inflammation associated with the disease. Furthermore, blocking the activity of sL-selectin could be a potential therapeutic target in treating T1DM. By blocking sL-selectin, it may be possible to reduce the trafficking of

immune cells to the pancreas, which would prevent further destruction of beta cells and preserve insulin production. In conclusion, the potential of sL-selectin as a marker for disease activity in T1DM and suggests that blocking its activity may be a promising therapeutic strategy for the disease. However, further studies are needed to fully understand the role of sL-selectin in T1DM and to develop effective therapeutic interventions (Kretowski et al. 2000).

1.9 ADAMS and ADAM17

ADAMs are a family of type I membrane anchored proteins with metalloproteinase and disintegrin function. ADAM family members are structurally relatives of snake venom disintegrins and have been implicated in a variety of processes that involve cell-extracellular matrix and cell-cell interactions. ADAMS are crucial in multitude of biological processes including development, regeneration, neurogenesis and inflammation. The ADAM family contains 21 members in humans. ADAMs are widely expressed by most immune cells; thirteen ADAMs encode a proteolytically active domain and share a common structure (Lambrecht, Vanderkerken, & Hammad, 2018). The best-known example of this is the cleavage of membrane-bound tumor necrosis factor (TNF) into soluble TNF (sTNF) by ADAM17. ADAM17 is a regulator of T-cell activation at sites of immune activity by cleaving L-selectin in naïve CD8 T-cells (Mohammed et al. 2019). Not all ADAMs are proteolytically active but those that are cleave the ectodomains of other transmembrane proteins. These 'sheddases' remove the ectodomain through their proteolytic activity thus generating a small membrane fragment. The proteolytically active ADAMs have a metal dependent metalloproteinase active site that carries out the shedding function creating a soluble form of the receptor protein. The proteolytic activity of ADAMs is a tightly regulated process to avoid excess or insufficient shedding that can otherwise lead to pathophysiological conditions. ADAMs localize to the perinuclear and plasma membranes to cleave their substrates (Schlondorff et al. 2000) functioning in *cis* or *trans* configuration cleaving substrates on the same cell surface or on the surface of the adjacent cells. ADAM17/TNF-α–converting enzyme, (TACE) and ADAM10 are the most characterized members of the ADAM family, having ∼50% sequence identity within the catalytic domain (Black et al. 1997).

ADAM17, a zinc-dependent metalloproteinase and a disintegrin responsible for L-selectin shedding in leukocytes belongs to adamalysin protein family and is one of the major ectodomain sheddases (Peschon et al. 1998; Li et al. 2006; Tang et al. 2011; Ager 2012). ADAM17 is involved in a variety of physiological housekeeping and pathophysiological processes including regeneration, differentiation, autoimmune diseases and cancer progression (Black et al. 1997; Moss et al. 1997; Peschon et al. 1998; Chalaris et al. 2010; Blaydon et al. 2011).

ADAM17 is also known as (TACE) Tumor Necrosis alpha converting enzyme for its proteolytic activity on membrane bound form of TNFα thereby releasing the soluble form of TNFα. ADAM17 is a significant mediator of cell signaling with its substrates ranging from growth factors such as Epidermal growth factor (EGF) and Epidermal growth factor receptor (EGFR), Toll-like receptors (TLRs), cytokine receptors ligands, G-protein coupled receptors (GPCRs) and cell adhesion proteins. The stimulators of ADAM17 can be physiological stimulators such as cytokines, or artificial agonist such as phorbol esters. TCR activation can also induce lymphocyte activation gene-3 (LAG-3) cleavage by ADAM17.

ADAM17 is ubiquitously expressed however the highest expression levels are observed in adult heart, placenta, skeletal muscle, pancreas, spleen, thymus, fetal brain, lung, liver and kidney. It is also expressed in neutrophils, monocytes and expressed on induced T-cell blasts (Ebsen et al. 2013). Elevated expression of ADAM17 gene has been observed in specific cell types derived from various autoimmune disease conditions. Furthermore, ADAM17 was recently shown to facilitate SARS-CoV-2 entry by spike protein S priming and ACE2 cleavage (Jocher et al 2022). The surface expression of ADAM17 is however tightly regulated as excess activity of ADAM17 on proinflammatory membrane bound receptors or growth receptors can cause chronic inflammation or tumorigenesis respectively. On the other hand, poor activity of ADAM17 on growth factors can cause developmental defects. Consistently, ADAM17-deficient mice have defects in multiple organs and tissues and as a result die between embryonic day 17.5 and the first few days after birth (Peschon et al. 1998).

The sheddase activity of ADAM17 is tightly regulated at multiple levels with different extracellular domains participating in such proteolytic activity. Since shedding of ectodomain via proteolysis is an irreversible step, shedding is tightly regulated to prevent excess or insufficient release of signal transmitting ectodomains such as epidermal growth factor receptor ligands.

1.9.1 Structure of ADAM17

ADAM17 is a multi-domain protein with a large extracellular region that has a 17 aa signal peptide (Figure 1.4). In addition, the ectodomain signal peptide sequence is followed by

a prodomain, a metalloenzyme or catalytic domain, a disintegrin domainand a membrane-proximal domain (MPD), as well as a short juxtamembrane segment called Conserved Adam seventeeN Dynamic Interaction Sequence (CANDIS). This is followed by a transmembrane domain leading to a short cytosolic region.

The domains in the extracellular region of ADAM17 are responsible for the shedding activity of ADAM17 are regulated by

a. β1-integrin binding and/ or interaction with tissue inhibitor of metalloproteinases-3 (TIMP3),
b. The conformation (disulphide isomerisation) of the membrane-proximal domain, which facilitates phosphatidylserine (PS) binding,
c. the availability of CANDIS for substrate binding.

Since ADAM17 can exert both positive and negative effects via its shedding activity, its role as a sheddase is tightly regulated at multiple levels by structural, conformational, phosphorylation of the cytosolic residues in ADAM17 and its substrates or inhibitors. Furthermore, processes and adaptor proteins that enable its forward trafficking, maturation, degradation and recycling are also under tight regulation.

1.9.1.1 The extracellular domains of ADAM17

The prodomain

The prodomain keeps the ADAM17 in an inactive state during the transport from the endoplasmic reticulum to the Golgi apparatus occurs. The catalytic activity is shut off by the ligation of a zinc ion to the cysteine containing motif (PKVCGY). The prodomain is cleaved off in the Golgi apparatus by Golgi resident calcium dependent serine endoprotease, furin (Grötzinger et al. 2017). The fate of cleaved prodomain is still unclear however recombinant soluble prodomain with various amino acid residues exchanges to stabilize the prodomain has been shown to inhibit the shedding by ADAM17 efficiently (Wong et al. 2016). The prodomain also functions as a chaperone for correct folding of ADAM17 in addition to maintaining the inactive state during transport.

Catalytic domain

ADAM17 belongs to the family of metallopeptidases. The catalytic domain is 215–473 aa with the canonical histidine rich HEXXHXXGXXH zinc binding motif (X being any amino acid residue) typical of metzincins. The catalytic center consists of zinc-binding site and a met-turn, tight 1,4-β-turn, in the tertiary structure positioned directly under the zinc-binding site. Valine is the most preferred amino acid in the cleavage site of the substrates for ADAM17 (Tucher et al. 2014).

The prodomain of ADAM17 and tissue inhibitor of metalloproteinases (TIMP-3) are the natural inhibitors of ADAM17. Loss of TIMP3 leads to increased IL-6R shedding causing microbiota-driven gut dysbiosis (Mavilio et al. 2016). TIMP-3 is thus a significant in vivo regulator of ADAM17 shedding activity.

The disintegrin domain

The disintegrin domain in ADAM proteases is homologous to the disintegrin domain in snake venom (Lu et al. 2010). This domain has specificity for the integrin interactions and functions as its antagonist. Each ADAM has a binding selectivity for the integrin interactions. ADAM17 interacts with $\alpha_5\beta_1$. The interaction between the integrin and ADAM17 leads to steric hindrance thus inhibiting the shedding activity by making the catalytic site inaccessible (Bax et al. 2004). Integrin and ADAM17 complexes occur in the storage areas of perinuclear space before transport of ADAM17 to the cell surface upon activation of integrin molecules (Gooz et al. 2012). Disintegrin domain provides stiffness to the C- shaped structure of ADAM17 and integrin interactions with it regulate the shedding activity of ADAM17.

The membrane proximal domain (MPD)

Both ADAM10 and ADAM17 unlike other ADAMs contain a membrane proximal domain (MPD) that is required for substrate binding and is crucial for regulation of ectodomain shedding activity (Zunke and Rose-John 2017). The human MPD exists in two conformations: flexible open and rigid closed. The two conformations exist due to differences in two disulfide bonds. Protein disulfide isomerase acts a negative regulator of ADAM17 shedding activity by acting on two MPD isomers changing the open

configuration to closed one (Düsterhöft et al. 2013). MPD is crucial in substrate recognition and shedding mechanism and (le Gall et al. 2010) showed that cytoplasmic tail is not required for the shedding activity. In the absence of cytoplasmic tail, another mechanism of relaying activation signals to the intracellular region occurs through the transfer of negatively charged phosphatidyl serine (PS) to the cell surface. The translocated PS act as negatively charged hubs for cations or positive charged residues. The positively charged residues in MPD interact with hubs on cell membrane leading to shedding process. Notably, the phosphatidylserine binding sequence in the MPD is in the flexible part of the domain which becomes rigid after PDI-mediated isomerization. The open conformation of MPD and not the closed conformation can bind the phosphatidyl serine (Sommer et al. 2016) that also allows for the neighboring conserved motif to bind substrates.

CANDIS (Conserved Adam seventeeN Dynamic Interaction Sequence)

The stalk region of ADAM17 is unique as it comprises of a conserved motif directly succeeding the MPD (Düsterhöft et al. 2014) that acts as a molecular switch of ADAM17 activity operated by protein disulfide isomerase on MPD. CANDIS forms an amphipathic helix and anchors the protease to the membrane but possesses low affinity for cholesterol. The activation of scramblases by ADAM17 stimuli through activated PKCs disturbs the membrane composition with an increase in the negatively charged phosphatidyl serine residues on the outer leaflet of the membrane. This resulting lower content of cholesterol and higher content of phosphatidylserine in the outer leaflet allows for CANDIS binding to the membrane. Consistently, depletion of cholesterol from the membrane leads to activation of ADAM17 mediated shedding process. It is proposed that binding of MPD and CANDIS to phosphatidylserine causes conformational change in the extracellular region of ADAM17 thereby positioning the catalytic domain with active site near the membrane. Additionally, CANDIS is essential for substrate recognition. CANDIS interacts with type I transmembrane substrates such as IL-6R and IL-1RII whereas its interaction with type II transmembrane substrates like TNFα is not efficient.

Dimeric or monomeric state of ADAM17 also regulates its shedding response (Lorenzen et al. 2011). The dimerized form of ADAM17 is inactive with no shedding activity as it

facilitates interaction with TIMP3. The regulation of dimerized state to monomeric state appears to be controlled by phosphorylation of cytoplasmic tail by MAPK such as p38 (Xu et al. 2012) The phosphorylation of Y735 leads to monomeric state of ADAM17 that cannot interact with TIMP3 and increase in cell surface expression of ADAM17. The removal of TIMP3 lifts the brakes on shedding function of ADAM17. Phosphorylation of the cytoplasmic tail also leads to increased cell surface expression of ADAM17 (Xu and Derynck 2010). Additionally, phosphorylation of S794 and T735 of murine ADAM17 increased the activity of ADAM17 (Diaz-Rodriguez 2002) (**Figure 1.4).**

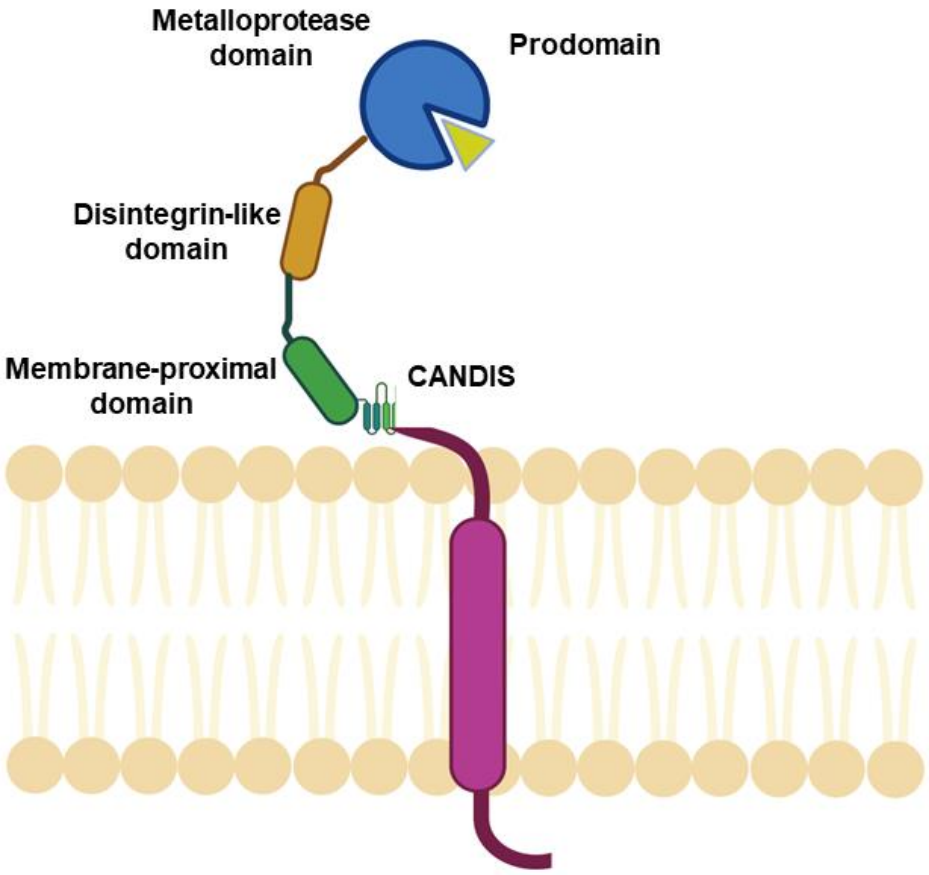

Figure 1.4. Structure of ADAM17. ADAM17 is a multi-domain protein with a large extracellular region with a prodomain, a metalloenzyme or catalytic domain, a disintegrin domain and a membrane-proximal domain (MPD), as well as a short juxtamembrane segment called Conserved Adam seventeeN Dynamic Interaction Sequence (CANDIS). This is followed by a transmembrane domain leading to a short cytosolic region that recruits adaptor proteins. Figure created using Biorender.com

1.9.2 Regulation of ADAM17 activity by substrate level selectivity

The activity of ADAM17 is also regulated at the level of substrate selectivity. For instance, CD9 is tetraspanin protein that protects SorLA (Sorting protein-related receptor containing LDLR class A repeats) from shedding by ADAM17 (Tsukamoto et al. 2014). Interestingly, CD9 was also demonstrated to bind ADAM17 and prevent it from shedding TNFα and ICAM1 (Gutiérrez-López et al. 2011). Recently, secreted frizzled related protein 3 was shown to bind ADAM17 and negatively regulate IL6R shedding (Oldefest et al. 2015)

1.9.3 Regulation of ADAM17 levels on the cell surface

The cell surface levels of mature ADAM17 are maintained at low levels to regulate the shedding activity of ADAM17. However, considerable levels of mature ADAM17 exist as intracellular pool. In addition, surface ADAM17 also undergoes clathrin-dependent internalization and PACS2 (phosphofurin acidic cluster sorting protein 2) -dependent recycling also occur. In the absence of PACS2, ADAM17 undergoes lysosomal degradation (Dombernowsky et al. 2015). Furthermore, phosphorylated paxillin can also shuttle ADAM17 to extracellular vesicles (Lee and Young 2013). Upon treatment with the phorbol ester PMA, surface levels of mature ADAM17 increase significantly within minutes with a gradual decline by internalization followed by lysosomal degradation. PMA mediated dysregulation thus leads to increased shedding activity of ADAM17. Additionally, ADAM17 released in extracellular vesicles is active and maintains the shedding response. HIV-protein Nef also shuttles ADAM17 in extracellular vesicles (Lee and Young 2013; Arenaccio et al. 2014; Lee et al. 2016). Furthermore, annexins affect the ADAM17 surface levels in different ways with annexin A2 decreasing the shedding activity whereas annexins A8 and A9 increasing the shedding activity (Nishiyama et al. 2012). Due to the role of annexins in exocytosis and endocytic functions within the cell, annexins are proposed to affect ADAM17 turnover rather than shedding activity. It is well established that only mature ADAM17 reaches the bilayer therefore the immature ADAM17 undergoes forward trafficking as it exits the ER to Golgi apparatus where it also matures. During this process, adaptor proteins iRhoms play a significant role.

1.9.4 Regulation of ADAM17 by iRhoms

In addition to the structurally regulated features of ADAM17 exerted via ectodomain regulation, forward trafficking of ADAM17 from the ER to Golgi and maturation of the

functional protease is also under regulation by iRhoms. iRhoms are pseudoproteases, belonging to the superfamily of rhomboid proteases (Urban et al. 2001; Lemberg and Freeman 2007).

Two iRhom proteins exist in vertebrates, namely iRhom1 (RHBDF1) and iRhom2 (RHBDF2). While iRhom1 is ubiquitously present, iRhom2 is expressed in immune cells. iRhom2 requires a structurally intact iRhom homology domain (IRHD) for ADAM17 binding and a complete iCERES (motif iCERES (iRhom Conserved ER to Golgi Export Sequence)) (Lee et al. 2016) within the IRHD for ER to Golgi transport. iRhoms represent a crucial ER-exit and forward trafficking receptor for ADAM17 (Lee et al. 2016). iRhoms are also crucial for maintaining the surface expression of ADAM17 by stabilizing it. Additionally, iRhom2 could play a separate role in substrate selectivity. Maretzky et al. (2013) demonstrated that no ADAM17-mediated shedding of HB-EGF or AREG could occur in mice deficient in iRhom2 whereas ADAM17- mediated shedding of TGFα and L-selectin was unaltered (Maretzky et al. 2013).

1.9.5 Functions of ADAM17

Ectodomain Shedding by Proteolytic Cleavage: With over 80 known substrates, ADAM17 can act upon diverse categories of these membrane bound substrates. The proteolytic cleavage of substrates by ADAM17 can lead to signal transduction events that may either lead to stimulation or dampening of response depending upon the target. The functional consequences of these can be cell proliferation, apoptosis, soluble cytokine release and lymphocyte migration. The cleaved proteins can exert their effect via autocrine, juxtacrine or paracrine mechanisms in the affected tissue or sometimes to distant organs (Reed and Ager 2022). For example, ADAM17 can cause the shedding of the soluble form of proinflammatory cytokine TNF-α that augments the initial inflammatory response through TNFR1 and TNFR2. However, since TNFR1 and TNFR2 are also ADAM17 substrates, shedding of these receptors instead negatively regulates the initial enhancement of the inflammatory response (Black et al. 1997; Bell et al. 2007). Similarly, ADAM17 can indirectly activate Epidermal Growth Factor Receptor (HB-EGFR) by cleaving HB-EGF that binds to EGFR to initiate cell proliferation (Gooz et al 2006). However, the receptor cleavage itself can prevent the ligand initiated signaling and hence inhibit the proliferation.

Interestingly, depending upon the pathway activated by EGFR, either proliferation or apoptosis could ensue.

Regulated Intramembrane Proteolysis (RIP): Receptor activation in many cellular processes can also lead to downstream regulated intramembrane proteolysis. For example, Notch signaling is crucial to early lymphocytic commitment. Notch 1 ligand-delta 1 binding to Notch 1 causes the ectodomain cleavage of Notch 1 by ADAM17. This leads to RIPing by γ-secretase presenilin resulting in translocation to the nucleus followed by the transcription of Notch 1 target genes. This further commits early progenitors to T-cell lineage rather than B-cells (Maillard et al. 2005; Tan et al. 2005).

Immune Cell Regulation by Clonal Expansion: CD3 mediated activation of the T-cell receptor can lead to induction of ADAM17 proteolysis of Lymphocyte activation gene 3 (LAG3) via PKCθ pathway. The release of soluble LAG3 gene product caused clonal expansion (Li et al. 2007). Furthermore, Mohammed et al (2019) studied the impact of L-selectin proteolysis by ADAM17 on T-cell activation in virus-infected mice. The authors showed that following virus infection of mice, L-selectin proteolysis promoted early clonal expansion of cytotoxic T-cells resulting in an 8-fold increase over T-cells with cleavage resistant L-selectin. This was associated with delayed proliferative responses in cleavage resistant T-cells in and lower CD25 expression.

1.9.6 ADAM17 mediated regulation of L-selectin

The metalloproteinase domain of ADAM17 cleaves L-selectin in the 15 aa membrane proximal extracellular region (Ager 2012). This activity regulates leukocyte adhesion and migration in activated leukocytes. Consistent with this, blocking of ADAM/MMP activity by synthetic or natural inhibitors can lead to arrest of lymphocyte migration across HEVs (Faveeuw et al. 2001). However, the ectodomain shedding of soluble form of L-selectin is also shown to contribute to non-homing related effects. TCR crosslinking is demonstrated to lead to ADAM17 mediated proteolytic cleavage of L-selectin via PKC signaling through PI3Kδ pathway (Chao et al. 1997; Sinclair et al. 2008). Studies on shedding resistant forms of L-selectin have showed the inability of antigen primed CD8+ T-cells to clonally expand in mice infected with vaccinia virus (Mohammed et al. 2019). However, the homing of these cells was still maintained. Activated neutrophils have been reported to shed L-selectin due to ADAM8 activity instead of ADAM17 (Gómez-Gaviro et al. 2007). Shedding of L-selectin in neutrophils is linked to phagocytosis of bacteria (Cappenberg et al. 2019).

1.9.7 Clinical significance of ADAM17 mediated L-selectin shedding

From a clinical perspective, the soluble circulating form of L-selectin (released as a consequence of ectodomain shedding) is sometimes used as a surrogate plasma/serum biomarker for leukocyte activity triggered during acute or chronic inflammation (JEAN-PAUL et al. 1999; Font et al. 2000; Jeff D. Fischer et al. 2000). Patients with rheumatic disease presented an increased prevalence of the splice variant transcript (human splice variant which lacks exon 7 encoding the transmembrane domain) which is thought to contribute to the increase in soluble L-selectin (Hirata et al. 2015).

Clinical application of the knowledge collected about L-selectin has not met with success. The use of CTLD blocking agents that target selectins non-specifically has not shown any efficacy in clinical trials (Raffler et al. 2005) indicating a requirement for L-selectin specific inhibitors in prevention of autoimmune diseases. Determining whether L-selectin undergoes regulated intramembrane proteolysis following activated TCR mediated ADAM17 shedding will be important to fully understand the role L-selectin in T-cell activation. The modulation of L-selectin shedding using small molecule inhibitors against tissue specific ADAM metalloproteinases that prevent shedding needs to be

studied. Consistently, while ADAM17 mediated TNF-a proteolytic cleavage can initiate inflammation, it was shown in a murine model of influenza infection that its inhibition led to reduction in CXCL2 expression causing reduction in the severity of lung inflammation with better survival outcome (DeBerge et al. 2013). Therefore, preventing lymphocyte migration through ADAM17 inhibition through either ADAM17 specific or tissue specific iRhom-2 inhibitors could have important implications to health and disease of humans.

Further, determining whether L-selectin undergoes regulated intramembrane proteolysis by γ-secretase/presenilins and, if it does, the fate of the release cyto tail following activated TCR mediated ADAM17 shedding will be important to fully understand the signalling role L-selectin during T-cell activation. This could enable the design of strategies targeting TCR specific ADAM17 responses that depend on proteolysis of L-selectin.

ADAM17 plays a crucial role in the development and progression of various diseases, including cancer, arthritis, and respiratory diseases. Targeting ADAM17 may have therapeutic potential in the management of these diseases, as it could potentially prevent the development of cancer or stop the progression of other diseases. ADAM17 may be a useful diagnostic marker for certain diseases, as its expression levels have been shown to correlate with disease severity. Overall, the potential clinical implications of targeting ADAM17 in the management of multiple diseases, both as a therapeutic target and a diagnostic marker. However, further research is needed to fully understand the role of ADAM17 in these diseases and to develop effective therapies targeting this metalloproteinase enzyme (Arribas & Esselens 2009).

1.10 Hypothesis and aims of the thesis

The following hypothesis was proposed to complete the work in this thesis and are summarized in Figure 1.5:

1) In an *in-vitro* model of T-cell activation using Molt3 cells transduced with a TCR which recognizes the SLY peptide, L-selectin is re-expressed and maintained on CD8+ T-cells the expression levels of L-selectin are regulated by ADAM17.
2) L-selectin and ADAM17 form a complex following TCR engagement with SLY peptide, which leads to L-selectin shedding.
3) The L-selectin membrane fragment generated following peptide-MHC induced ADAM17 activation is retained following inhibition of γ-secretase and the proteasome.

To test these hypotheses the following aims where achieved:

- Flow cytometric staining methods were optimized to create an *in vitro* model of B-cell based peptide-MHC presentation to T-cells expressing a peptide-specific TCR to study L-selectin expression.
- Peptide concentrations required to stimulate TCR-induced shedding of L-selectin were optimized.
- Correlated the ADAM17 activation status by immunoblotting to detect L-selectin and ADAM17 fragments
- Dissected the mechanisms that regulate cyclical expression of L-selectin in cytotoxic T lymphocytes following TCR engagement.
- Validated methods to pulldown L-selectin-V5-his-tagged using cobalt coated beads.

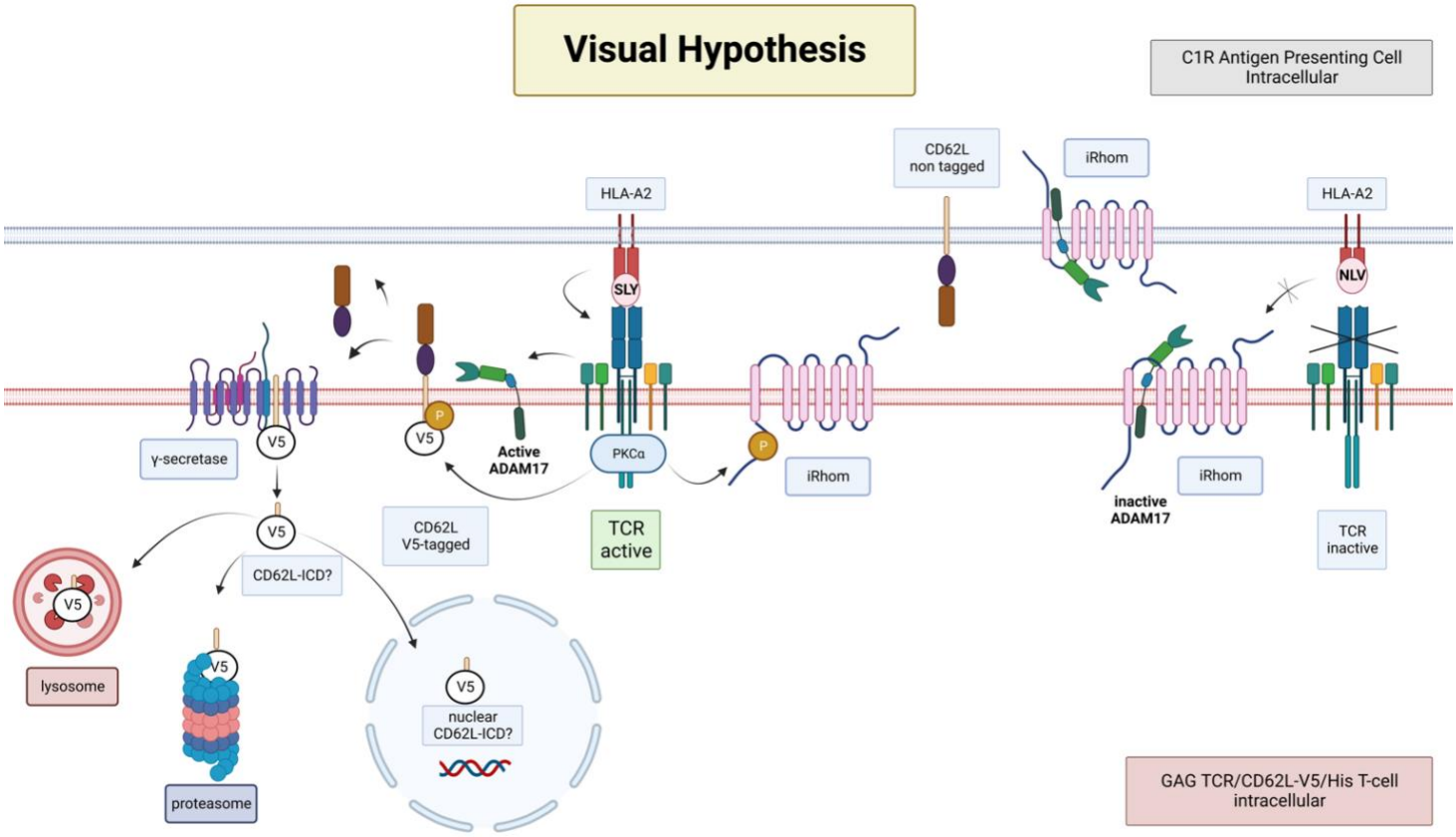

Figure 1.5. Visual Hypothesis of L-selectin shedding and internalization following peptide activation. ADAM17 and iRhom interactions bring ADAM17 to the unactivated T-cell surface. Following TCR engagement, cell surface L-selectin is cleaved by ADAM17 to generate soluble L-selectin and L-selectin MRF. MRF RIPing by γ-secretase leads to released L-selectin cytotail which goes to nucleus as well as being degraded by being targeted to lysosomes or the proteasome. Figure created using Biorender.com

2 Materials and Methods

2.1 Tissue Culture

All the ingredients for the cell culture medium were from Thermo Fisher Scientific, with the exception of the fetal calf serum, which was from Gibco. The composition of the cell culture medium is described in Table 2.3. The cells were grown at 37 °C with 5% CO2 in a humidified incubator.

2.1.1 Cell Lines

The HEK293T cells (Knock down ADAM17 and parental) kindly gifted cell line from Michael Tomlinson, University of Birmingham, Molt-3 T-cells (ATCC; CRL-1552; Molt-3) expressing the 868TCR, and C1R B-cell lymphoblastoid line were kindly provided by John Bridgeman. The 868TCR recognizes the HIV gag-specific peptide (SLYNTVATL) and has been characterized elsewhere (Varela-Rohena et al. 2008). The 868 TCR positive Molt-3 T-cells were transduced by Professor John Bridgeman, University of Liverpool, to express the HIV-gag 868TCR and were kindly gifted to the Ager lab as part of a collaboration. These cells will be referred to as Molt-3 T-cells in the thesis and were also transduced by Dr Andrew Newman, Cardiff University, with human L-selectin (Newman 2017). Nunc cell culture dishes, plates, and flasks were purchased from Thermo Fisher Scientific. Cells were counted using a LUNA-FLTM Dual Fluorescence Cell Counter with either 1:1 Trypan Blue or 1:10 AO/PI Cell viability reagent (Logos Biosystems; Thermo Fisher Scientific). The cell culture media are detailed in Table 2.3.

2.1.2 Cell Thawing

The cells were taken from liquid nitrogen storage and placed on dry ice for transport. The cryovials were then placed in a 37°C water bath for rapid thawing. After thawing, 1 mL of the cell solution was added to 20 mL of pre-warmed D10 or R10 medium (Table 2.3) and centrifuged at 500 g for 5 minutes. The supernatant was removed, the cells were resuspended in pre-warmed D10 or R10 medium (Table 2.3) and placed into T25 or T75 flasks for culturing.

2.1.3 Adherent Cell Passaging

All cell culturing was conducted in a sterile environment in a class II laminar flow cabinet. After the cells reached 80-100% confluency, the media was removed from the flask and washed with phosphate-buffered saline (PBS) to remove any remaining media. 10% Trypsin supplemented with 0.25% EDTA (Gibco) was added to the cells and incubated at 37°C in 5% CO2 in air for several minutes until the cells detached from the flask. Pre-warmed D10 media (table 2.3) was added to the flask to neutralize the trypsin-EDTA, and the cells were removed and placed into a 50 mL falcon tube. The cells were centrifuged at 500 g for 5 minutes at 37°C. The supernatant was discarded, and the cells were resuspended in pre-warmed D10 (Table 2.3) media diluted 1:10 every two days and placed into a fresh flask for further culturing.

2.1.4 Suspension Cells Passaging

Molt-3 T-cells and derived cell lines were seeded at 3 $x10^6$ cells per T75 flask, cultured in R10 (Table 2.3) and diluted 1:10 every two days. The cells were seeded in 2 mL complete T-cell medium (1 $x10^6$ cells) per well in a 12-well dish and the medium was changed every two days upon confluency by replacing the top 1 mL without disturbing the suspended cells at the bottom of the well.

2.1.5 Cell Cryopreservation

For long-term storage, confluent cells (80 % confluency) were frozen in a 1 mL solution of 10% (v/v) dimethyl sulfoxide (DMSO)/foetal calf serum (FCS) freezing medium (table 2.3). at a concentration of $3x10^6$ cells/mL. Cells were placed into a labelled cryovial and placed into a 'Mr Frosty freezing container (ThermoFisher) for -80^oC storage at a freezing rate of -1^oC per minute. 1 day later cells were transferred to liquid nitrogen (LN_2) Dewar.

2.2 Cell Activation and Treatments

2.2.1 T-Cell Receptor Activation

The SLYNTVATL (SLY) peptide used to activate T-cells expressing the 868 gag TCR was purchased from Peptide Synthetics, reconstituted to 5 mM in DMSO and stored at -80°C. The NLVPMVATV (NLV) peptide used as a negative control was purchased from Peptide Synthetics and kindly provided by Edward Wang, Cardiff University. L-selectin shedding in response to cognate peptide stimulation were studied using SLYNTVATL peptide to activate gag TCR expressing cells and NLVPMVATV control peptide. Molt-3 T-cells and HLA-A2^{+} C1R peptide-MHC were rested for 1h in R2 medium (Table 2.3) at 1 x 10^{6} cells/ml. Then C1R cells were resuspended to 1 x 10^{6} cells/ml in R2 medium, in the presence or absence of SLY (10^{-4} M to 10^{-7} M) or NLV peptide (10^{-5} M) and 100 µl of the cells added into wells of a 96 well U-bottom plate. All peptide concentrations were set up in triplicates and cells were incubated for 1 h at 37°C before being washed once in R2 medium (Table 2.3). Molt-3 cells were added in 100 µl at 1.5 x 10^{6} cells/ml in R2 medium, giving a final 3:1 ratio of T: peptide-MHC ratio. The cells were incubated for 1 h at 37°C, washed and stained with Abs for flow cytometry, lysed for western blot, or stored supernatant for ELISA.

2.2.2 Inhibition of ADAM17 Treatments

To study the effect of shedding inhibitors, Molt-3 T-cells were preincubated with D1(A12) ADAM17 antibody was obtained from Professor Gillian Murphy (Cambridge University) and used at a concentration of 100 nM, proteasome inhibitor MG132 (Sigma-Aldrich; Pinazza et al. 2018) was used at 10 µM, γ-secretase inhibitor L-685 (Sigma Aldrich) was used at 10 µM, hydroxamate-based ADAM17/ADAM10 metalloproteinase inhibitor GW280264X, or DMSO for 60 min. Then the Molt-3 T-cells suspension in the R2 medium (Table 2.3) containing the inhibitors were added to peptide-pulsed, washed C1R cells pellet. Cells were then stimulated in the presence of the inhibitors or DMSO control.

2.3 Flow Cytometry

2.3.1 Extracellular Cell Staining

$1x10^6$ cells were dispensed into individual wells of a 96-well plate. Supernatant was removed by rapid inversion following a 5-minute centrifugation (260g, 5min at 4^0C). Cells were washed with PBS and then incubated at room temperature for 30 minutes in 50 µL fixable Live/Dead aqua stain in accordance with manufacturer's instructions (Thermo Fisher). The cells were again centrifuged, and the supernatant removed before suspending the cells in 50 µl FACS buffer (2% FCS in PBS). The cells were then incubated at 4 ^{o}C to prevent cross-linking and internalisation for 30 minutes in prepared antibody solution. The antibody labelled cells were fixed in 4% formaldehyde in PBS (prepared diluting 40% formaldehyde 1/10) at room temperature for 15 minutes. The cells were suspended in FACS buffer, and the plate stored at 4-8^0C in the dark before analysis. Table 2.1 contains details for the reagent dilutions used in this analysis. To ensure robust control of the assay and set compensation parameters an AbC (antibody control), ArC (amine reactive control) and negative control beads were included in the analysis as directed by the package insert (Invitrogen).

2.3.2 Controls and compensation

For flow cytometry, UltraComp eBeads (Invitrogen; 01-2222-41) were stained individually with antibodies and for Live/Dead Aqua compensation, a V500- conjugated antibody (BD; 561391) was used as the Live/Dead stain cannot bind eBeads. Either isotype controls or fluorescence minus one (FMO) stain were used as controls and this is shown in the gating strategy of each experiment.

2.3.3 Antibodies Used in Flow Cytometric Staining (Table 2.1)

Cells were stained in a 96-well plate with a volume of 50 µL. The working concentrations of the antibody were diluted in 2% (v/v) FCS/PBS (FACS buffer). The cells were incubated with the antibody for 30 minutes at 4 degrees Celsius in the dark.

Antibody Target Antigen	Host species	Clone or RRID	Fluorophore conjugate	Stock concentration	Working concentration (Dilution)	Manufacturer and product catalogue (#)
Anti-human L-selectin Ectodomain	Mouse	DREG-56	PE	0.125 mg/mL	1:10	Invitrogen Catalog number# 12-0629-42
Anti-human CD19	Mouse	SJ25-C1	APC	0.05 mg/mL	1:10	Invitrogen Catalog number# MHCD1905
Anti-human CD19	Mouse	SJ25-C1	FITC	0.05 mg/mL	1:10	Invitrogen Catalog number# MHCD1901-4
Anti-human L-selectin Ectodomain	Mouse	DREG-56	FITC	0.2 mg/mL	1:10	Invitrogen Catalog number# 11-0629-42
Anti-human ADAM17	Mouse	MM0561-8C13	PE	0.38 mg/mL	1:5	Novusbio Catalog number# NBP2-12018PE
isotype control	Mouse IgG1, k	P3.6.2.8.1	PE	0.125 mg/mL	1:10	Invitrogen Catalog number# 12-4714-82
isotype control	Mouse IgG1, k	P3.6.2.1	APC	0.05 mg/mL	1:10	Invitrogen Catalog number# 17-4714-42
isotype control	Mouse IgG1, k	P3.6.2.8.1	FITC	0.05 mg/mL	1:10	Invitrogen Catalog number# 11-4714-81
isotype control	Mouse	11711	PE	0.05 mg/mL	1:5	R&D Catalog number# IC002P
Live/Dead aqua	DMSO	N/A	Aqua	200 assays	1:50	Invitrogen Catalog number# L34957
Unsuccessful Stained Antibody						
Anti-human ADAM17	Mouse	111633	Alexa Fluor® 647	100 ug	1:5	R&D Catalog number# FAB9301R-100UG
Anti-human ADAM17	Mouse	111633	PE	100 ug	1:5	R&D Catalog number# FAB9301R-100UG
Anti-human ADAM17	Mouse	111633	Alexa Fluor® 488	100 ug	1:5	R&D Catalog number# FAB9301R-100UG

Table 2.1 Antibodies and cell stains used for flow cytometry used in this thesis.

2.4 Soluble L-selectin analysis via ELISA (Sandwich ELISA)

An enzyme-linked immunosorbent assay (ELISA) was performed on soluble human L-selectin using Duoset ELISA kits and ancillary reagent kits from R&D Systems. The ELISA involved coating 96-well microplates with capture antibodies, washing the plates and adding cell culture supernatant. Detection antibodies were then added, and the plates were washed, followed by the addition of streptavidin-HRP. The plates were washed again, and substrate solution was added, followed by the addition of stop solution. The absorbance of the plates was then measured at 450 nm wavelength using a CLARIOstar Plus Microplate Reader.

2.5 Pulldown of L-selectin

Pelleted 6 x 10^6 Molt-3 tagged T-cells on GAG TCR/CD62L-V5-His lysed in 140 µL cell lysis buffer for 35 min on ice. After lysis, 80 µl of lysate was stored in -80 °C until further analysis. The remaining lysate was diluted in 700 µL of 1X binding/wash buffer and added to 50 µL His tag isolation and pulldown dynabeads (Thermo Fisher) and incubated on a roller for 10 min at 4 °C. Dynabeads were magnetically collected using a DynaMag-5 magnet (Thermo Fisher) and washed 4X in binding/wash buffer (100 mM sodium phosphate (pH 8.0), 600 mM sodium chloride, 0.02 % Tween 20 (v/v)). His-tagged L-selectin (Table 2.4) was released from dynabeads by incubation in 100 µL His-elution buffer at room temperature for 10 min. Dynabeads were magnetically pelleted and the collected sample was stored at -80 °C until further analysis.

2.6 Protein Analysis by Western Blotting

2.6.1 Western Blotting for Chapter 3 and Chapter 4

1 x10^6 Molt-3 T-cells and 3.33 x10^5 peptide-MHC (C1R cells) pulsed with control peptide (NLV) or activation peptide (SLY) were added per well of a 96-well plate and following experimentation I used a series of methods to lyse cells, extract proteins, and determine the protein concentrations in the samples. The cells were grown in 96-well plates. Cells were lysed with commercially purchased RIPA lysis buffer (Table 2.5) containing protease inhibitors (Table 2.5). Lysis buffer was prepared by 1 protease inhibitor tablet per 10 mL of RIPA buffer. The lysates were incubated on ice and then centrifuged to separate the soluble proteins from the cell debris. The protein concentrations were determined using a Bicinchoninic Assay Kit and a standard curve made from BSA solutions. The samples were pipetted in duplicates into a 96-well plate and a dilution of reagent A and reagent B from the assay kit was added to each well. This was used to measure the protein concentrations accurately and precisely in the samples. After the samples were prepared in the 96-well plate, the plate was incubated for 30 minutes at 37°C. This step allows the biuret reaction, which is used to measure protein concentration, to proceed and produce a measurable signal. After incubation, the absorbance of the samples was measured at 570 nm using a microplate reader. The absorbance is a measure of the amount of light absorbed by the sample, which is directly proportional to the concentration of protein in the sample. The protein concentrations in the samples were then calculated by performing linear regression on the standard curve. Linear regression is a statistical method for finding the line of best fit through a set of data points. By fitting a line to the standard curve, the protein concentrations of the samples can be determined by interpolation. This allows to measure the protein concentrations accurately and precisely in the samples. Protein quantification was performed as discussed in 2.6.4.

2.6.2 Glycine SDS-PAGE

In this experiment, I used Sodium dodecyl sulphate polyacrylamide-gel electrophoresis (SDS-PAGE) to separate proteins based on their size and charge. SDS-PAGE is a common technique used to resolve proteins in a mixture based on their molecular weights. In SDS-PAGE, proteins are first denatured and then subjected to an electric field in a gel matrix. The proteins migrate through the gel based on their size, shape, and charge, resulting in the separation of the proteins into distinct bands. I used 4-20% pre-cast gradient gels from Bio-Rad for the SDS-PAGE experiments. Each well of the gel was loaded with 20 µg of protein lysate. The samples were diluted in 2x SDS loading buffer, which contains the detergent sodium dodecyl sulphate (SDS) and other chemicals that help to denature and solubilize the proteins. The samples were run alongside a pre-stained protein ladder for 60-80 minutes at 120 V. After the proteins were separated in the gel, they were transferred onto a Polyvinylidene-difluoride (PVDF) membrane at 75 Volts for 2h. The PVDF membrane is a type of membrane with a high affinity for proteins, which allows the proteins to be efficiently transferred and immobilized on the membrane. The membrane was then blocked with 5% non-fat milk in Tris-buffer saline-Tween (TBS-T) to reduce non-specific binding and background noise. To detect specific proteins, I incubated the membrane with primary antibodies that specifically bind to the proteins of interest. The primary antibodies were incubated with the membrane overnight at 4˚C to allow for efficient binding. The membrane was then washed and incubated with secondary antibodies (Table 2.2) that specifically bind to the primary antibodies. The secondary antibodies were incubated with the membrane for 1 hour at room temperature. To visualize the bound antibodies and detect the proteins of interest, I used an enhanced chemiluminescence kit (ECL) and exposed the membrane to ECL films. The ECL reaction produces light, which is captured on the film, producing an image of the proteins on the membrane. I also used the iBright 1500 Developer from Invitrogen to develop the blots. PVDF membranes were stripped according to manufacturer's protocol (Thermo Fisher Scientific, 21059; 15 min, 37 ^{o}C) before washing 5x in PBS-T (5 min, RT, rocking), blocking with 5 % PBS-T and re-probing for ADAM17. The re-probing followed the same protocol as blotting for anti-V5 antibody but used the anti-ADAM17 antibody (Table 2.2) (60 min, RT, rocking) primary antibody. For long-term storage, PVDF membranes were

sealed in bags with PBS-T (4 ^{o}C). Protein quantification was performed as discussed in 2.6.4.

2.6.3 Western Blotting for Chapter 5

Cells were then lysed as described in 2.6.1. Lysates were boiled (at 100 ^{o}C, for 10 min) to reduce viscosity prior to the addition of a half-volume of 4 % reducing buffer (3.5 mL dH_2O, 1.25 mL of 0.5 M Tris-HCl at pH 6.8, 2.5 mL glycerol, 4 mL of 10 % SDS, 0.2 mL of 0.5 % bromophenol blue) with β-mercaptoethanol (add 50 µL of β-mercaptoethanol to 950 µL of reducing buffer prior to use) and centrifuged (30 min, 10,062 g) on a benchtop centrifuge. Lysates were then run (35 min, 200 V) using the X-cell module (Invitrogen; EI0002) alongside a SeeBlue pre-labelled protein ladder (Invitrogen; LC5625) using MES-SDS running buffer (Thermo Fisher Scientific; NP0002). Proteins were transferred to a PVDF transfer membrane (methanol, 30s, RT) with a pore size of 0.2 µm (Thermo Fisher Scientific; 88520) and captured using the X-cell module (60 min, 30 V). The PVDF membrane was then kept in PBS-T (1 mL Tween-20 in 999 mL PBS) at 4 ^{o}C and blocked with 5% PBS-T containing milk powder before being stained for anti-V5 antibody (overnight, rocking, 4 ^{o}C) (Table 2.2). The PVDF membrane was then washed and treated with a HRP-conjugated secondary antibody before being developed using a chemiluminescent substrate and imaged using a Syngene G:Box. The PVDF membrane was then stripped and re-probed for GAPDH using the same protocol as the L-selectin staining, with an anti-GAPDH primary antibody. After imaging, the PVDF membranes were sealed in bags with PBS-T and stored at 4 ^{o}C. The following day, the PVDF membrane was washed 5x in PBS-T (5 min, RT, rocking) before addition of the secondary antibody (Table 2.2) (60 min, RT, rocking). The PVDF membrane was washed 5x in PBS-T (5 min, RT, rocking). Then I also used the iBright 1500 Developer from Invitrogen to develop the blots. Following imaging, PVDF membranes were stripped according to manufacturer's protocol (Thermo Fisher Scientific, 21059; 15 min, 37 ^{o}C) before washing 5x in PBS-T (5 min, RT, rocking), blocking with 5 % PBS-T and re-probing for GAPDH. The re-probing followed the same protocol as blotting for anti-V5 antibody but used the anti-GAPDH (Table 2.2) (60 min, RT, rocking) primary antibody. For long-term storage, PVDF membranes were sealed in bags with PBS-T (4 ^{o}C). Protein quantification was performed as discussed in 2.6.4.

Antibodies used in Western Blotting:

Specificity	**Origin**	**Concentration**
Mouse anti-V5 tag	Thermo Fisher Scientific Catalog number# R960-25	1:2000
Rabbit anti-ADAM17	Abcam Catalog number# ab39162	1:2000
Rabbit anti-GAPDH	Abcam Catalog number ab128915	1:2000
Secondary Antibodies		
Specificity	**Origin**	**Concentration**
Rabbit anti-mouse	Jackson ImmunoResearch	1:5000
Rabbit anti-goat	Jackson ImmunoResearch	1:5000
Donkey anti-Rabbit	Jackson ImmunoResearch	1:5000

Table 2.2 The Antibodies used in Western Blotting in this thesis

2.6.4 Densitometry

iBright Analysis Software from Invitrogen to quantify the band intensities. The iBright Analysis Software is a software program that allows users to analyze and process images of protein blots. I captured images of the exposed membranes using the iBright developer and stored the images in G2i file formats. The images were then loaded into the iBright analysis software for analysis. The software allows users to mark the bands of interest on the images using a rectangular selection tool from the Analyze section. The software also has an automatic band detection mode, which allows the software to automatically detect and quantify the band intensities within the plot lanes. The band intensities were quantified using a local background correction, which subtracts the background noise from the signal to improve the accuracy of the measurements. Protein quantification is illustrated in (Figure 2.1). The band intensities were then compared to the housekeeping protein controls, which are used as references to normalize the data. The analysis was performed on at least 3 independent blots to improve the reliability and reproducibility of the results (Figure 2.1).

A.

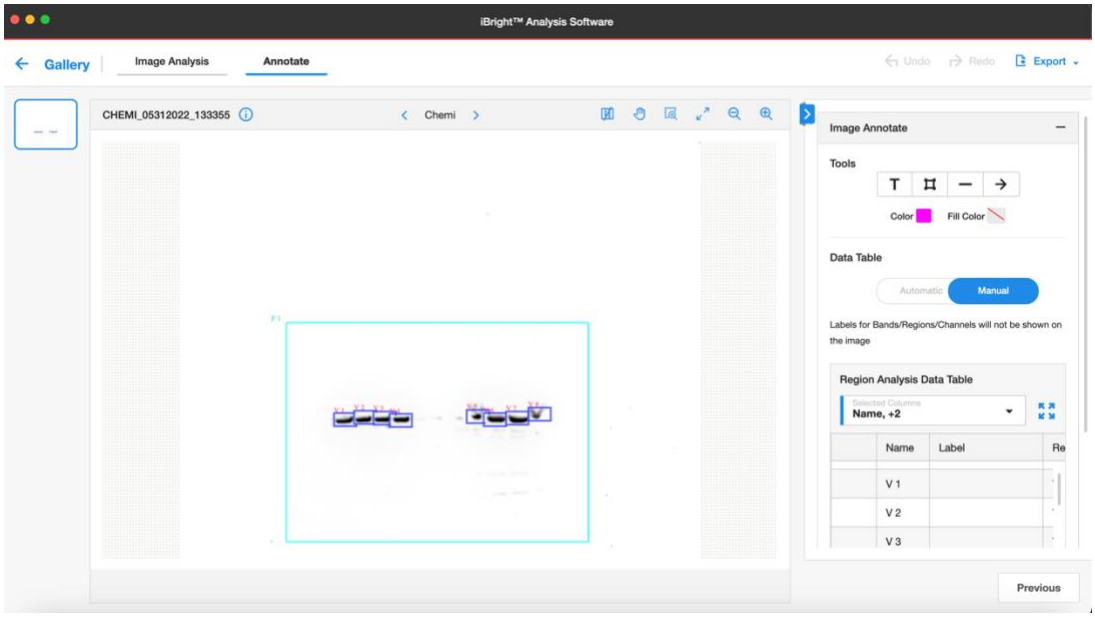

B.

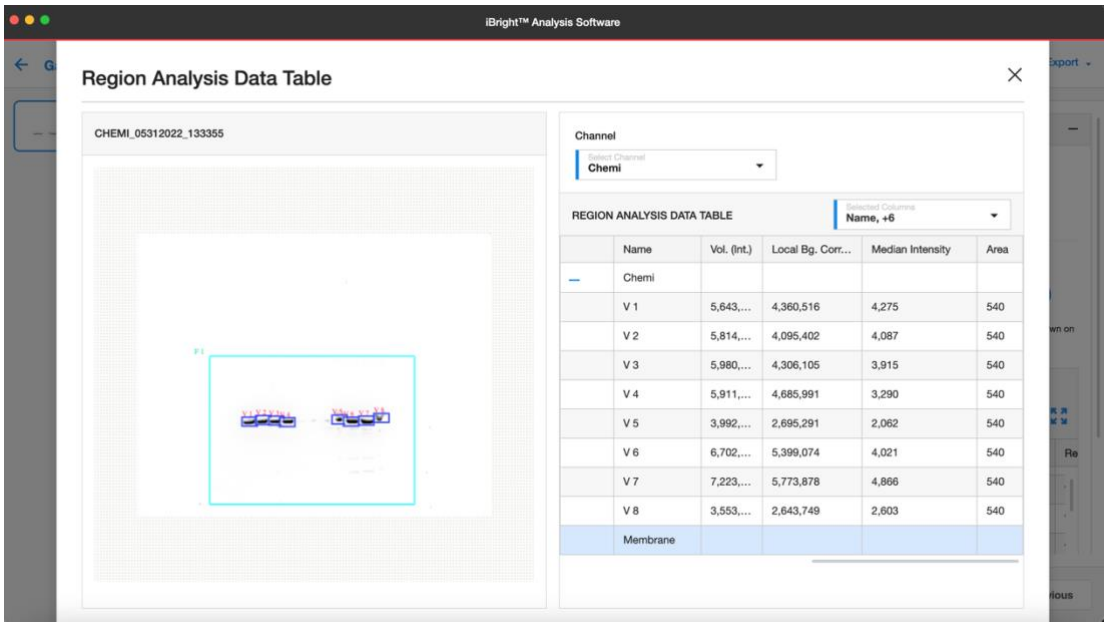

Figure 2.1. iBright was used to quantify western blots. (A) The rectangular selection tool marks the bands of interest on the image. **(B)** The data table containing the intensity of each band can be exported and analysed by comparing to the housekeeping protein controls which serve to normalize the data.

2.7 Statistical Analysis

All statistical analyses were performed using Prism 9.0 software (GraphPad). To test for whether the data was normally distributed the D'Agostino & Pearson test was performed. For comparing three or more groups, a one-way ANOVA was performed with Tukey's post-hoc test for data found to be normally distributed. Error bars on bar graphs represent the standard error of the mean. A p-value of less than 0.05 was considered statistically significant. Each experiment contains data from 3 independent experiments (n=3).

For flow cytometry analysis, the expression of cell surface L-selectin and ADAM17 on Molt-3 T-cells was calculated as a percentage relative to non-TCR stimulated cells, after subtracting the mean fluorescence intensity (MFI) of the isotype control from all samples.

2.8 List of reagents

2.8.1 Media

Medium	Composition	Use
R10 (complete RPMI)	RPMI 1640 (4.5 g/L glucose), 10 % FCS, 2mM L-Glutamine, 100 IU penicillin, 100 µg/mL streptomycin and 1 mM sodium pyruvate.	Culturing Molt-3 868TCR^{+} T-cells and derived cell lines.
R1	RPMI 1640 (4.5 g/L glucose), 1 % FCS, 2mM L-Glutamine, 100 IU penicillin, 100 µg/mL streptomycin and 1 mM sodium pyruvate.	L-selectin shedding experiments
R2	RPMI 1640 (4.5 g/L glucose), 2% FCS, 2 mM L-Glutamine, 100 IU penicillin, 100 µg/ml streptomycin and 1 mM sodium pyruvate	Used to culture Molt-3 T-cells during T-cell activation protocols, (e.g., Peptide activation of T-cells)
D10	DMEM (4.5 g/L glucose and 4 mM L- glutamine), 10 % FCS, 100 IU penicillin, 100 µg/mL streptomycin and 1 mM sodium pyruvate	Culturing HEK 293T cells
Trypsin-EDTA	Trypsin supplemented with 0.25% EDTA (Gibco)	Used for subculturing HEK 293T cells
Freezing Media	10% DMSO, 90 % FCS	Used to freeze cells for liquid nitrogen storage.

Table 2.3. Composition of all cell culture media used in this thesis.

2.8.2 General Buffers

Buffer	Composition and preparation
FCS	Foetal calf serum used to supplement media and for freezing was purchased from Sigma-Aldrich and heat inactivated for 30 minutes at 56^{o}C to reduce the risk of contamination by bacteria or fungi and to inactivate any enzymes or other proteins that might interfere with cell culture experiments. FCS is often heat inactivated at a temperature of 56°C for 30 minutes because this is sufficient to inactivate many types of enzymes and other proteins without damaging the FCS itself or denaturing the proteins it contains. Heat inactivation also helps to reduce the risk of contamination by killing any microorganisms that may be present in the FCS
Dimethyl sulfoxide (DMSO)	DMSO was purchased from Sigma-Aldrich and used for cell freezing media (90% FCS, 10% DMSO) or as a vehicle control for peptide and inhibitor treatments.
FACS buffer	FACS buffer was made using 2% v/v sterile FCS/PBS. 50 mL aliquots were created and stored at 4^{O}C. FACS buffer was used for flow cytometric staining.
Live/dead (LD) Aqua	LD aqua was purchased from Invitrogen (L34957) and each vial was resuspended in 50 µL DMSO, as per manufacturer instructions. 5 µL aliquots were stored at -20^{O}C.
4% Formaldehyde fix	37%-40% formalin solution was diluted in sterile PBS to a working solution of 4% formaldehyde (FA) fix. 4% FA fix was used to fix cells for flow cytometric analysis.
Dynabeads™ His-Tag Isolation and Pulldown	Commercially bought from Thermofisher, Catalog number# 10103D.

Table 2.4. Composition of general buffers used in this thesis.

2.8.3 Western Blot Buffers

Buffer	Composition and preparation
Sample Buffer, Laemmli 2× Concentrate	Commercially bought from Sigma-Aldrich, Catalog number# S3401. A total of 1 x 10^6 pelleted Molt-3 T-cells were directly lysed in 35 µL Laemmli buffer containing 660 mM Tris-HCl (pH 6.8), 26 % glycerol (v/v), 4 % SDS (w/v), 0.01 % bromophenol blue (w/v), 5 % β2-meracaptoethanol (v/v). Cell lysates were sonicated on ice for 15 sec using a Sonic Dismembrator model-120 (Thermo Scientific) and centrifuged at 13,000 rpm. Collected supernatants were immediately used for SDS-PAGE and western blot analysis.
Cell lysis buffer (RIPA lysis buffer)	Commercially bought from Thermofisher, Catalog number# 89901
Protease Inhibitor Cocktail	Commercially bought from Merck – Roche, Catalog number# 04693116001. 1 tablet in 10ml RIPA lysis buffer
Tris-Buffered Saline (TBS) pH 8.0	50nM Tris-HCl 150nM NaCl
Reducing sample buffer (2x)	65nm Tris-HCl pH 6.8 2% SDS 4% glycerol 0.01% bromophenol blue 5% β-mercaptoethanol
Non-reducing sample buffer (2x)	65nm Tris-HCl pH 6.8 2% SDS 4% glycerol 0.01% bromophenol blue
Western blot transfer buffer	25nM Tris 190nM glycine 20% methanol
TBS-Tween pH 8.0	TBS with 0.05% Tween-20
SuperSignal™ West Pico PLUS Chemiluminescent Substrate	Commercially bought from Thermofisher, Catalog number# 34577
Restore™ PLUS Western Blot Stripping Buffer	Commercially bought from Thermofisher, Catalog number# 46428

Table 2.5. Composition of Western Blot buffers used in this thesis

2.9 Software

For analysis, iBright Analysis Software (Invitrogen) was used to quantify western blots, FlowJo 10 (FlowJo LLC) was used to analyse conventional flow cytometry data (BD). To create figures, Biorender.com, Affinity Designer (Serif Europe LLC) were used. This thesis was compiled in Microsoft word (Microsoft Corporation).

2.10 Equipment

Cells were centrifuged using a Heraeus Megafuge 4R (Thermo Fisher Scientific) and counted using a LUNA-FLTM Dual Fluorescence Cell Counter in a 1:1 ratio with Trypan Blue (Logos Biosystems; Thermo Fisher Scientific). Stained cells underwent FACS using a BD FACSCanto II (BD). To collect conventional flow cytometry data, BD FACSDIVA (BD) software packages was used.

3 A Cell-Based Model of Cyclical Expression of L-selectin Following TCR Engagement

3.1 Introduction

L-selectin is expressed by naïve and central memory T lymphocytes and is involved in the multistep adhesion cascade of leucocyte recruitment from the bloodstream into tissues. L-selectin binds to glycoproteins termed peripheral node addressins (PNAd) expressed on HEVs in lymph nodes and supports naïve and central memory T-cell recruitment into lymph nodes during immunosurveillance (Girard et al. 2012). Whilst it is known that TCR activation induces downregulation of L-selectin, it was recently found that L-selectin is re-expressed and maintained on primed virus-specific CD8+ T-cells and is required for recruitment to virus infected organs and for protective immunity (Mohammed et al. 2016). Understanding how L-selectin re-expression is regulated may have important implications for endogenous responses as well as clinical implications in adoptive T-cell therapies for viral infection treatment and cancer (Mohammed et al. 2016). This may also have important implications for our understanding of the immune system and its response to infection and inflammation. For example, if we understand how L-selectin expression is regulated, we may be able to develop strategies to enhance or suppress its expression in order to improve the immune system's ability to fight infections and cancer or to reduce the severity of autoimmune disorders.

Additionally, understanding how L-selectin expression is regulated may have clinical implications, such as the development of new drugs or therapies that target L-selectin expression in order to treat or prevent a variety of immune-related disorders. It is known that ectodomain proteolytic shedding of L-selectin is regulated by ADAM17 (Mohammed et al. 2019). Whether L-selectin re-expression following shedding requires either downregulation of ADAM17 activity or loss of cell surface expression or both is not currently known. This chapter describes the use of an in vitro model of T-cell activation to dissect the mechanisms underlying re-expression of L-selectin and to further delineate the role of ADAM17 in this process.

3.2 Chapter Aims

- To optimize staining methods required to distinguish antigen presenting B-cells from T-cells by flow cytometry.
- To optimize peptide concentrations required to stimulate TCR-induced shedding of L-selectin.
- To examine surface level expression of L-selectin and ADAM17 by flow cytometry following SLY activation of Molt-3 cells.
- To examine at the whole protein level, L-selectin and ADAM17 expression following SLY activation of Molt-3 cells using western blot.

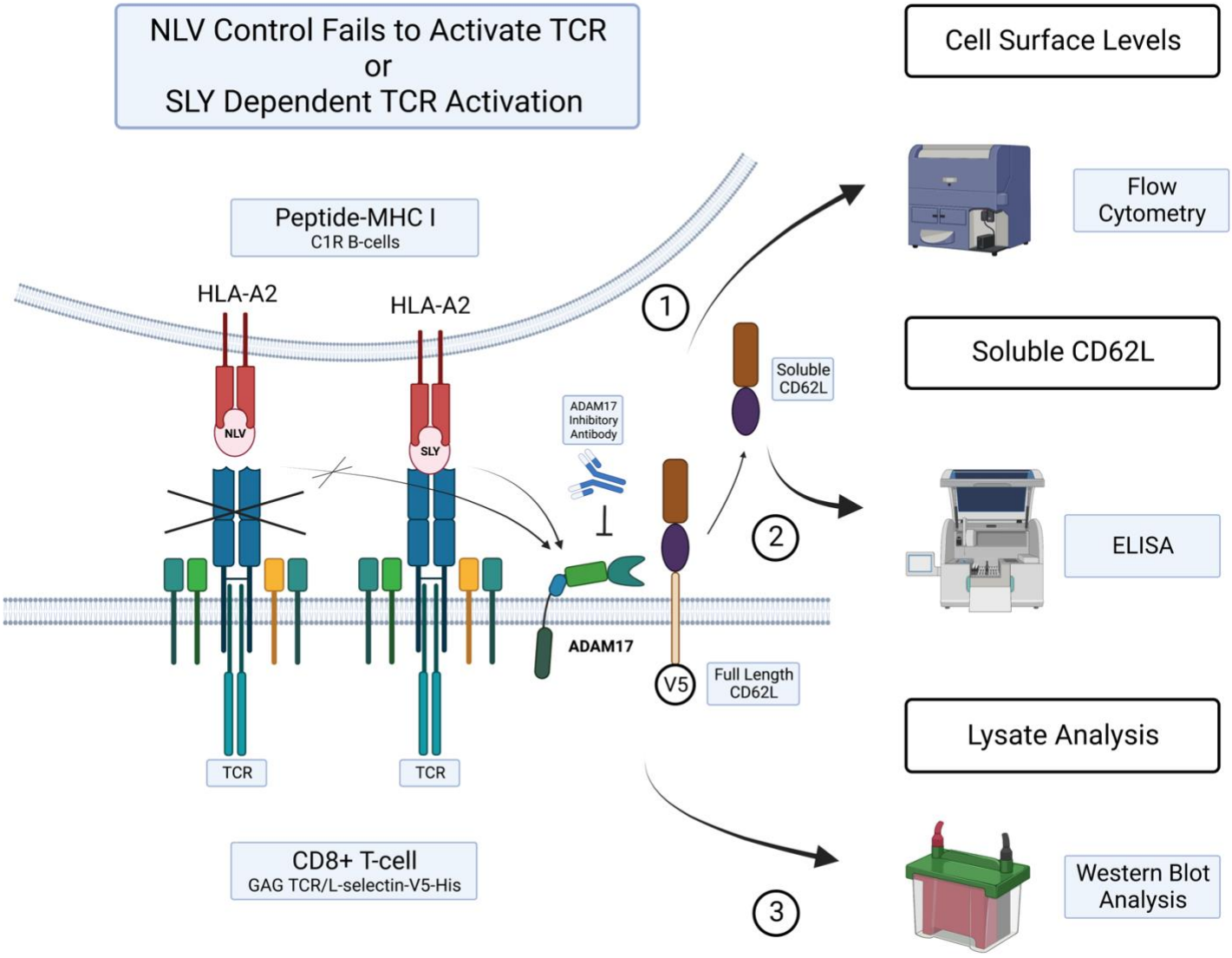

Figure 3.1. Workflow for methods used in this chapter to investigate the role of ADAM17 in L-selectin re-expression in-vitro. (1) Cell surface levels of L-selectin and ADAM17 on Molt-3 T-cells were assessed by Flow cytometry. **(2)** Soluble L-selectin shed from surface of Molt-3 T-cells was measured by ELISA. **(3)** Lysate analysis for fragments of L-selectin and ADAM17 was measured by Western blot analysis. Figure created using Biorender.com

3.3 Optimising Staining to distinguish antigen presenting B-cells from T-cells by flow cytometry.

3.3.1 Antigen presenting cell (APC) staining:

Molt-3 cells are a human T lymphoblastic leukemia cell line which does not express L-selectin endogenously. Therefore, we introduced human L-selectin tagged at carboxy terminus with V5-His tags via lentiviral transduction to investigate the regulation of its expression (Newman 2017). In order to study TCR induced shedding by peptide-MHC, the virus-specific TCR (HIV-1 Gag SLYNTVATL-specific TCR (868) was transduced into Molt-3 cells (Mohammed et al. 2019) and HLA-A2 transduced human B lymphoblastic (CIR) cells were used to present cognate peptide. To track L-selectin expression in Molt-3 868TCR+ T-cells it was important to gate out C1R B-cells which express L-selectin. CD19 is a common B-cell marker and was used to exclude C1R cells from our analysis so that we could specifically examine Molt-3 T-cell expression of L-selectin (Figure 3.2).

3.3.2 ADAM17 staining:

To validate the ADAM17 antibody, HEK293T ADAM17 Wild Type cells and HEK293T ADAM17 Knock out cells (C-Z. Koo & M. Tomlinson, unpublished) were used, respectively, as a positive and negative control. The first anti-ADAM17 antibody (clone 111633) was unable to stain for ADAM17 on Molt-3 T cells and C1R B-cells (Figure 3.3A&B). However, the anti-ADAM17 antibody (clone# MM0561-8C13 and Catalog number# NBP2-12018PE) (Table 2.1) was found to stain HEK293T ADAM17 Wild Type cells (Figure 3.3C) and not HEK293T ADAM17 knock out cells (Figure 3.3D) and was hence chosen for all further experiments.

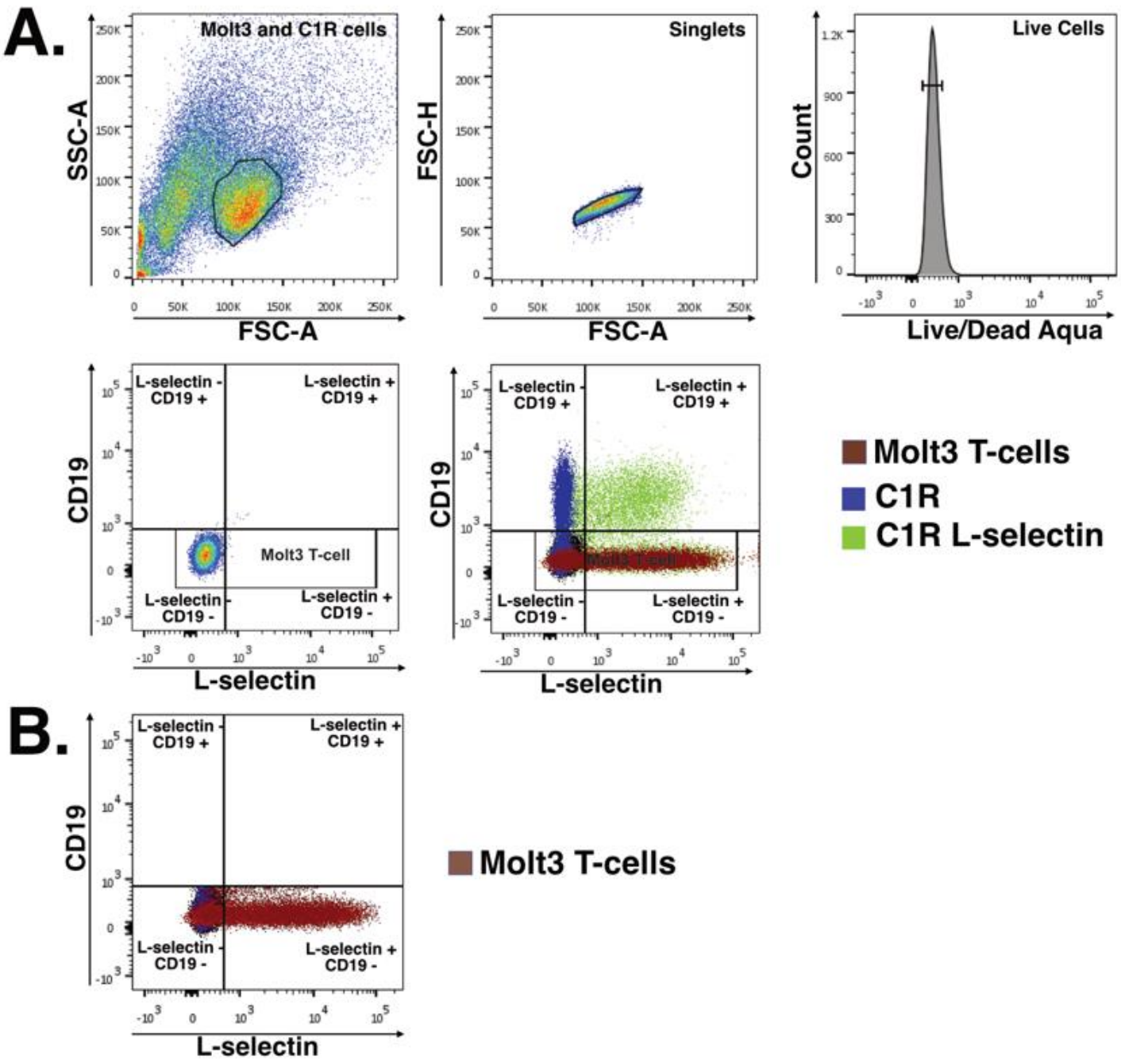

Figure 3.2. CD19 can be used to distinguish C1R cells from a mixed population of Molt-3 and C1R cells. C1R B-cells were co-cultured with Molt-3 868TCR^{+} T-cells and stained with CD62L and CD19. (**A**) The gating strategy by which CD19-, Live, Single, Molt-3 and C1R cells. (**B**) Gating strategy for examining the Molt-3 T-cell population (CD19-) which can be assessed for L-selectin expression specifically on this population.

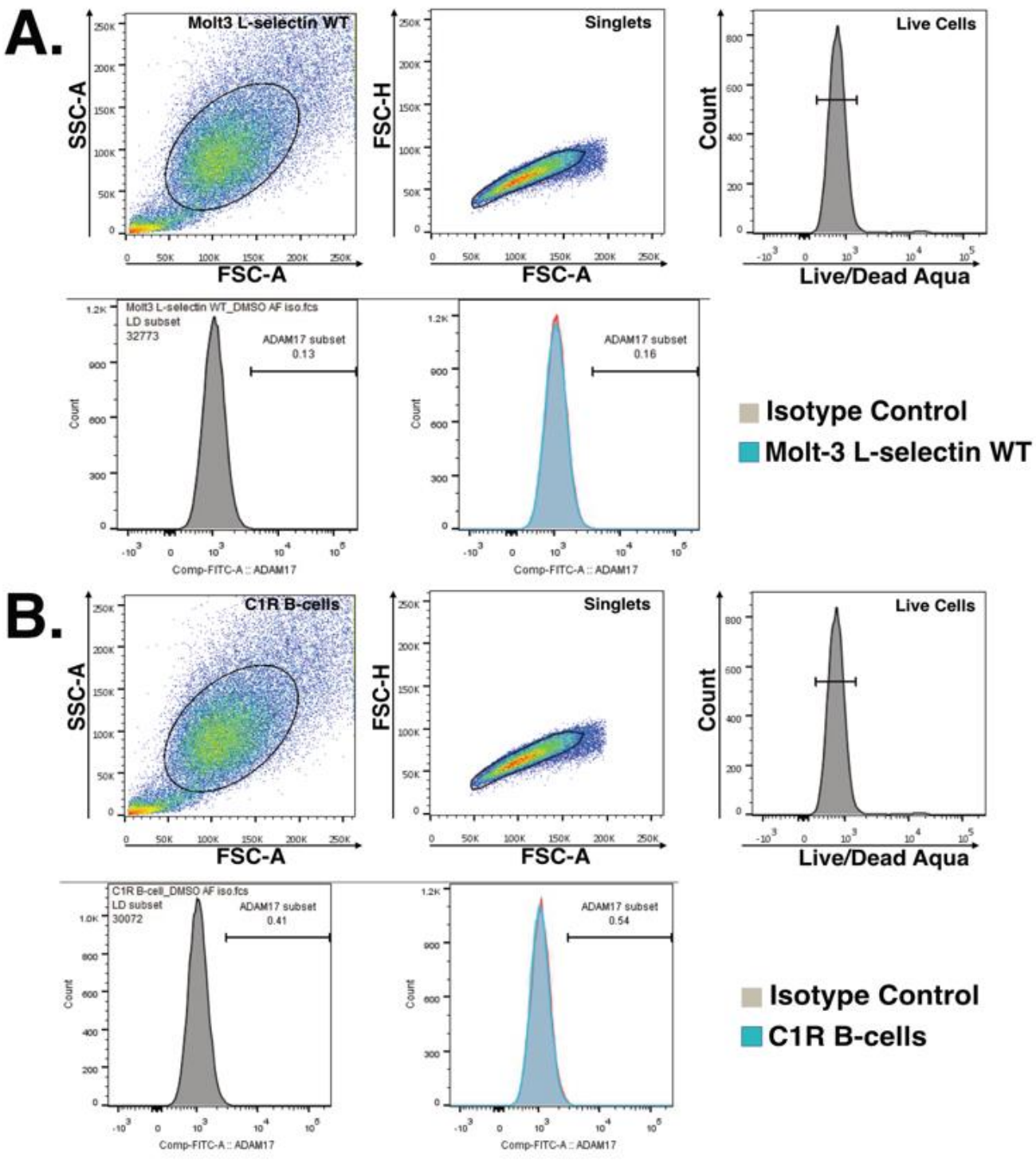
A.
Molt3 L-selectin WT
SSC-A
FSC-A
Singlets
FSC-H
FSC-A
Live Cells
Count
Live/Dead Aqua
Molt3 L-selectin WT_DMSO AF iso.fcs
LD subset
32773
ADAM17 subset
0.13
Count
Comp-FITC-A :: ADAM17
ADAM17 subset
0.16
Count
Comp-FITC-A :: ADAM17
Isotype Control
Molt-3 L-selectin WT
B.
C1R B-cells
SSC-A
FSC-A
Singlets
FSC-H
FSC-A
Live Cells
Count
Live/Dead Aqua
C1R B-cell_DMSO AF iso.fcs
LD subset
30072
ADAM17 subset
0.41
Count
Comp-FITC-A :: ADAM17
ADAM17 subset
0.54
Count
Comp-FITC-A :: ADAM17
Isotype Control
C1R B-cells

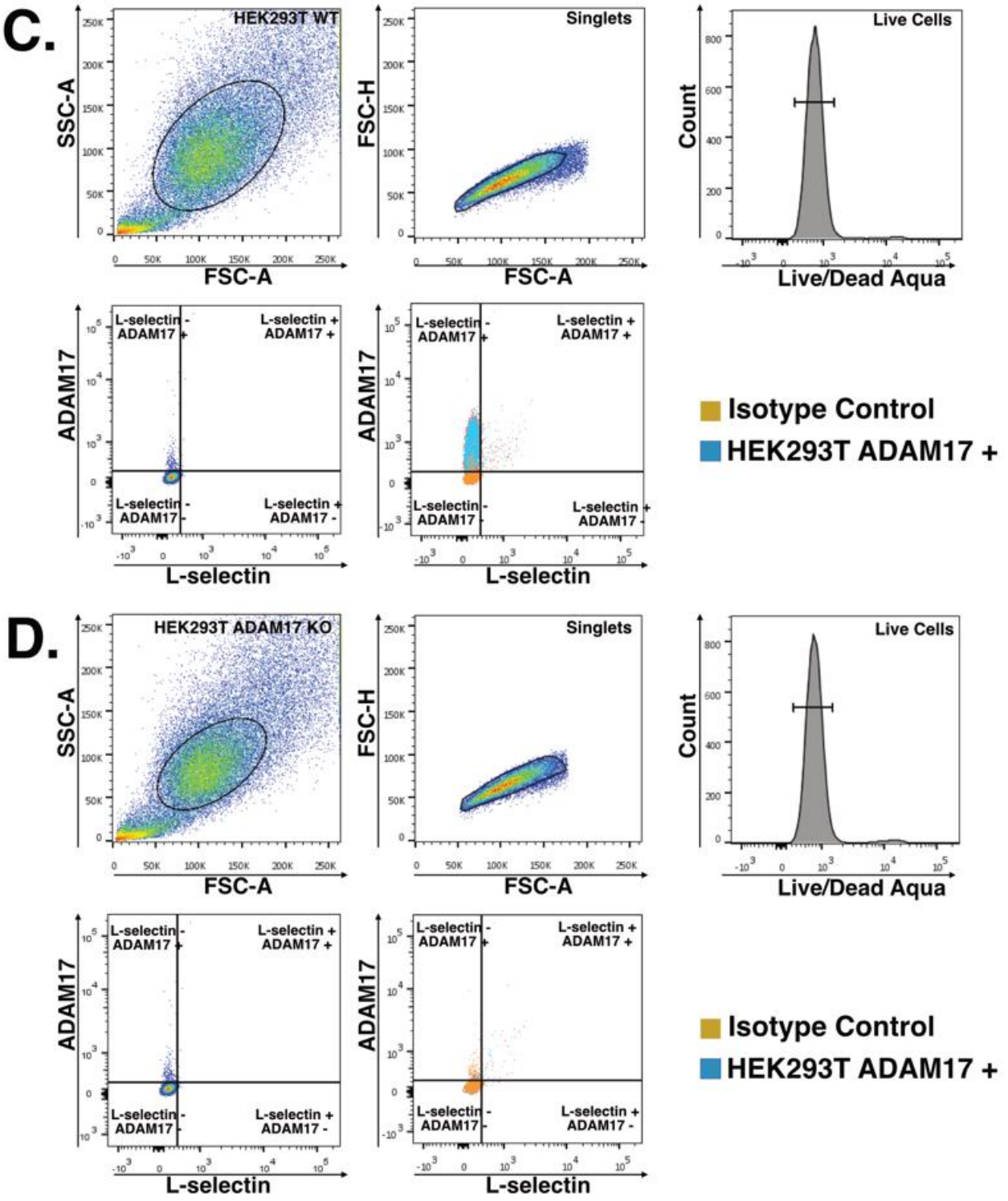

Figure 3.3. Validation of antibodies to ADAM17 for analysis of cell surface expression by flow cytometry. (A) Molt-3 868TCR+ T-cells and **(B)** C1R B-cells cells gated on live cells (stained with Live/Dead Aqua) were stained with anti-ADAM17 (Table 2.1; Clone# 111633 and Catalog number# FAB9301R-100UG FAB9301R). ADAM17 was not detected on the cell surface using this antibody. **(C)** HEK293T WT cells were stained with anti-ADAM17 (MM0561-8C13) and Live/Dead Aqua antibodies to examine expression. HEK293 WT cells stained positive for ADAM17 and did not stain positive for LD. **(D)** HEK293T ADAM17 KO cells were stained with anti-ADAM17 and Live/Dead Aqua antibodies to examine expression. HEK293 KO cells did not stain positive for ADAM17.

3.4 TCR activation dependent shedding of L-selectin:

It was first important to confirm whether the post-translational (ADAM17 cleavage) regulation of L-selectin expression was comparable in the leukemic Molt-3 868TCR cell line as in virus-specific memory CD8+ T-cells. L-selectin expression on Molt-3 868TCR+ cells following activation with cognate SLY peptide was compared with control (NLV) peptide, which binds to HLA-A2 but is not recognized by 868 TCR. The SLY and NLV peptides were pulsed onto C1R B-cells and incubated with Molt-3 868TCR+ T-cells for 60 mins. SLY peptide stimulated a dose-dependent downregulation of cell surface L-selectin between 10^{-7} and 10^{-4} M whereas NLV peptide had no effect on L-selectin expression (Figure 3.4, A).

3.5 L-selectin re-expression in Molt-3 868 TCR$^+$ cells following T-cell receptor engagement

To determine if L-selectin levels would recover to starting levels, due to re-expression. Molt-3 868 TCR+ cells were activated with SLY and L-selectin expression measured over a 24-hour time course (Figure 3.4, C). L-selectin expression was downregulated after 1 hour from ~750 expression of L-selectin (gMFI) to ~480 expression of L-selectin (gMFI) but after 4 hours there was a trend towards re-expression of L-selectin. However, L-selectin expression decreased between 4 and 24 h to very low levels of ~250 expression of L-selectin (gMFI). L-selectin expression decreased to similarly low levels in NLV peptide treated cells suggesting that this was not due to TCR engagement but instead correlated with Molt-3 868TCR$^+$ T-cells death observed at 24h (Figure 3.4, D). The data indicated that cells were undergoing apoptosis which was supported by the fact that the media turned yellow. Therefore, a further experiment was done to determine whether frequent medium change prevented cell death over the course of the 24h experiment. Frequent medium exchange, every 4h, prevented cell death (Figure 3.4, B) and therefore this was incorporated into the experimental protocol. By replenishing the media every 4 hours cell viability was significantly improved (Figure 3.4, B). This modified protocol was used for L-selectin detection over a 20 hours of peptide stimulation to test whether it is re-expressed.

After TCR activation with SLY-peptide pulsed APC but not NLV peptide or vehicle control (DMSO) treated APC there was also a significant reduction in L-selectin expression levels on T-cell when compared to the control treatment at the 1-hour time point (Figure 3.4, E). L-selectin levels were monitored over a 24h time frame. The data demonstrate that L-selectin levels increased steadily and reached a level equivalent to that of starting levels at 24 hours. The analysis of live dead staining (Figure 3.4, F) showed that cell viability remained stable. Therefore, I have overcome the previous difficulty in maintaining cell viability.

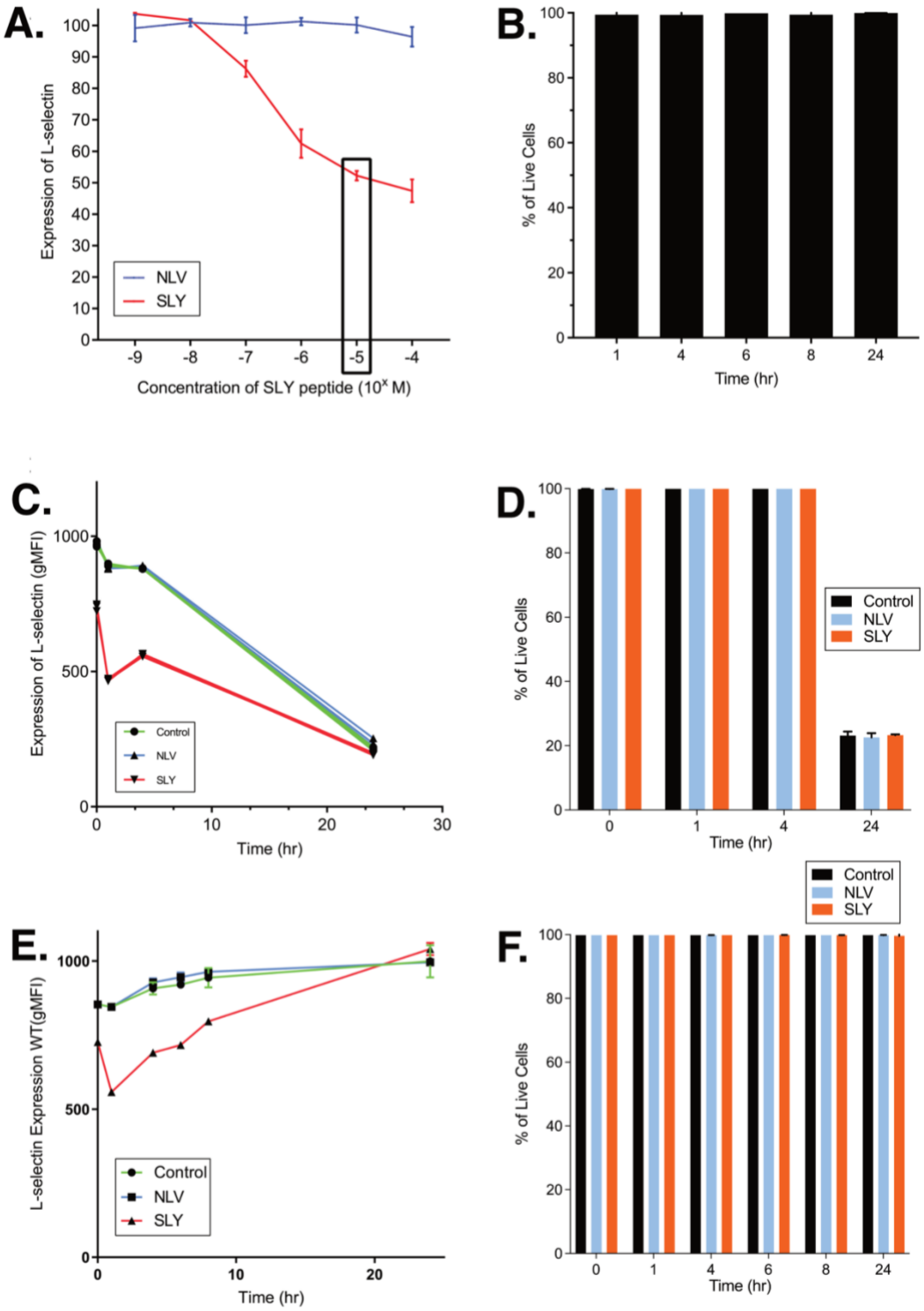

Figure 3.4: Effect of TCR dependent activation on L-selectin expression and viability of Molt-3 868 TCR+ cells. C1R B-cells were pulsed with SLY or NLV peptide (10^{-9}-10^{-4} M) for 1 hour, co-cultured with Molt-3 868TCR^{+} T-cells for up to 24 h and L-selectin expression levels and cell viability determined by flow cytometry. (A) Cell surface L-selectin after 1 h **(B)** Viability of both Molt-3 868TCR+ and C1R B-cells using LD Aqua stain at different time points (0-24 hours) whilst media was replenished every 6 hours. **(C)** Cell surface L-selectin determined between 0 and 24 h without media replenishment. **(D)** Molt-3 868TCR+ T-cell viability at 0-24 h without media replenishment. **(E)** Cell surface L-selectin determined between 0 and 24 h with media replenishment.). **(F)** Molt-3 868TCR+ T-cell viability at 0-24 h with media replenishment. Statistical significance was determined by Two-way ANOVA (Repeated measures ANOVA, *p < 0.05 **P < 0.0). Error bars represent SEM. Data from 3 independent experiments (n=3).

3.6 L-selectin and ADAM17 expression in Molt-3 868TCR^{+} L-selectin cells following T-cell receptor engagement

3.6.1 Characterization of cell surface and soluble levels of L-selectin and ADAM17 by flow cytometry and L-selectin by ELISA

In order to examine the surface expression levels of L-selectin and ADAM17 prior to and following peptide stimulation APC cells were pulsed with vehicle control (DMSO), NLV or SLY peptide (10^{-5} M) for 1 hour and co-cultured with Molt-3 868TCR+ T-cells and expression levels were measured over several time points (24-hour period) as shown in (Figure 3.7). Molt-3 868TCR+ T-cells were identified and distinguished from C1R cells using the gating strategy shown in Figure 3.5. Firstly, to know whether Molt-3 T-cell activation will have an impact on the expression of ADAM17 and L-selectin on C1R B-cells, it was important to look at expression levels of ADAM17 and L-selectin on C1R B-cells from the same experiment. All C1R B-cells showed stable expression levels of ADAM17 (Figure 3.6A) and L-selectin (Figure 3.6B) across the entire time course. Unstimulated Molt-3 T-cells had detectable expression levels of both L-selectin (Figure 3.5A) and ADAM17 (Figure 3.5B). Following peptide stimulation, L-selectin surface expression levels were initially downregulated (Figure 3.7A). After 1 hour there was a trend towards re-expression of L-selectin (Figure 3.7A) which is consistent with the results shown in Figure 3.4E. Interestingly, ADAM17 levels were initially upregulated and after 4 hours there was a trend for decreased ADAM17 expression (Figure 3.7B). This suggests that the activation of ADAM17 following peptide stimulation leads to the downregulation of L-selectin surface expression levels. Indeed, blocking ADAM17 with D1(A12) prevented L-selectin shedding on Molt-3 cells (Figure 3.7C&D). To confirm that ADAM17 dependent downregulation of L-selectin was due to ectodomain shedding, soluble L-selectin expression levels were measured by ELISA. Soluble L-selectin levels were detected at 0h only in the presence of SLY suggesting rapid activation of Molt-3 T-cells and L-selectin shedding. Soluble L-selectin levels significantly increased 1 hour after peptide stimulation which was completely abrogated in the presence of D1(A12) suggesting upregulation of ADAM17 following peptide stimulation (Figure 3.8B) leads to the downregulation of L-selectin surface expression levels (Figure 3.8B).

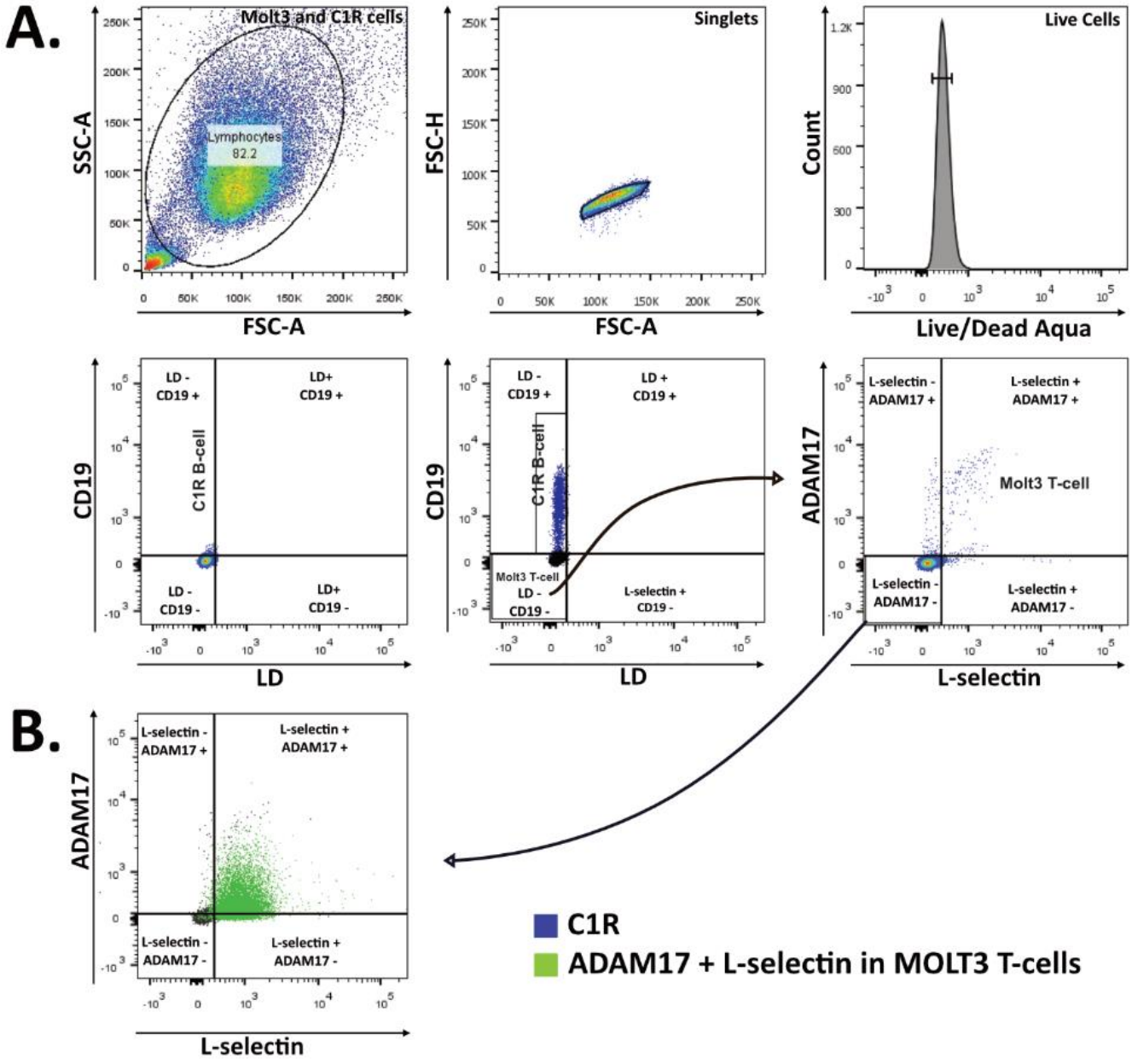

Figure 3.5. Gating strategy for distinguishing C1R cells from Molt-3 cells and further identifying populations of ADAM17+ and L-selectin+ Molt-3 cells. C1R B-cells were co-cultured with Molt-3 868TCR^{+} T-cells and stained with CD62L, CD19 and ADAM17. (**A**) The gating strategy by which CD19-, live, single, Molt-3 were identified and distinguished from CD19+, live, C1R cells. (**B**) The CD19-, live, Molt-3 T-cell population to be assessed for L-selectin and ADAM17 expression.

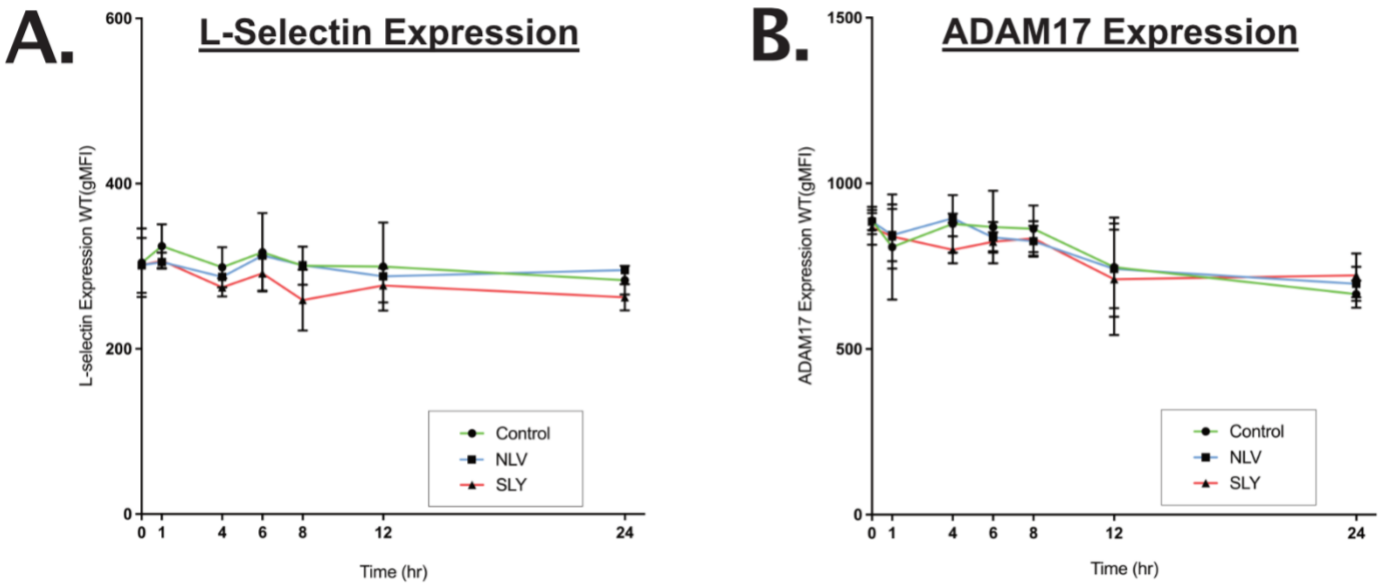

Figure 3.6. Expression levels of L-selectin and ADAM17 on C1R B-cells following peptide stimulation. APC cells were pulsed with Control (DMSO), NLV or SLY (10^{-5} Molar) for 1 hour and co-cultured with Molt-3 868TCR+ T-cells over several time points (0-24 hours). **(A)** L-selectin expression levels on C1R B-cells over a 24-hour period. (**B**) ADAM17 expression levels on C1R B-cells over a 24-hour period. Statistical significance was determined by Two-way ANOVA (Repeated measures ANOVA, *p < 0.05 **P < 0.0). Error bars represent SEM. Data from 3 independent experiments (n=3).

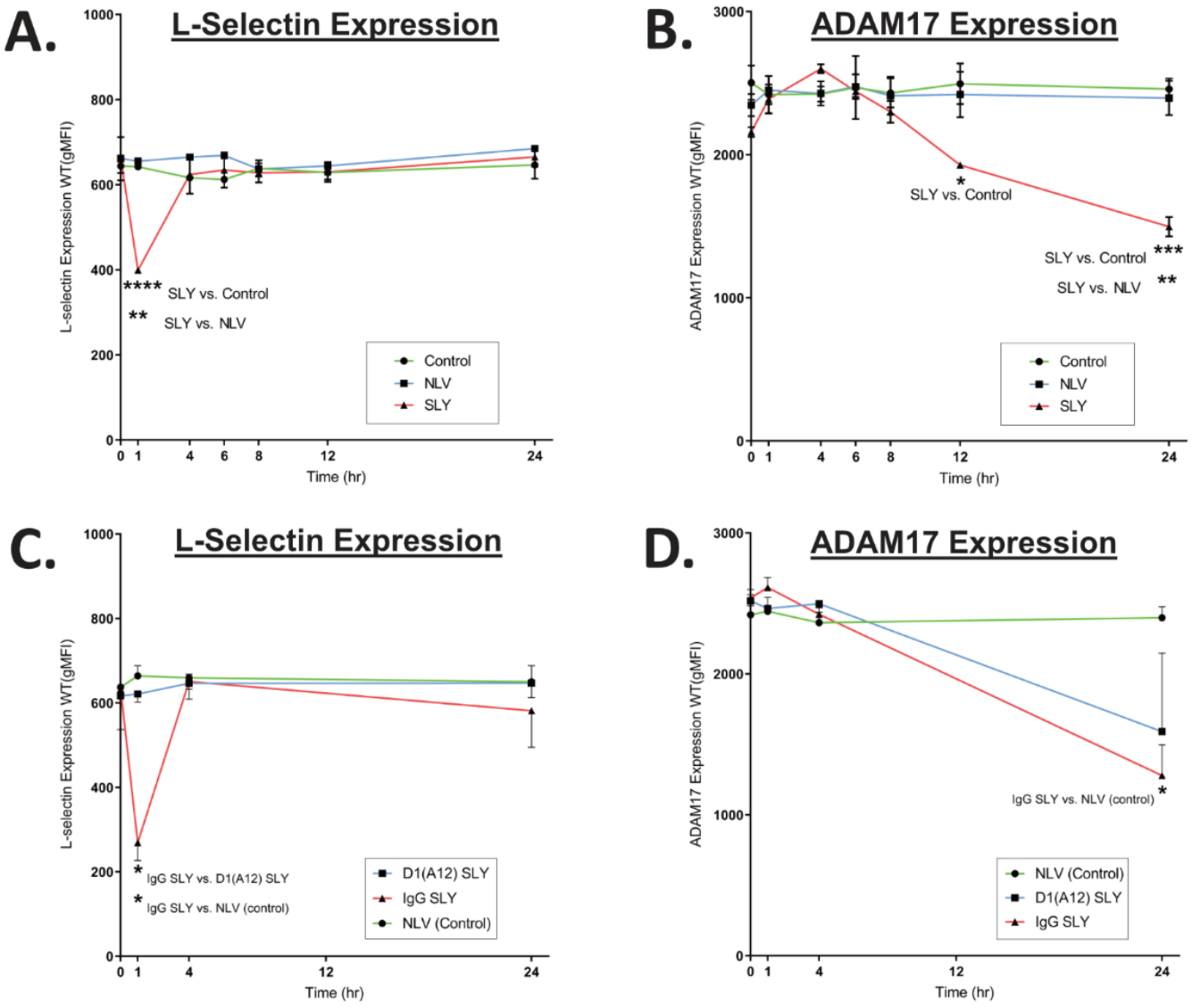

Figure 3.7. Expression levels of L-selectin and ADAM17 on Molt-3 868TCR+ T-cells following TCR stimulation. APC cells were pulsed with Control (DMSO), NLV or SLY peptides (10^{-5} M) for 1 hour, co-cultured with Molt-3 868TCR+ T-cells for up to 24 h and cell surface expression of L-selectin (**A**) and ADAM17 (**B**) on Molt-3 868TCR+ T-cells determined. APC cells were pulsed with Control (DMSO), NLV, SLY + D1(A12) and SLY + IgG (10^{-5} M) for 1 hour and co-cultured with Molt-3 868TCR+ T-cells for up to 24 h and cell surface expression of L-selectin (**C**) and ADAM17 (**D**) determined by flow cytometry. Statistical significance was determined by Two-way ANOVA (ANOVA, *p < 0.05, **P < 0.01, ***P < 0.001, ****P < 000.1). Error bars represent SEM. Data from 3 independent experiments (n=3).

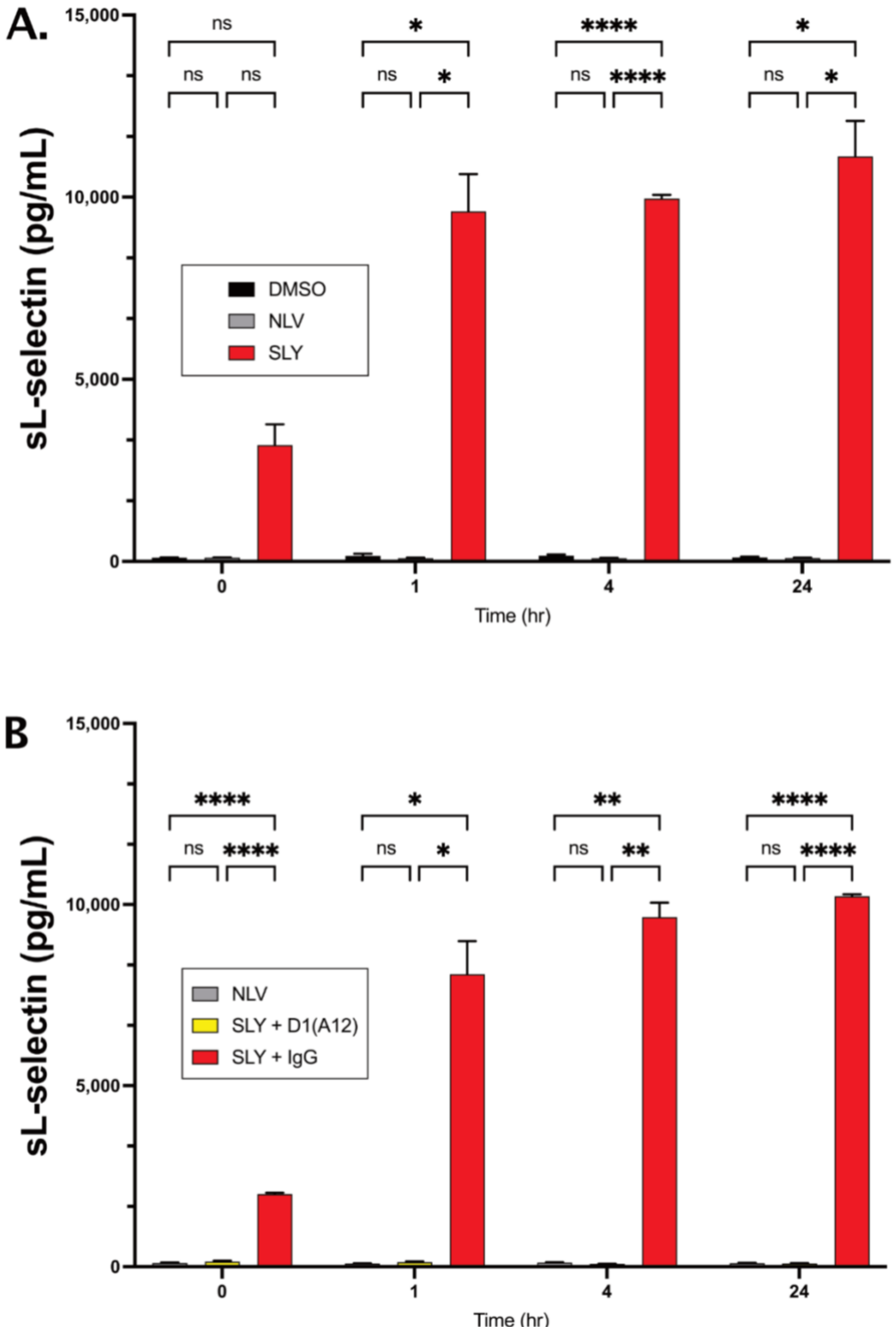

Figure 3.8. Soluble L-selectin expression levels detected by ELISA following Molt-3 868TCR+ T-cells peptide stimulation and ADAM17 blocking. **(A)** APC cells were pulsed with Control (DMSO), NLV or SLY (10^{-5} M) for 1 hour and co-cultured with Molt-3 868TCR+ T-cells over several time points (0-24 hours). The supernatant from this experiment (same time course experiment as in **(Figure 3.7A&B)** was collected and soluble L-selectin levels were quantified by ELISA. **(B)** APC cells were pulsed with Control (DMSO), NLV, SLY + D1(A12) and SLY + IgG (10^{-5} M) for 1 hour and co-cultured with Molt-3 868TCR+ T-cells over several time points (0-24 hours) and L-selectin soluble levels were detected by ELISA. Statistical significance was determined by Two-way ANOVA (ANOVA, *p < 0.05, **P < 0.01, ****P < 000.1). Error bars represent SEM. Data from 3 independent experiments (n=3).

3.6.2 Western blot analysis of L-selectin fragments and ADAM17 fragments

Changes in L-selectin and ADAM17 expression levels were also examined by western blotting. The specificity of the ADAM17 antibody for detecting ADAM was first confirmed using ADAM17 WT at molecular weight of ~100 kDA and ADAM17 KO HEK293 cells (Figure 3.9A). The cells from the same experiment whereby L-selectin surface expression were examined following peptide stimulation, in Figure 3.7A&B were collected and lysed with lysis buffer and frozen down after which western blotting was performed. A 3 -fold reduction in ADAM17 expression level in SLY-treated conditions (Figure 3.9 B&C) and a 2-fold reduction in full length L-selectin (Figure 3.9D&E) was also seen at the 24-hour time point. In NLV control peptide treated samples there was no change. The presence of a 180kDA ADAM17 band was also seen (Figure 3.9B) which could be explained by a dimer form of full length ADAM17 (~100 kDA) and mature form lacking the pro-domain (~80kDA) (Xu et al. 2016).

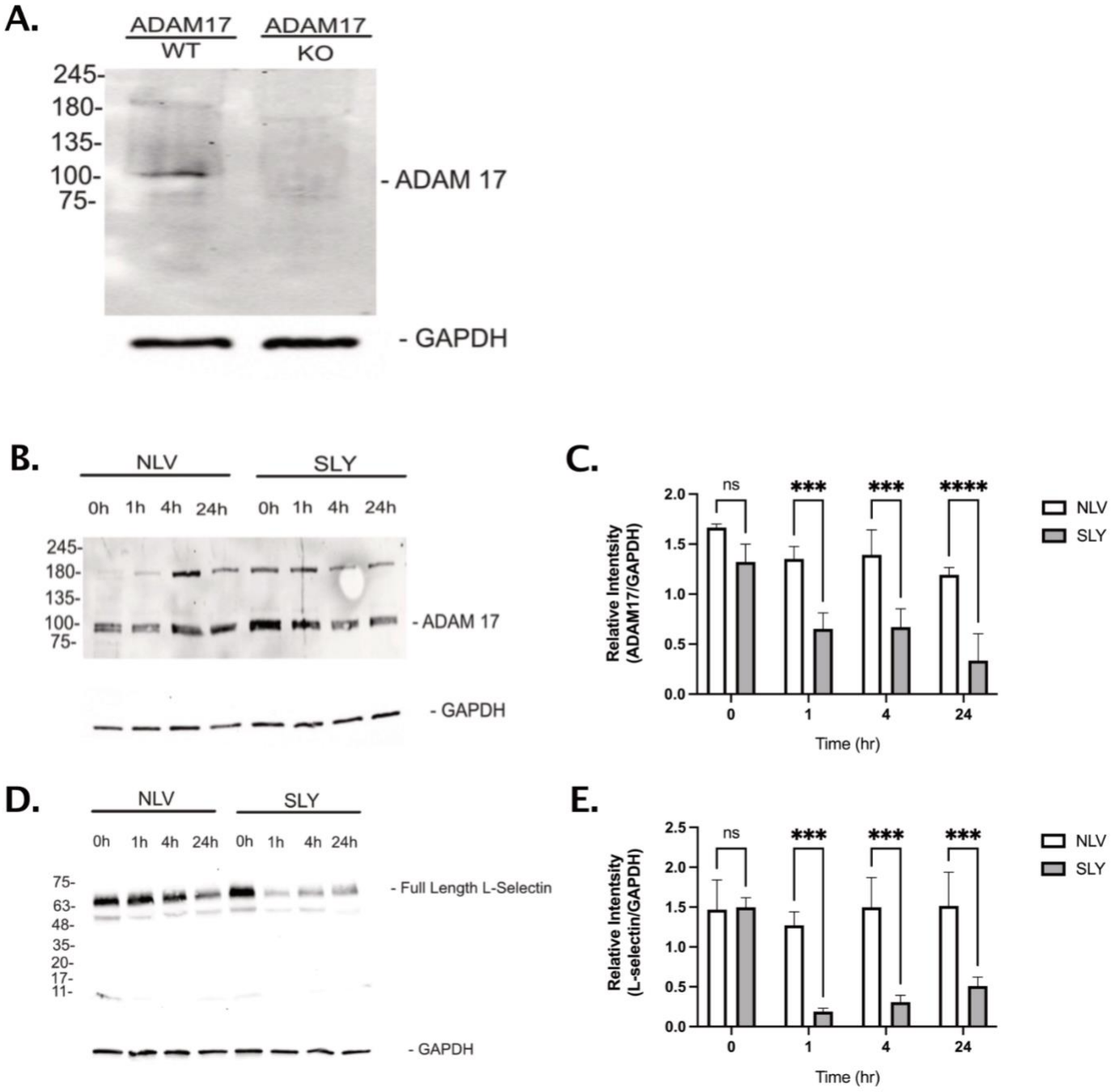

Figure 3.9. Western blot analysis of L-selectin fragments and ADAM17 fragments following peptide stimulation. APC cells were pulsed with Control (DMSO), NLV or SLY (10^{-5} Molar) for 1 hour and co-cultured with Molt-3 868TCR+ T-cells over several time points (0-24 hours). Cells were lysed and western blotting (WB) was performed with V5 Ab and A17 Ab. **A)** Western blot of A17 WT and A17 KO to validate antibodies. **B)** Western blot of A17 at several time points (0-24 hours). **C)** Quantification of A17 relative to GAPDH. **D)** Western blot of full-length L-selectin and C-terminal fragments at several time points (0-24 hours). **E)** Quantification of L-selectin relative to GAPDH. Statistical significance was determined by Two-way ANOVA (ANOVA, **P < 0.01, ***P < 0.001, ****P < 000.1). Data shown is mean with error bars representing SEM. Data from 3 independent experiments (n=3).

3.7 Discussion

L-selectin is an essential surface molecule whose functions can be summarized with these three roles: adhesion, shedding and signaling. This triad of events is tightly regulated and proper functioning of all three processes is essential for leukocyte circulation, recruitment, and homing. To investigate changes in L-selectin expression on T-cells during viral infection the appropriate concentrations of fluorescent antibodies for labelling L-selectin and C1R B-cells were optimized. Several commercial ADAM17 antibodies were tested and only the clone (MM0561-8C13) (Table 2.1) was found to work by flow cytometry. The CD19 biomarker was used to gate out L-selectin expressing APC cells to allow detection of L-selectin expression by Molt-3 T-cells only. At least 10^{-7} M of pulsed peptide was required for L-selectin shedding. L-selectin is re-expressed in human T-cells (Molt-3) which are transduced to co-express an HLA-A2 restricted T-cell receptor for the gag protein from HIV (868) and wildtype human L-selectin. This allowed for examining cell surface L-selectin levels which were found to be initially downregulated at 1 hour following SLY peptide engagement and then re-expressed at 4 hours after activation. Increased levels of soluble L-selectin were detected by ELISA and coincided with cell-surface downregulation of L-selectin. ADAM17 cell surface expression was also found to be initially upregulated and after 4 hours there was a trend for decreased ADAM17 expression. This is consistent with the possibility that the activation of ADAM17 following peptide stimulation leads to the downregulation of L-selectin surface expression levels.

The western blot data did not show convincing re-expression of full-length L-selectin following peptide activation whereas surface level examination by flow cytometry revealed re-expression within 4 h. Similarly, the loss of ADAM17 by western blot was greater than cell surface levels by flow cytometry. The degradation of ADAM17 shown in the western blot is not a result of ADAM17 degradation in APCs. Overall, this Chapter describes the development of a novel *in-vitro* model which allows for measuring L-selectin and ADAM17 cell surface levels and lysate levels following peptide engagement. Importantly, this method is in line with the finding from studies in the Ager lab that L-selectin is re-

expressed on virus-specific CD8 T-cells *in-vivo* 48 hour following virus infection (Mohammed et al. 2016).

L-selectin re-expression following shedding is associated with downregulation of ADAM17 activity or loss of cell surface expression. In order to examine this further it would be important to test whether re-expressed L-selectin can still be shed if ADAM17 has been downregulated as it may have important implications in T-cell expansion and trafficking (Mohammed et al. 2019). This could be examined by re-stimulating Molt-3 cells with SLY peptide after 24 hours and examining again the cell-surface ADAM17 levels and L-selectin shedding using flow cytometry for cell surface examination and ELISA for measuring soluble L-selectin levels.

4 Investigating the L-selectin Interaction with ADAM17 Following TCR Activation Using a Pulldown Approach

4.1 Introduction

Data from Chapter 3 show that stimulation of the TCR causes activation of ADAM17. After ADAM17 activation L-selectin is cleaved at the ectodomain generating a membrane retained fragment (MRF) comprising of the transmembrane region and a 17-amino acid L-selectin ICD sequence (Figure 4.1) which is V5-His-tagged. In Chapter 3 (Figure 3.8) I showed that soluble L-selectin levels were immediately increased after peptide stimulation of the TCR with SLY peptide at the 0h timepoint which indicates how rapid shedding occurs after TCR stimulation. In this study, Molt-3 T-cells were incubated with peptide-MHC (C1R cells) pulsed with control peptide (NLV: Figure 4.1 A) or TCR activating peptide (SLY: Figure 4.1 B).

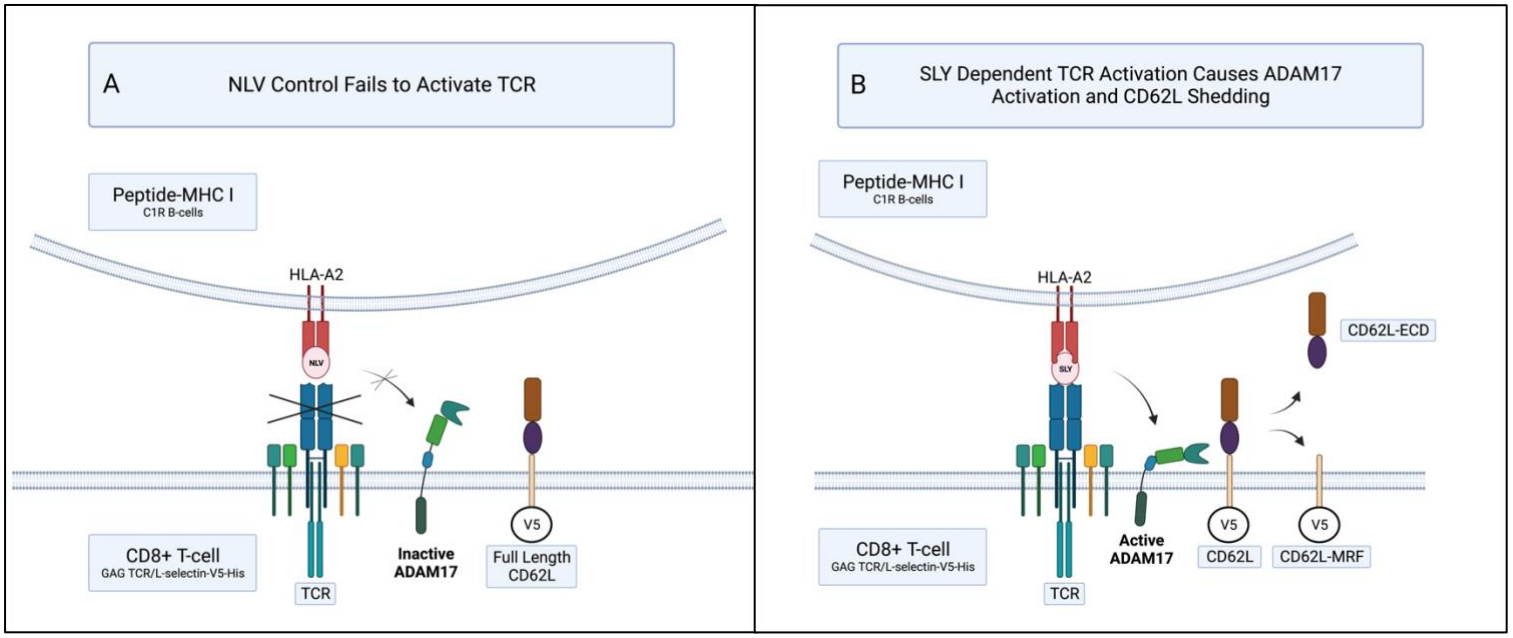

Figure 4.1: The cognate peptide is presented by human leucocyte HLA A2 antigen on antigen presenting cells and binds to the TCR. This shows the two different approaches of TCR non-stimulation or TCR stimulation. **(A)** TCR non-activation using NLV peptide pulsed C1R cells. C1R cells (NLV) binds to MHC but not to TCR on the surface of Molt-3 T-cells. TCR stimulation will not happen, ADAM17 will not be activated and there will be no cleavage of L-selectin. **(B)** TCR activation using SLY peptide pulsed C1R cells. C1R cells present a cognate (SLY) peptide to gag TCR on the surface of Molt-3 T-cells. After TCR stimulation, ADAM17 becomes activated and cleaves L-selectin. Figure created using Biorender.com

A pulldown assay was then performed to see whether the V5 his tag WT L-selectin directly interacts with ADAM17 in both non-activated and TCR activated T-cells. I hypothesised that TCR activation induces an interaction between L-selectin and ADAM17 which would result in proteolysis. Cobalt coated dynabeads were used to bind to the His tag of the L-selectin-V5-His protein allowing me to extract potential L-selectin/ADAM17 complexes from the original cell lysate (Figure 4.2).

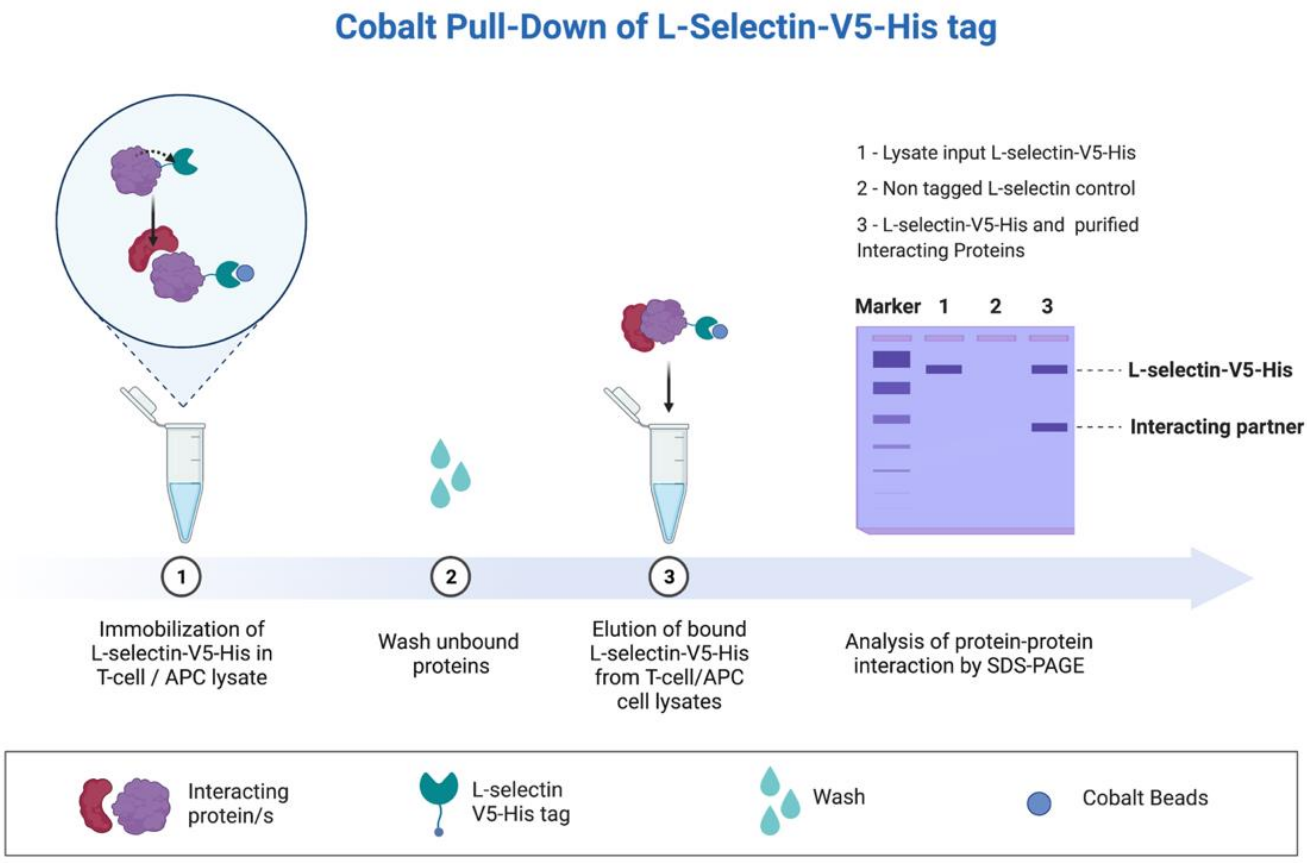

Figure 4.2. Workflow of methods used in this chapter to investigate the potential formation of an ADAM17 and L-selectin complex in Molt-3 L-selectin T-cells. Pulldown of L-selectin V5 His using cobalt ion covered dynabeads. The His tag region of L-selectin binds to cobalt ions presented on the surface of the dynabeads. This allows the isolation and pulldown of potential L-selectin/ADAM17 complexes. Only binding partners from T-cells would be isolated using this approach as the APC expresses non-tagged L-selectin. Figure created using Biorender.com

4.2 Chapter Aims

- To validate methods to pulldown L-selectin-V5-his-tagged using cobalt coated beads.
- To study whether ADAM17 forms a complex with L-selectin in both non TCR-activated and TCR-activated T-cells.

4.3 Validating pull-down of the his-tagged L-selectin from cell lysates using western blot analysis

First, it was important to validate the V5 tag monoclonal antibody (Catalog # R960-2) in western blotting by comparing L-selectin negative Molt-3 T-cells expressing a gag TCR (control Molt-3 T-cells) and L-selectin+ (V5 His) Molt-3 T-cells (Figure 4.3 A). Different time points were analysed following TCR activation and compared with unactivated T-cells (Figure 4.3 B, C). As shown in (Figure 4.3A) L-selectin-V5-tagged was successful pulled down by cobalt beads at molecular weight of 75 kDA in the NLV treated samples (control) for 0, 1, 4 and 24 hour time points. While, in the SLY treated samples there was a reduction in the signal intensity for L-selectin-V5-His at 1, 4 and 24 hour time points when compared with the corresponding to NLV treated samples. As a negative control, Molt-3 T-cells which lack L-selectin (Figure 4.3 B) were used to show that the eluted proteins were specific to tagged L-selectin. Which means using either L-selectin null Molt-3 T-cells or from Molt-3 T-cells expressing wild type non tagged L-selectin failed to produce any signal, indicating that only L-selectin was isolated and non-tagged Molt-3 T-cells do not bind to cobalt beads (Figure 4.3 B and C).

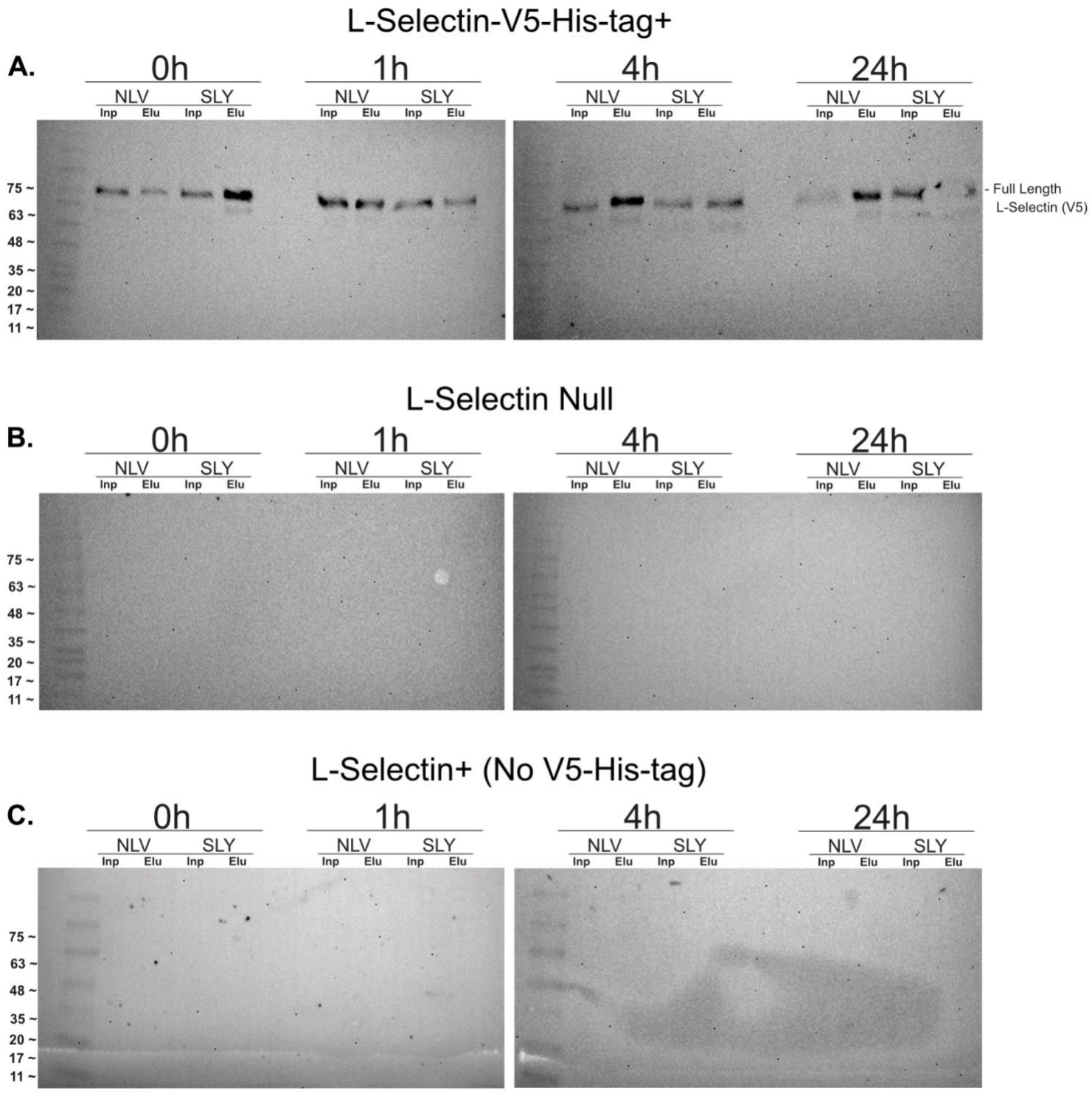

Figure 4.3. Pulldown of L-selectin-V5-his-tagged in unactivated and TCR activated Molt-3 + cells in Western blots. Molt-3 T-cells expressing gag TCR with without untagged and His-tagged L-selectin were incubated with control (NLV) or cognate (SLY) peptide for 1, 4 and 24h and cell lysates before (input) and following incubation with and elution from cobalt covered dynabeads (elute) analysed by western blotting for V5 tag. **(A)** L-selectin-His tag expressing Molt-3 T-cells. **(B)** L-selectin null Molt-3 T-cells. **(C)** Molt-3 T-cells expressing non-tagged L-selectin. (n=1).

4.4 Studying the interactions between L-selectin and ADAM17 in non TCR-activated and TCR-activated Molt-3 T-cells

In order to test the hypothesis that ADAM17 forms a complex with its substrate L-selectin I performed pull-down experiments using cell lysates from 868 TCR+ Molt-3 T-cell expressing L-selectin-V5-his-tagged. Molt-3 T-cells were incubated with APC presenting either activation SLY peptide or non-activating NLV peptide to the gag TCR on the Molt-3 T-cells for up to 24 h. Cells were lysed at 0h, 1h, 4h and 24h time points and L-selectin-V5-his-tagged and potential binding partners isolated using cobalt beads. Although APC express wild type non-tagged L-selectin, the levels are 10-fold lower than L-selectin-V5-his-tagged Molt-3 T-cells (see Figure 3.6) and, as shown above, non-tagged L-selectin does not bind to cobalt beads. Thus, only binding partners from T-cells expressing L-selectin-V5-his-tagged would be isolated using this approach.

L-selectin-V5-his-tagged was successfully isolated from the cell lysate at 0h for both NLV and SLY conditions (Figure 4.4B). During prolonged treatment the signal intensity for L-selectin-V5-his-tag was reduced where the SLY peptide had been presented to the GAG-TCR (see Figure 4.4B at 24h SLY treated). In contrast, in the presence of NLV the L-selectin-V5-his-tag signal was maintained over 24h (Figure 4.4B NLV treated). This indicates that L-selectin-V5-his-tag was cleaved, leading to loss of signal intensity over time (Figure 4.4B).

Pulldowns were initially stained for ADAM17 before being stained for the L-selectin-V5-his-tag. This allowed for probing in parallel of the western blots from the pulldowns for the presence of mature ADAM17 at 93 kDA (Figure 4.4A) in the original starting material as well as the eluation. The western blot shows that ADAM17 was only found in the input samples and not in the pulldowns irrespective of NLV or SLY treatment. ADAM17 does not interact with L-selectin in either resting T-cells and after TCR-activation (Figure 4.4A). One possibility, as it has been shown in Chapter 3 (Figure 3.9E) with the loss of ADAM17 across different time points is linked to the rapid degradation of ADAM17 after TCR activation which prevented its detection it when I pulled down V5-his-tagged L-selectin.

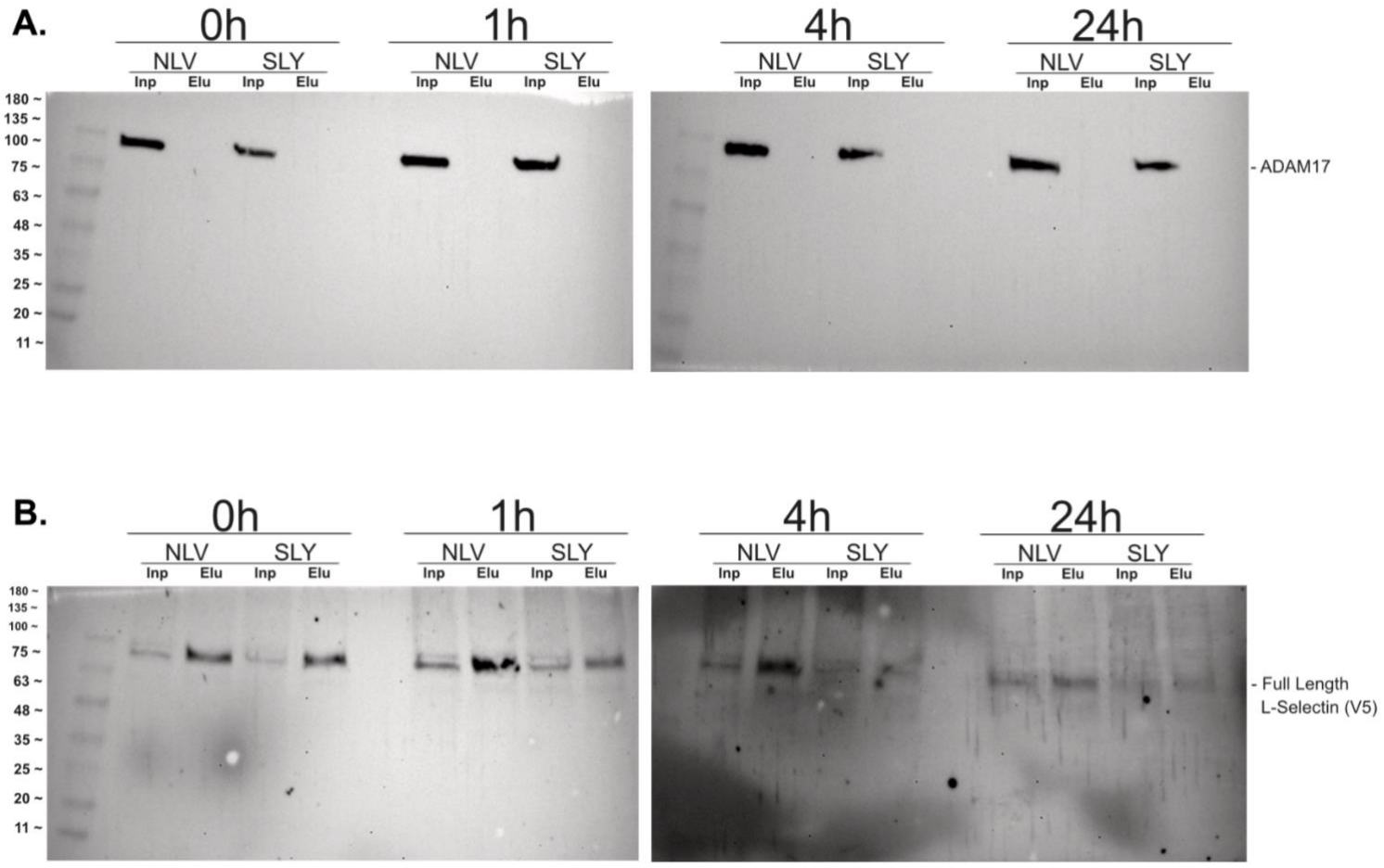

Figure 4.4. Pulldown of L-selectin-V5-his-tagged in unactivated and TCR activated Molt-3+ cells. A) Molt-3 T-cells expressing gag TCR with and without untagged or His-tagged L-selectin were incubated with antigen presented cells primed with either control (NLV) or stimulated with cognate (SLY) peptide for 0, 1, 4 and 24h and cell lysates before (input) and following incubation with and elution from cobalt covered dynabeads (elute) analysed by western blotting for V5 tag and ADAM17. Lysates from L-selectin+ V5-His-tagged Molt-3 T-cells were stained for ADAM17 **(A)** and L-selectin-V5-his-tagged **(B)**. Data from 2 independent experiments (n=2).

4.5 ADAM17 does not form a complex with L-selectin when shedding of the ectodomain of L-selectin is prevented

Data from Chapter 3 show that stimulation of the TCR causes activation of ADAM17 dependent ectodomain shedding of L-selectin and maximal release of the cleaved ectodomain within the first 60 mins of TCR stimulation. If L-selectin binding to ADAM17 in TCR activated cells depends on an intact ectodomain, it would not be detected unless ADAM17 shedding of L-selectin is inhibited. As results from my previous experiments showed that L-selectin did not bind to ADAM17 in TCR-activated Molt-3 cells, I next wanted to investigate whether pretreatment with an ADAM17 inhibitor would allow the isolation of an enzyme-substrate complex. I selected a small molecule ADAM17 inhibitor, rather than an inhibitory antibody to ensure that I did not induce any steric hindrance that would prevent enzyme-substrate complex formation in response to TCR activation. To investigate further, the only way to capture a complex (ADAM17 and L-selectin), would be by blocking cleavage. To determine whether ADAM 17 and L-selectin interaction requires prior blocking agent which binds to the ADAM17 active site and prevent cleaving of L-selectin, the same experiment as in Figure 4.4 was performed, but in the presence of metalloproteinase inhibitors to capture enzyme substrate complexes as previously shown (Hartmann, et al. 2015). Molt-3 T-cells were pretreated with DMSO or GW280264X (ADAM17 inhibitor) for 1h and cells were then incubated with peptide pulsed APCs for 1h. Lysates were then incubated with cobalt beads (elute) to capture L-selectin containing complexes. The elution from the cobalt beads and the input were analysed by western blotting (Figure 4.5).

A fraction of the original lysate labeled as the input sample and served as a positive control for ADAM17 and L-selectin-V5-His signals. ADAM17 was only found in the appropriate input sample and not in the pulldowns irrespective of NLV or SLY treatment, in the presence or absence of the metalloproteinase inhibitor GW280264X (Figure 4.5A). The ADAMA17 blot was reported for L-selection-V5-His and only75 kDA full length L-selectin-V5-His was detected in the NLV input and elution samples in the absence of GW280264X. In contract, SLY treatment led to loss of L-selectin-V5-His signal in the appropriate elution from the SLY samples (Figure. 4.5B). In the presence pf the ADAMI7 inhibition GW280264X full length L-selectin-V5-His was found in both NLV and SLY treated conditions (Figure. 4.5B). This indicated that GW280264X blocked L-selectin cleavage successfully, however, ADAM17 protein could not be enriched in the appropriate elution from the beads. ADAM17 does not interact with L-selectin in both resting T-cells and after TCR-activation (Figure 4.5A). Whilst the inhibitor blocked shedding of L-selectin as expected (noticeably denser full-length L-Selectin band in ADAM17 inhibitor treated group) (Figure 4.5B), ADAM17 was not found to be eluted. This could be because the complex disassociates rapidly (Figure 4.5A).

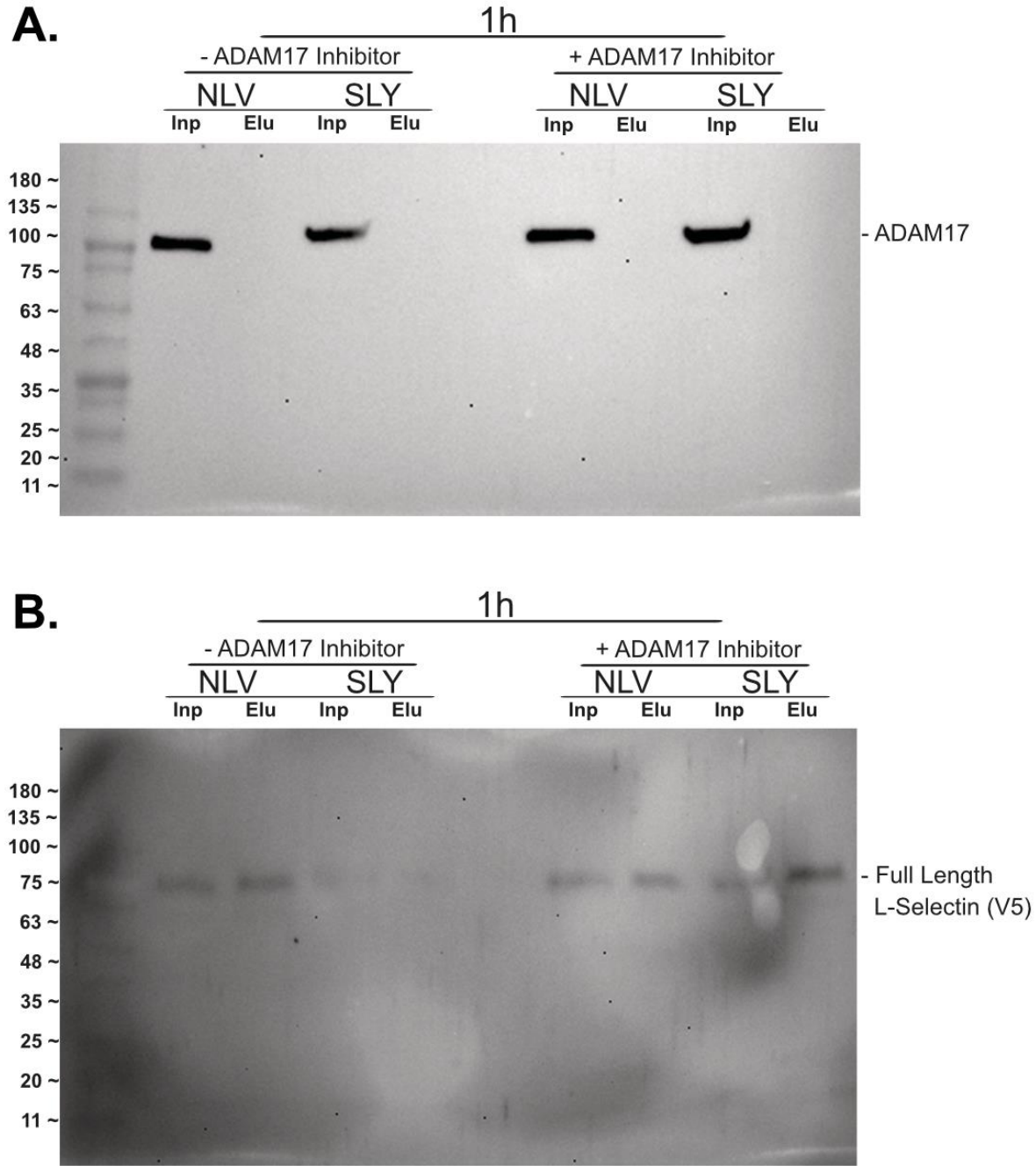

Figure 4.5. Pulldown of L-selectin-V5-his-tagged from control and TCR activated Molt-3 T-cells in Western blots for 1h with or without metalloproteinase inhibitor. A) Lysates from L-selectin-V5-His-tagged Molt-3 T-cells were incubated with cobalt covered dynabeads (elute) and Lysates from L-selectin-V5-His-tagged Molt-3 T-cells were not incubated with cobalt covered dynabeads (input). Lysates for both elute and input were used for western blot analysis and stained for ADAM17. Anti-ADAM17 antibody was used to detect ADAM17 for 1h with absence or presence of metalloproteinase inhibitor. **B)** Lysates from L-selectin-V5-His-tagged Molt-3 T-cells were incubated with cobalt covered dynabeads (elute) and Lysates from L-selectin+ V5-His-tagged Molt-3 T-cells were not incubated with cobalt covered dynabeads (input). Lysates for both elute and input were used for western blot analysis and stained for L-selectin. Anti-V5 antibody was used to detect L-selectin-V5-His-tagged for 1h with absence or presence of metalloproteinase inhibitor. Data from 2 independent experiments (n=2).

4.6 Discussion

The use of V5 His tagged L-selectin allows for the effective isolation of L-selectin (via His tag isolation and pulldown dynabeads) and further downstream analysis of L-selectin binding partners. The C terminal V5 His tag of L-selectin was previously shown not to interfere with ADAM17 proteolysis after TCR stimulation (Newman 2017). In this chapter, L-selectin and ADAM17 were found not to form a complex in resting T-cells or after TCR-activation even when blocking ADAM17 by (GW280264X) (Mohammed et al. 2019), but further investigation is needed. A different blocking agent should be applied in the future. One explanation is that the rapid dissociation of the complex happens very quickly. As such it is recommended to try a shorter time point e.g., 5min, 10min, or 30min. Proteomic analysis of the samples pull-down (elute) vs non-pull-down (input) would be worth doing as it will show all the changes that happen on the phosphorylation level. Previously described co-precipitation experiments which include the inclusion of a pre-clearing step which overcomes the detection of false binders based on charge have led to the identification of several L-selectin binding partners (Ivetic et al., 2019). Whilst several L-selectin binders such as Alpha-actinin and Calmodulin have been identified, ADAM17 has not been reported. It would be important to validate the pulldown approach by probing for other L-selectin binding partners such as alpha-actinin, calmodulin and ERMs. This would serve as a positive control to that show the pulldown approach which was used in this thesis is a valid approach.

The presence of the V5 his tag in the L-selectin tail could potentially hinder interaction with protein binding partners which in turn regulate metalloproteinase dependent ectodomain proteolysis. Disruption of the interaction between ezrin and mosein which interact with L-selectin ICD has been shown to drive resistance to PMA induced shedding (Ivetic, et al. 2002; Ivetic, et al. 2004). This may explain why ADAM-17 in a complex with L-selectin could not be detected in this work. The presence of calmodulin could hinder this interaction as well since calmodulin inhibitors such as trifluroperazine have been shown to induce metalloproteinase dependent shedding of L-selectin (Kahn, et al. 1998).

The finding from this Chapter is that ADAM17 and L-selectin do not form a complex. Blot quantification would allow the extent of reduction in full length L-selectin to be quantitated to demonstrate clearly that shedding was inhibited by GW280264X. This would allow for comparison the differences in NLV and SLY peptide which are detectable in this assay as well. However due to the elution step, GAPDH and other housekeeping proteins have been removed and quantification cannot be performed as I have done for western blots of whole cell lysates for L-selectin-V5-his tag and ADAM17 in Chapter 3. Alternatively, the data could be normalized to the input (cell lysates before the pulldowns) in order to perform quantification.

5 Studying the fate of L-selectin's cytoplasmic tail following ADAM17 dependent shedding in response to peptide-MHC dependent TCR activation

5.1 Introduction

Previous work by (Mohammed et al. 2019) used naïve $CD8^+$ T-cells expressing $H2D^b$ restricted influenza A nucleoprotein peptide 366/374 (NP68)-specific TCR (F5) and either wild type L-selectin (F5/B6) or non-cleavable L-selectin (F5/LΔP) to study clonal expansion in an adoptive transfer model of influenza infection in naïve B6 mice. CFSE prelabelled naïve $CD8^+$ T-cells from wild type (F5/B6) and non-cleavable L-selectin (F5/LΔP) mice were injected into B6 mice prior to viral challenge 24h later. Analysis demonstrated that donor $CD8^+$ T-cell numbers from wild type mice two days after virus infection had increased in the draining mediastinal lymph node, which correlated with increased early clonal expansion of cytotoxic T-cells, when compared to T-cells expressing non cleavable L-selectin. This showed that the proteolysis of CD62L results in an 8-fold increase in early clonal expansion of cytotoxic T-cells, which also correlated with an increase in CD25 expression in the transferred T-cells (Figure 5.1). This suggests that by preventing L-selectin proteolysis the proliferation kinetics of LΔP T-cells could be delayed for therapeutic benefit for example until the T-cells reach the target tissue site of interest such as tumor or viral infected tissues (Figure 5.1). The hypothesis of this Chapter is that the L-selectin membrane fragment generated following peptide-MHC induced ADAM17 activation is retained following inhibition of γ-secretase and the proteasome as was previously shown using anti-CD3/CD28 and PMA for T-cell activation (Newman 2017; Moon 2021) (Figure 5.2). Therefore, it is possible that the cell associated L-selectin membrane retained fragment (MRF) or a yet unknown intracellular fragment could drive cell proliferation in T-cells where ADAM17 dependent ectodomain shedding of L-selectin is intact. ADAM17 dependent proteolysis of other cell surface proteins, such as epidermal growth factor ligands, or the Notch-receptor is known to regulate the proliferation of target cells (Zunke and Rose-John 2017). Whether these events are dependent on extracellular fragments (e.g., EGFR-ligands) or intracellular fragments (e.g., Notch-ICD) is currently unclear for L-selectin (Figure 5.2).

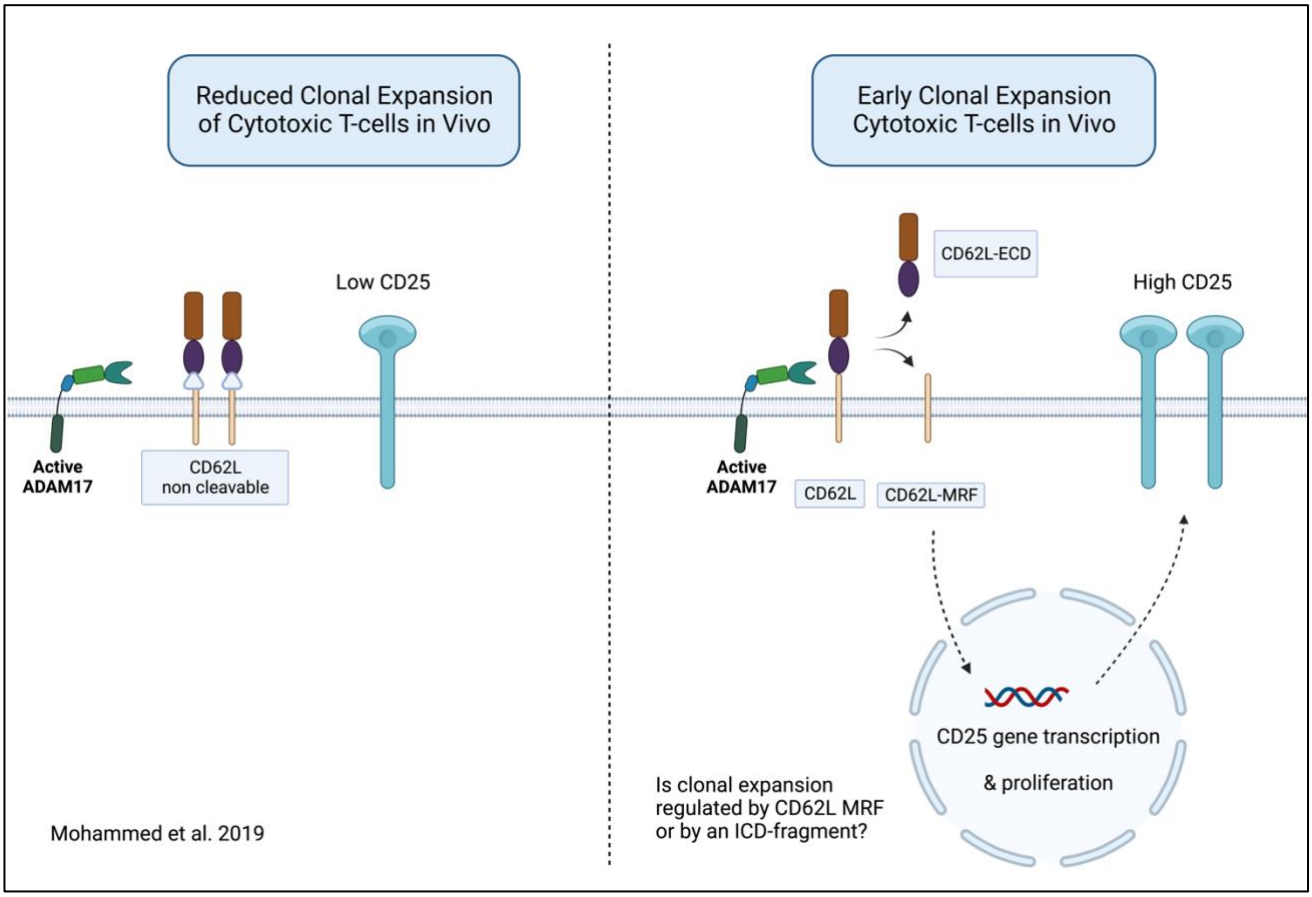

Figure 5.1: ADAM17-dependent proteolysis of L-selectin promotes early clonal expansion of cytotoxic T-cells. Cleavage of L-selectin (CD62L) allows early clonal expansion of cytotoxic T-cells through upregulation of CD25 expression. Cleavage of L-selectin may result in the formation of a fragment with signaling potential that regulates the early clonal expansion of $CD8^+$ T-cells in the above model. Figure adapted from (Mohammed et al. 2019). Figure created using Biorender.com

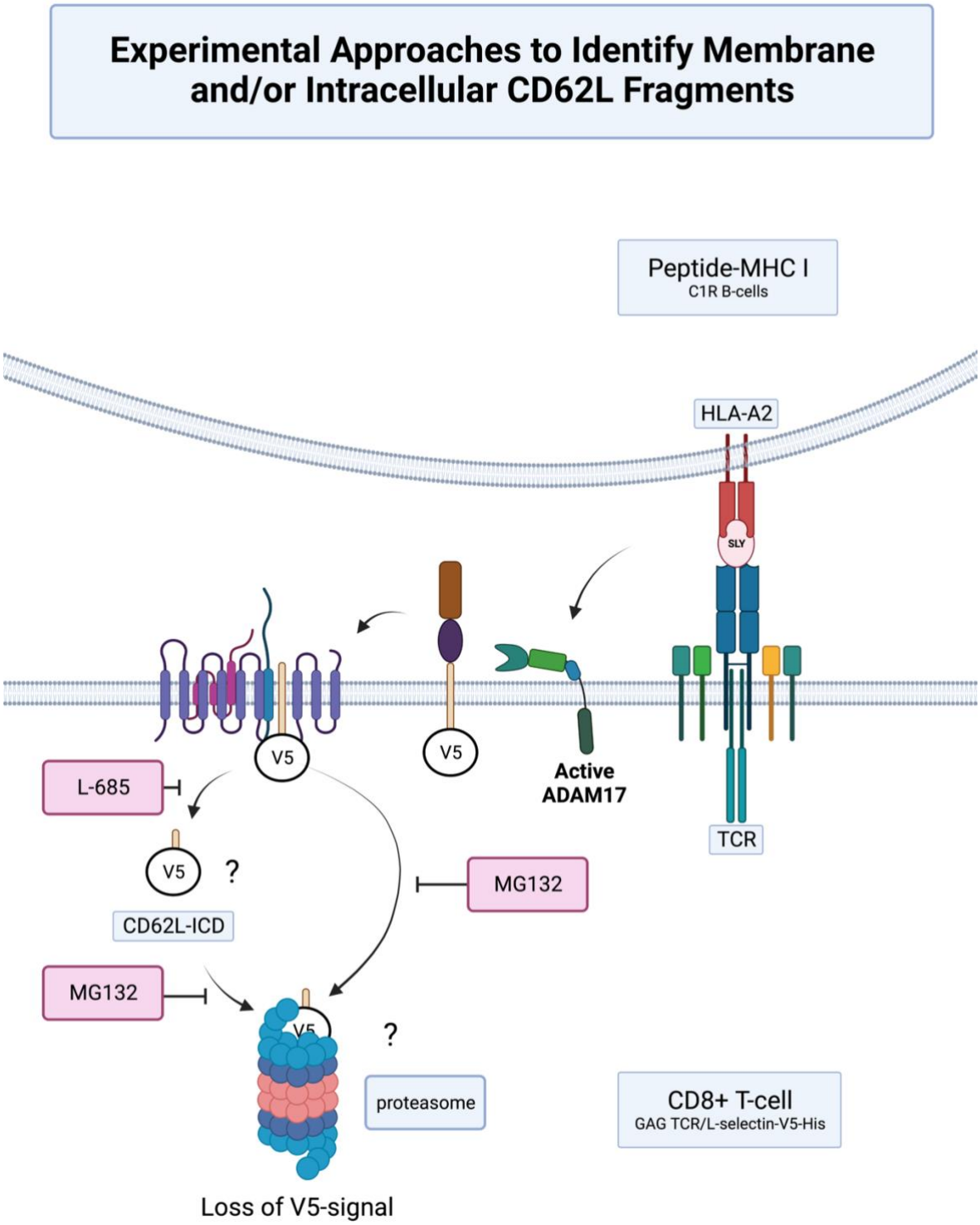

Figure 5.2: Experimental Approaches to Identify Membrane and/or Intracellular CD62L Fragments. The cognate peptide is presented by human leucocyte HLA A2 antigen on antigen presenting cells and binds to the TCR. This shows two different approaches of TCR non-stimulation or stimulation. TCR activation using SLY peptide pulsed C1R cells. C1R cells present a cognate (SLY) peptide to GAG TCR/L-selectin-V5-His T-cell. After TCR stimulation, ADAM17 becomes activated and cleaves L-selectin generating the L-selectin membrane fragment. Whether the L-selectin membrane fragment is retained following inhibition of γ-secretase and the proteasome was examined by performing by Western blot analysis. Figure created using Biorender.com

5.2 Chapter Aim

- This chapter therefore set out to determine whether the MRF of L-selectin was subject to further degradation by γ-secretase leading to the formation of an intracellular fragment with signaling potential.

5.3 Proteolysis of cytoplasmic tail of L-selectin is inhibited by γ-secretase inhibition (L-685) and proteasome inhibition (MG132) after TCR induced shedding by SLY peptide

In previous chapters I showed that the L-selectin MRF was difficult to detect by Western blotting. To test the hypothesis that the L-selectin MRF released following SLY induced ADAM17 activation is further processed by γ-secretase activity, I pre-treated cells with γ-secretase inhibitor L-685. T-Cells were then stimulated with peptide-MHC presenting SLY to activate TCR on GAG TCR/CD62L-V5-His T-cells, leading to ADAM17 activation, which was compared to NLV control conditions in the presence and absence of inhibitor. peptide-MHC express wild type non-tagged L-selectin, the levels are 10-fold lower than L-selectin-V5-his-tagged T-cells on GAG TCR/CD62L-V5-His (see Figure 3.6) and staining for V5-epitope tag only detects T-cell L-selectin and its fragments in this experimental setup. In Figure 5.3 NLV treatment demonstrated that L-selectin remained a full-length molecule in the presence or absence of L-685. In response to SLY dependent activation of ADAM17 the blot shows that the MRF cannot be detected in DMSO solvent conditions, but γ-secretase inhibition allowed the detection of the MRF at 11 kDa (Figure 5.3A SLY, L685 lane; Figure 5.3B for quantification of MRF). This indicates that the MRF is processed by γ-secretase, leading to a fragment, that cannot be detected by western blotting under the experimental conditions.

To investigate this further, the proteasome inhibitor MG132 was tested to enrich for a smaller L-selectin fragment. T-cells were pretreated with MG132 and then stimulated with peptide-MHC carrying either activating SLY or NLV control peptide in the presence or absence of MG132. In NLV conditions, no L-selectin fragments were detected. Surprisingly, MG132 treatment did not enrich a smaller ICD-L-selectin fragment but enriched the MRF fragment in the cell lysate (Figure 5.3A SLY, MG132 lane; Figure 5.3B for quantification of MRF, Figure 5.3C for quantification of full-length L-selectin).

To see whether L685 and MG132 had an additive effect and increased MRF levels further, T-cells were pretreated with both inhibitors and TCR stimulated with peptide-MHC as above. Western blot analysis demonstrates that NLV treatment had no effect on L-selectin. In SLY conditions the treatment with both inhibitors enriched the MRF to detectable levels, but these were not significantly different from the DMSO control treatment (Figure 5.3 SLY L685-MG132 lane; B for quantification of MRF).

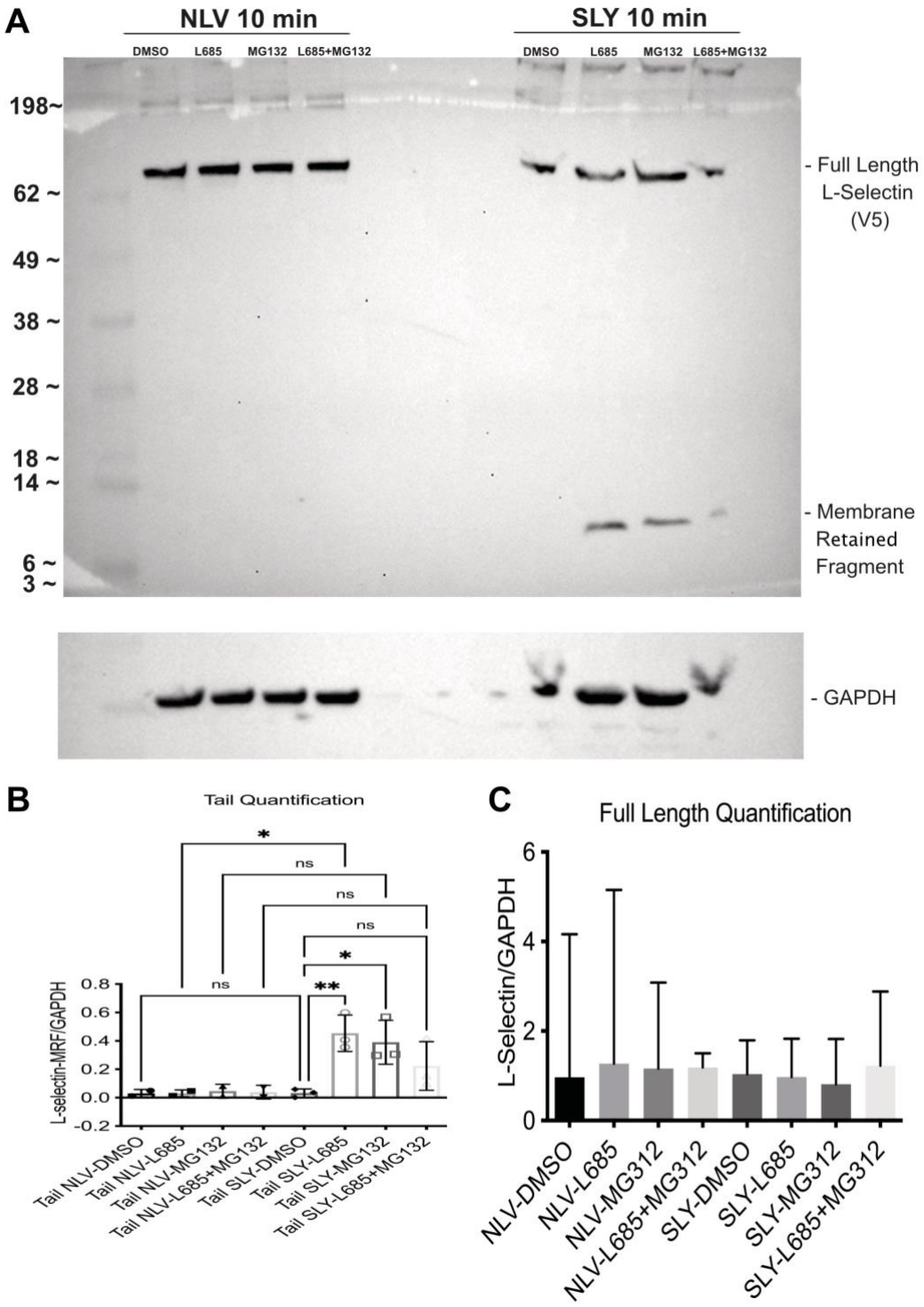

Figure 5.3: Analysis of MRF-CD62L fragment levels in GAG TCR/CD62L-V5-His T-cells in response to T-cell activation in the presence and absence of γ-secretase or proteasome inhibitors. The proteasomal inhibitor MG132, γ-secretase inhibitor L685, or both inhibitors stabilise the L-selectin MRF. Molt-3 T-cells were treated with the indicated inhibitors or DMSO control prior to SLY Peptide induced proteolysis or NLV Peptide control before lysis and immunoblotting for L-selectin's V5/His tagged cytosolic tail. **(A)** A representative western blot for full-length and L-selectin fragment tail. **(B)** the quantification of MRF relative to GAPDH control and presentation as fold change following Peptide treatment. **(C)** the quantification of full-length L-selectin relative to GAPDH control and presentation as fold change following Peptide treatment. Statistical significance was determined by Two-way ANOVA (Repeated measures ANOVA, *p < 0.05 **P < 0.0). Error bars represent SEM. Data from 3 independent experiments (n=3).

5.4 Discussion

In this chapter, the L-selectin MRF released following SLY induced ADAM17 activation was found to be retained following the inhibition of γ-secretase (L-685) and the proteasome (MG132). This is consistent with previous work whereby CD3/CD28 was used to activate L-selectin-His-V5 tagged 868 TCR+ Molt-3 cells (Newman 2017) and PMA was used to activate Molt-3 cells (Moon 2021). Both experiments showed that L-selectin MRF is retained when the proteosome and γ-secretase are inhibited using the same inhibitors (Newman 2017; Moon 2021). Imaging flow cytometry experiments further showed that the MRF signal was lost from the cells consistent with the MRF being further degraded (Newman 2017; Moon 2021). Interestingly the use of both inhibitors did not increase the MRF signal but rather a smaller band was seen (Figure 5.3). This could be because the inhibitors interfere with each other, eg, MG132 prevents γ-secretase from working properly or L685 prevent proteasome from working properly which will require further investigation.

Overall, this work is in line with the work by Mohammed et al which showed that cleaved L-selectin to drive CD25 expression and clonal T-cell expansion (Mohammed et al. 2019). However, in order to determine if γ-secretase generated fragments of the MRF could get to the nucleus and acting as transcriptional factors which drive CD25 expression and T-cell expansion, requires further research. To identify the location where the catalytic component of γ-secretase cleaves L-selectin MRF, the detected form of the protein will be analyzed using mass spectroscopy. This information can then be used to create synthetic peptides, which will be tested in a chromatin immunoprecipitation assay to see if cleaved L-selectin ICD binds to a specific DNA sequence. If L-selectin ICD does bind to DNA, the expression of genes like CD25 can be examined using DNA microarray analysis and mRNA from T-cells activated by the TCR and expressing either cleavable or non-cleavable forms of L-selectin (Figure 5.4). Substrates such as amyloid precursor protein (AICD) and Notch (NICD) are known to be rapidly degraded by the ubiquitin proteasome pathway (De Strooper et al. 1999; Schweisguth 2004; Selkoe and Kopan 2003).

Previous attempts to detect L-selectin ICD by western blot have proven difficult (Newman 2017) and could be explained by rapid degradation as well. However cleaved AICD and NICD have been shown to enter the nucleus and act as gene transcriptional factors (von Rotz et al. 2004; Schroeter et al. 1998). L-selectin ICD could therefore act in a similar way.

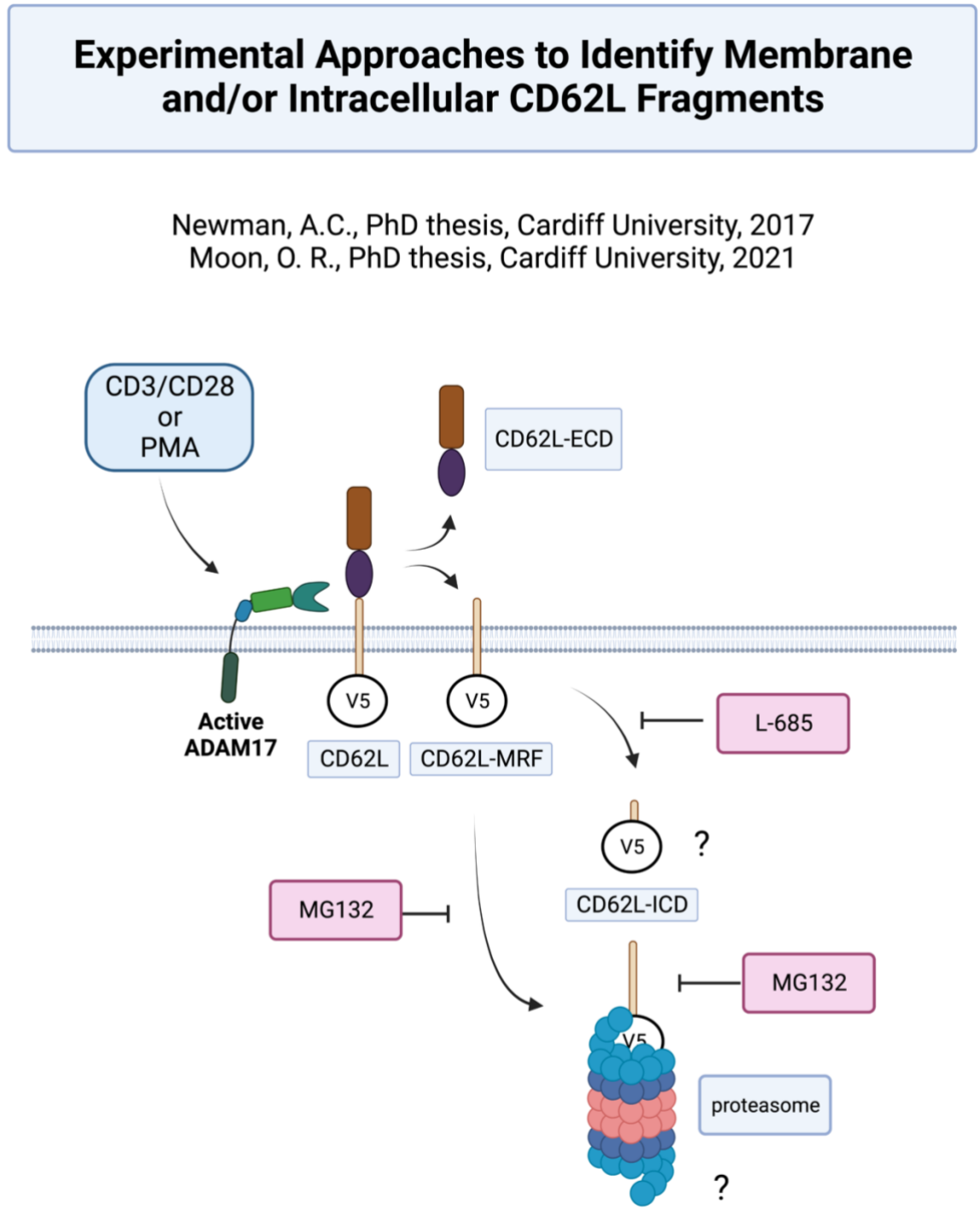

Figure 5.4: Experimental Approaches to Identify Membrane and/or Intracellular CD62L Fragments. This shows two different approaches of TCR stimulation. TCR activation using anti-CD3/CD28 or PMA. After TCR stimulation, ADAM17 becomes activated and cleaves L-selectin. The Lysate analysis was used for studying the fragments of L-selectin by Western blot analysis. Figure adapted from (Newman 2017; Moon 2021). Figure created using Biorender.com

6 Final Discussion

6.1 Summary of Results

In Chapter 3 of this thesis, I showed that cell surface L-selectin levels were found to be initially downregulated at 1 hour following SLY peptide engagement and then re-expressed at 4 hours after activation. Downregulation of cell-surface L-selectin coincided with L-selectin shedding as increased levels of soluble L-selectin were detected by ELISA within 1 hour. ADAM17 cell surface expression was also examined and found to be initially upregulated and after 4 hours there was a trend for decreased ADAM17 expression. This is consistent with the possibility that the activation of ADAM17 following peptide stimulation leads to the downregulation of L-selectin surface expression levels. In Chapter 4 of this thesis, pull down experiments were performed to examine whether L-selectin and ADAM17 form a complex as it was hypothesized that TCR activation induces an interaction between L-selectin and ADAM17 which would result in proteolysis. Pulldown experiments did not reveal the formation of a complex however further investigation will be needed to examine why this was the case. Lastly in Chapter 5 of this thesis, the retention of the L-selectin membrane fragment released following SLY induced ADAM17 activation was examined following the inhibition of γ-secretase and the proteasome. Blocking either of the two pathways was found to lead to the retention of L-selectin membrane fragment.

6.2 Limitations

L-selectin expression has previously been shown to be regulated by endogenous regulators such as serine/threonine kinase Pak1 (Dios-Esponera et al. 2019) and KLF2 (Preston et al. 2013). In Pak1-null mice, there was a decrease in the recruitment of immune cells to the lymph node compared to wildtype mice due to reduced transcripts and surface expression of L-selectin and CCR7 (Dios-Esponera et al. 2019). KLF2 is a transcription factor that positively regulates SELL (gene for L-selectin) and whose transcripts are significantly reduced following peptide specific T-cell activation (Preston et al. 2013).This is particularly true for higher affinity TCRs and high IL2 concentrations (Preston et al. 2013). However, in this work, the Molt-3 T-cell line (GAG TCR/CD62L-V5-His) was used which did not allow for the investigation of SELL by endogenous regulators because the cells were transduced to express L-selectin under an exogenous promoter.

In Chapter 3, it was shown that on unactivated T-cells, both ADAM17 and L-selectin are detected at the cells surface by flow cytometry. ADAM17 does not shed L-selectin in NLV peptide non-activated T-cells but does shed L-selectin in SLY peptide activated T-cells. An important question is how are ADAM17 and L-selectin kept apart in NLV/non-activated T-cells and how do ADAM17 and L-selectin come together in the membrane following peptide-MHC-TCR activation? L-selectin and TCR have been shown to colocalise on microvilli on T-cells (Sarin et al. 2011). Signals downstream of the TCR may therefore directly operate on ADAM17 and/or L-selectin e.g., serine phosphorylation especially since it is already known that PKC alpha regulates TCR induced L-selectin shedding (Gharbi et al. 2013). The phosphorylation of serines in the cyto tail of L-selectin and/or ADAM17 may bring them together in the membrane and this could be tested in a future experiment by mutating the serines to alanines in either or both L-selectin and ADAM17 and examining the impact this has on shedding.

Nevertheless, the pulldown experiments described in Chapter 4 may not be a suitable approach for detecting L-selectin and ADAM17 complexes as the interaction may be short lived. Other factors such as CD53 which has been shown to prevent L-selectin shedding by metalloproteases may impact this interaction as well (Demaria et al. 2020). A different approach would be to cross link closely positioned proteins in the membrane or a FRET where the transfer of fluorescence energy between closely positioned proteins could be measured (Ivetic et al. 2019). It would also be worth staining with antibodies targeted against non-tagged L-selectin to validate that all of the L-selectin was V5 tagged and subsequently pulled down (Demaria et al. 2020).

6.3 Role of L-selectin ICD initiating a proliferative response

T-cell proliferation kinetics in mice were recently shown to be regulated by the ectodomain proteolysis of L-selectin which correlated with upregulation of the high affinity IL-2 receptor (CD25) which was associated with increased clonal expansion of CD8 T-cells (Mohammed et al. 2019). Furthermore, CD8+ T-cells expressing LΔP L-selectin were shown to have delayed viral clearance in comparison to WT L-selectin, to a recombinant vaccinia virus (Richards et al. 2008). L-selectin ICD could therefore regulate the transcriptional control of CD25 activity which increases the kinetics of viral clearance. As such future experiments should aim to measure the transcriptional activity of CD25 during L-selectin proteolysis. Transcriptional activity could be measured by real-time quantitative PCR q-PCR or RNA sequencing in GAG TCR/CD62L-V5-His Molt-3 T-cell line following SLY peptide engagement. If transcriptional activity of CD25 is found to be elevated, then this could be confirmed on the protein level by flow cytometry analysis. Furthermore, the transcriptional and translational activity of CD25 could be examined in Molt-3 cells which express presenilin-resistant I351W L-selectin or alternatively using the inhibitors described in Chapter 5. This could be compared with Molt-3 T-cell lines expressing cleavable or non-cleavable L-selectin to confirm the role of proteolyzed L-selectin.

6.4 Clinical significance of ADAM17 mediated L-selectin shedding

From a clinical perspective, the soluble circulating form of L-selectin (released as a consequence of ectodomain shedding) is sometimes used as a surrogate plasma/serum biomarker for leukocyte activity triggered during acute or chronic inflammation (Font et al. 2000). Patients with rheumatic disease presented an increased prevalence of the splice variant transcript, which is thought to contribute to the increase in soluble L-selectin (Hirata et al. 2015).

The L-selectin MRF released following SLY induced ADAM17 activation was found to be retained following the inhibition of γ-secretase (L-685) and the proteasome (MG132). This is consistent with previous work by Owen Moon and Andy Newman who showed using anti-CD3/CD28 and PMA that L-selectin MRF is retained when the proteosome and γ-secretase are inhibited using the same inhibitors (Newman 2017; Moon 2021). Overall, this work is in line with the work by Mohammed et al which showed that cleavable L-selectin drives CD25 expression and clonal T-cell expansion (Newman 2017; Moon 2021). However, in order to determine if the γ-secretase generated fragments of the L-selectin MRF translocate to the nucleus and have a role as a transcriptional factor in driving CD25 expression and T-cell expansion, requires further research. Whether soluble L-selectin plays a role in T-cell expansion cannot also be excluded. Whilst LΔP T-cells do not shed L-selectin in response to peptide-MHC I (Mohammed et al. 2019) WT T-cells still do so, it is possible that shed L-selectin in WT T-cells regulates expansion. Further, determining whether L-selectin undergoes regulated intramembrane proteolysis by γ-secretase/presenilins and, if it does, the fate of the release cyto tail following activated TCR mediated ADAM17 shedding will be important to fully understand the signalling role L-selectin during T-cell activation. This could enable the design of strategies targeting TCR specific ADAM17 responses that depend on proteolysis of L-selectin.

6.5 Conclusion

L-selectin and ADAM17 expression can be detected by flow cytometry and western blotting before and following activation of GAG TCR/CD62L-V5-His T-cells with SLY peptide-MHC complexes. L-selectin and ADAM17 are not present in a preformed complex in the cell before activation and were not detectable in a complex after TCR engagement so it is still unclear how ADAM17 comes to cleave L-selectin. The released tail of L-selectin is degraded by either the proteasome or γ-secretase as was shown using specific inhibitors of both pathways. The proteolysis product of the L-selectin MRF and its function remains to be determined in future experiments.

The approaches described in this thesis to uncover L-selectin regulation by ADAM17 are of clinical relevance as they could have significant implications for inflammatory diseases, viral clearance and cancer. For example, since soluble L-selectin is a biomarker for leukocyte activity during inflammation, understanding the mechanisms of L-selectin shedding under such conditions using the novel approaches described in this thesis could potentially lead to new therapeutic strategies. As discussed earlier, L-selectin shedding has been implicated in T-cell activation and proliferation. In this thesis it was demonstrated that antigen specific T cell activation (via SLY activation) leads to L-selectin shedding and retention of L-selectin MRF when γ-secretase and the proteasome are inhibited. This is in line with the possibility that L-selectin ICD can drive increased clonal T-cell expansion (Mohammed et al. 2019) and effective viral clearance (Richards et al. 2008). This finding extends the relevance of L-selectin shedding in the human setting and could have significant implications for human diseases including autoimmune diseases and cancer. If L-selectin shedding is found to be a key regulator of T-cell activation and proliferation (through downstream ICD signaling), then this could potentially be targeted for therapeutic purposes.

7 References

Ager, A. 2012. ADAMs and Ectododomain Proteolytic Shedding in Leucocyte Migration: Focus on L-Selectin and ADAM17. The Journal of investigative dermatology 132(4), pp. 965-976. doi: 10.1038/jid.2011.418.

Ager, A. and May, M.J. 2015. Understanding high endothelial venules: Lessons for cancer immunology. OncoImmunology 4(6). doi: 10.1080/2162402X.2015.1008791.

Arribas, J. and Esselens, C. 2009. ADAM17 as a Therapeutic Target in Multiple Diseases. *Current Pharmaceutical Design* 15(20). doi:10.2174/138161209788682398.

Asano, M., Toda, M., Sakaguchi, N., Sakaguchi, S. 1996. Autoimmune disease as a consequence of developmental abnormality of a T cell subpopulation. *J Exp Med*. 184(2), pp.387-96.

von Andrian, U.H. and Mempel, T.R. 2003. Homing and cellular traffic in lymph nodes. Nature Reviews Immunology 3(11), pp. 867–878. doi: 10.1038/nri1222.

Arbones, M.L. et al. 1994. Lymphocyte Homing and Leukocyte Rolling and Migration Are Impaired in L-Selectin-Deficient Mice. Immunity 1(4), pp. 247-260. doi: 10.1016/1074-7613(94)90076-0.

Arenaccio, C. et al. 2014. Exosomes from Human Immunodeficiency Virus Type 1 (HIV-1)-Infected Cells License Quiescent CD4 + T Lymphocytes to Replicate HIV-1 through a Nef- and ADAM17-Dependent Mechanism. Journal of Virology 88(19), pp. 11529–11539. doi: 10.1128/jvi.01712-14.

Bai, A., Hu, H., Yeung, M. and Chen, J. 2007. Krüppel-Like Factor 2 Controls T Cell Trafficking by Activating L-Selectin (CD62L) and Sphingosine-1-Phosphate Receptor 1

Transcription. The Journal of Immunology 178(12), pp. 7632–7639. doi: 10.4049/jimmunol.178.12.7632.

Banchereau, J. et al. 2000. Immunobiology of dendritic cells. Annu Rev Immunol. 2000(18), pp.767-811. doi: 10.1146/annurev.Immunol.18.1.767.

Bax, D. v., Messent, A.J., Tart, J., van Hoang, M., Kott, J., Maciewicz, R.A. and Humphries, M.J. 2004. Integrin α5β1 and ADAM-17 interact in vitro and co-localize in migrating HeLa cells. Journal of Biological Chemistry 279(21), pp. 22377–22386. doi: 10.1074/jbc.M400180200.

Bell, J.H., Herrera, A.H., Li, Y. and Walcheck, B. 2007. Role of ADAM17 in the ectodomain shedding of TNF- and its receptors by neutrophils and macrophages. Journal of Leukocyte Biology 82(1), pp. 173–176. doi: 10.1189/jlb.0307193.

Björkström, N.K., Strunz, B. and Ljunggren, H.G. 2022. Natural killer cells in antiviral immunity. Nature Reviews Immunology 22(2), pp. 112–123. doi: 10.1038/s41577-021-00558-3.

Black, R.A., Charles T. Rauch, Carl J. Kozlosky, J.J.P.J.L.S., Martin F. Wolfson, B.J. and Douglas Pat Cerretti 1997. A metalloproteinase disintegrin that releases tumour-necrosis factor-a from cells.

Blaydon, D.C. et al. 2011. Inflammatory Skin and Bowel Disease Linked to ADAM17 Deletion. The New England journal of medicine 365(16), pp.1502–1508. doi: 10.1056/NEJMoa1100721.

Bogoslowski, A., Butcher, E.C. and Kubes, P. 2018. Neutrophils recruited through high endothelial venules of the lymph nodes via PNAd intercept disseminating Staphylococcus aureus. Proceedings of the National Academy of Sciences of the United States of America 115(10), pp. 2449–2454. doi: 10.1073/pnas.1715756115.

Boscacci, R.T. et al. 2010. Comprehensive analysis of lymph node stroma-expressed Ig superfamily members reveals redundant and nonredundant roles for ICAM-1, ICAM-2, and VCAM-1 in lymphocyte homing. Blood 116(6), pp. 915–925. doi: 10.1182/blood-2009-11-254334.

Bretscher, A. 1983. Purification of an 80,000-dalton Protein That is a Component of the Isolated Microvillus Cytoskeleton, and Its Localization in Nonmuscle Cells. The Journal of Cell Biology 97, pp. 425–432.

Bretscher, A., Reczek, D. and Berryman, M. 1997. Ezrin: a protein requiring conformational activation to link microfilaments to the plasma membrane in the assembly of cell surface structures. Journal of Cell Science 110, pp. 3011–3018.

Buscher, K., Riese, S.B., Shakibaei, M., Reich, C., Dernedde, J., Tauber, R. and Ley, K. 2010. The transmembrane domains of L-selectin and CD44 regulate receptor cell surface positioning and leukocyte adhesion under flow. Journal of Biological Chemistry 285(18), pp. 13490–13497. doi: 10.1074/jbc.M110.102640.

Butcher, Eugene.C. and Picker, Louis.J. 1996. Lymphocyte Homing and Homeostasis. Science 272(5258), pp. 60–67.

Cappenberg, A. et al. 2019. L-selectin shedding affects bacterial clearance in the lung: a new regulatory pathway for integrin outside-in signaling. Blood 134 (17), pp. 1445-1455. doi:10.1182/blood.2019000685.

Carlin, L.E., Hemann, E.A., Zacharias, Z.R., Heusel, J.W. and Legge, K.L. 2018. Natural killer cell recruitment to the lung during influenza A virus infection is dependent on CXCR3, CCR5, and virus exposure dose. Frontiers in Immunology 9(4). doi: 10.3389/fimmu.2018.00781.

Chalaris, A. et al. 2010. Critical role of the disintegrin metalloprotease ADAM17 for intestinal inflammation and regeneration in mice. Journal of Experimental Medicine 207(8), pp. 1617–1624. doi: 10.1084/jem.20092366.

Chao, Q., Rothenberg, M., Solano, R., Roman, G., Terzaghi, W. and Ecker, J.R. 1997. Activation of the ethylene gas response pathway in Arabidopsis by the nuclear protein ETHYLENE-INSENSITIVE3 and related proteins. Cell 89(7), pp. 1133–1144. doi: 10.1016/S0092-8674(00)80300-1.

Chen, S., Kawashima, H., Lowe, J.B., Lanier, L.L. and Fukuda, M. 2005. Suppression of tumor formation in lymph nodes by L-selectin-mediated natural killer cell recruitment. Journal of Experimental Medicine 202(12), pp. 1679–1689. doi: 10.1084/jem.20051473.

Christopherson, I., Piechoki, M., Liu, G., Ratner, S. and Galy, A. 2001. Regulation of l -selectin expression by a dominant negative Ikaros protein. Journal of Leukocyte Biology 69(4), pp. 675–683. doi: 10.1189/jlb.69.4.675.

Condon, T.P., Flournoy, S., Sawyer, G.J. and Baker, B.F. 2001. “ADAM17 but not ADAM10 mediates tumor necrosis factor-alpha and L-selectin shedding from leukocyte membranes.” Antisense & nucleic acid drug development 11(2), pp. 107–116.

Dang, X., Raffler, N.A. and Ley, K. 2009. Transcriptional regulation of mouse l-selectin. Biochimica et Biophysica Acta - Gene Regulatory Mechanisms 1789(2), pp. 146–152. doi: 10.1016/j.bbagrm.2008.10.004.

DeBerge, M.P., Ely, K.H., Cheng, G.S. and Enelow, R.I. 2013. ADAM17-mediated processing of TNF-α expressed by antiviral effector CD8+ T cells is required for severe T-cell-mediated lung injury. PLoS ONE 8(11). doi: 10.1371/journal.pone.0079340.

Demaria, M.C. et al. 2020. Tetraspanin CD53 Promotes Lymphocyte Recirculation by Stabilizing L-Selectin Surface Expression. iScience 23(5). doi: 10.1016/j.isci.2020.101104.

De Strooper, B., Annaert, W., Cupers, P., Saftig, P., Craessaerts, K., Mumm, J. S., & Goate, A. 1999. A PS-1-dependent γ-secretase-like protease mediates release of Notch intracellular domain. *Nature* 398(6727), pp.518-522.

Dib, K., Tikhonova, I.G., Ivetic, A. and Schu, P. 2017. The cytoplasmic tail of L-selectin interacts with the adaptor-protein complex AP-1 subunit μ1A via a novel basic binding motif. Journal of Biological Chemistry 292(16), pp. 6703–6714. doi: 10.1074/jbc.M116.768598.

Dios-Esponera, A., Melis, N., Subramanian, B.C., Weigert, R. and Samelson, L.E. 2019. PAK1 kinase promotes activated T cell trafficking by regulating the expression of L-selectin and CCR7. Frontiers in Immunology 10(3). doi: 10.3389/fimmu.2019.00370.

Dombernowsky, S.L. et al. 2015. The sorting protein PACS-2 promotes ErbB signalling by regulating recycling of the metalloproteinase ADAM17. Nature Communications 6. doi: 10.1038/ncomms8518.

Drost, E.M. and MacNee, W. 2002. Potential role of IL-8, platelet-activating factor and TNF-α in the sequestration of neutrophils in the lung: Effects on neutrophil deformability, adhesion receptor expression, and chemotaxis. European Journal of Immunology 32(2), pp. 393–403. doi: 10.1002/1521-4141(200202)32:2<393::AID-IMMU393>3.0.CO;2-5.

Düsterhöft, S. et al. 2014. A disintegrin and metalloprotease 17 dynamic interaction sequence, the sweet tooth for the human interleukin 6 receptor. Journal of Biological Chemistry 289(23), pp. 16336–16348. doi: 10.1074/jbc.M114.557322.

Düsterhöft, S., Jung, S., Hung, C.W., Tholey, A., Sönnichsen, F.D., Grötzinger, J. and Lorenzen, I. 2013. Membrane-proximal domain of a disintegrin and metalloprotease-17 represents the putative molecular switch of its shedding activity operated by protein-disulfide isomerase. Journal of the American Chemical Society 135(15), pp. 5776–5781. doi: 10.1021/ja400340u.

Dustin, M. and Dustin, L. 2001. The immunological relay race: B cells take antigen by synapse. Natural Immunology 2(6), pp. 480–482.

Ebsen, H., Schröder, A., Kabelitz, D. and Janssen, O. 2013. Differential Surface Expression of ADAM10 and ADAM17 on Human T Lymphocytes and Tumor Cells. PLoS ONE 8(10). doi: 10.1371/journal.pone.0076853.

Ermann J, Hoffmann P, Edinger M, Dutt S, Blankenberg FG, Higgins JP, et al. 2005. Only the CD62L+ subpopulation of CD4+CD25+ regulatory T cells protects from lethal acute GVHD. Blood 105(5), pp.2220–6. doi: 10.1182/blood-2004-05-2044

Evans, S.S., Collea, R.E., Appenheimer, M.M. and Gollnick, S.O. 1993. Interferon-c Induces the Expression of the L-Selectin Homing Receptor in Human B Lymphoid Cells. Cell Biology 123(6), pp. 1889–1898.

Faveeuw, C., Preece, G. and Ager, A. 2001. Transendothelial migration of lymphocytes across high endothelial venules into lymph nodes is affected by metalloproteinases. Blood 98(3), pp. 688-695.

Font, J., Pizcueta, P., Ramos-Casals, M., Cervera, R., Garci´a, M., Garci´a-Carrasco, G. and Navarro, M. 2000. Increased serum levels of soluble L-selectin (CD62L) in patients with active systemic lupus erythematosus (SLE). Clinical and Experimental Immunology 119(1), pp.169–174.

Fors, B.P., Goodarzi, K. and von Andrian, U.H. 2001. L-Selectin Shedding Is Independent of Its Subsurface Structures and Topographic Distribution 1. Immunol 167 (7), pp. 3642–3651.

Förster, R., Davalos-Misslitz, A.C. and Rot, A. 2008. CCR7 and its ligands: Balancing immunity and tolerance. Nature Reviews Immunology 8(5), pp. 362–371. doi: 10.1038/nri2297.

Fu, S. et al. 2004. CD4+ CD25+ CD62+ T-Regulatory Cell Subset Has Optimal Suppressive and Proliferative Potential. American Journal of Transplantation 4(1), pp. 65–78. doi: 10.1046/j.1600-6143.2003.00293.x.

Furukawa, T.A. et al. 2008a. The performance of the Japanese version of the K6 and K10 in the World Mental Health Survey Japan. International Journal of Methods in Psychiatric Research 17(3), pp. 152–158. doi: 10.1002/mpr.257.

Furukawa, Y., Umemoto, E., Myoung, H.J., Tohya, K., Miyasaka, M. and Hirata, T. 2008. Identification of novel isoforms of mouse L-selectin with different carboxyl-terminal tails. Journal of Biological Chemistry 283(18), pp. 12112–12119. doi: 10.1074/jbc.M801745200.

Le Gall, S.M. et al. 2010. ADAM17 is regulated by a rapid and reversible mechanism that controls access to its catalytic site. Journal of Cell Science 123(22), pp. 3913–3922. doi: 10.1242/jcs.069997.

Gallatin WM, Weissman IL, Butcher EC.1983. A cell-surface molecule involved in organ-specific homing of lymphocytes*. J Immunol*. 2006(177), pp. 5–9.

Gharbi, S.I., Avila-Flores, A., Soutar, D., Orive, A., Koretzky, G.A., Albar, J.P. and Mérida, I. 2013. Transient PKCα shuttling to the immunological synapse is governed by DGKζ

and regulates L-selectin shedding. Journal of Cell Science 126(10), pp. 2176–2186. doi: 10.1242/jcs.118513.

Girard, J.P., Moussion, C. and Förster, R. 2012. HEVs, lymphatics and homeostatic immune cell trafficking in lymph nodes. Nature Reviews Immunology 12(11), pp. 762–773.

Girard, J.-P. and Springer, T.A. 1995. High endothelial venules (HEVs): specialized endothelium for lymphocyte migration. Immunology Today 16(9), pp. 449–457.

Gómez-Gaviro, M. et al. 2007. Expression and Regulation of the Metalloproteinase ADAM-8 during Human Neutrophil Pathophysiological Activation and Its Catalytic Activity on L-Selectin Shedding. The Journal of Immunology 178(12), pp. 8053–8063. doi: 10.4049/jimmunol.178.12.8053.

Gooz, P., Dang, Y., Higashiyama, S., Twal, W.O., Haycraft, C.J. and Gooz, M. 2012. A disintegrin and metalloenzyme (ADAM) 17 activation is regulated by α5β1 integrin in kidney mesangial cells. PLoS ONE 7(3). doi: 10.1371/journal.pone.0033350.

Grötzinger, J., Lorenzen, I. and Düsterhöft, S. 2017. Molecular insights into the multilayered regulation of ADAM17: The role of the extracellular region. Biochimica et Biophysica Acta - Molecular Cell Research 1864(11), pp. 2088–2095. doi: 10.1016/j.bbamcr.2017.05.024.

Gutiérrez-López, M.D. et al. 2011. The sheddase activity of ADAM17/TACE is regulated by the tetraspanin CD9. Cellular and Molecular Life Sciences 68(19), pp. 3275–3292. doi: 10.1007/s00018-011-0639-0.

Hemmerich, S., Butcher, E.C. and Rosen, S.D. 1994. Sulfation-dependent Recognition of High Endothelial Venules (HEV)-Ligands by L-Selectin and MECA 79, an Adhesion-blocking Monoclonal Antibody. Experimental Medicine 180, pp. 2219–2226.

Hengel, R.L. et al. 2003. Cutting Edge: L-Selectin (CD62L) Expression Distinguishes Small Resting Memory CD4 + T Cells That Preferentially Respond to Recall Antigen . The Journal of Immunology 170(1), pp. 28–32. doi: 10.4049/jimmunol.170.1.28.

Hirata, T., Usui, T., Kobayashi, S. and Mimori, T. 2015. A novel splice variant of human L-selectin encodes a soluble molecule that is elevated in serum of patients with rheumatic diseases. Biochemical and Biophysical Research Communications 462(4), pp. 371–377. doi: 10.1016/j.bbrc.2015.05.002.

Imai, Y., Singer, M.S., Fennie, C., Lasky, L.A. and Rosen, S.D. 1991. Identification of a Carbohydrate-based Endothelial Ligand for a Lymphocyte Homing Receptor. The Journal of Cell Biology 113(5), pp. 1213–1221.

Imhof', B.A. and Dunont, D. 1995. Basic mechanism of leukocyte migration. Hormone and metabolic research 29(12), pp.614-621. doi: 10.1055/s-2007-979112.

Ivetic, A. 2004. The telling tail of L-selectin. Biochemical Society Transactions 32(6), pp. 1118–1121. doi: 10.1042/BST0321118.

Ivetic, A., Hoskins Green, H.L. and Hart, S.J. 2013. L-selectin: A Major Regulator of Leukocyte Adhesion, Migration and Signaling. *Biomolecules* 3(1), pp. 258-277.

Ivetic, A. 2018. A head-to-tail view of L-selectin and its impact on neutrophil behaviour. Cell and Tissue Research 371(3), pp. 437–453. doi: 10.1007/s00441-017-2774-x.

Ivetic, A., Green, H.L.H. and Hart, S.J. 2019a. L-selectin: A major regulator of leukocyte adhesion, migration and signaling. Frontiers in Immunology 10(MAY). doi: 10.3389/fimmu.2019.01068.

Janeway, J., Travers, P., Walport, M. et al. 2011. Immunobiology: The Immune System in Health and Disease. 5th edition. New York: Garland Science.

Jean-Paul, A., Paul, V. and Boris, L. 1999. Soluble L-Selectin Level Is a Marker for Coronary Artery Disease in Type 2 Diabetic Patients. DIABETESCARE 22(12), pp. 2044–2048.

Jeff D. Fischer, Min H. Song, A. Benjamin Suttle, William D. Heizer, Charles B. Burns and Dennis L. Vargo 2000. Comparison of zafirlukast (Accolate) absorption after oral and colonic administration in humans. Pharmaceutical Research 17(2), pp. 154–159.

Jenkins, M.R. and Griffiths, G.M. 2010. The synapse and cytolytic machinery of cytotoxic T cells. Current Opinion in Immunology 22(3), pp. 308–313. doi: 10.1016/j.coi.2010.02.008.

Jocher, G. 2022. ADAM10 and ADAM17 promote SARS-CoV-2 cell entry and spike protein-mediated lung cell fusion. *EMBO Reports* 23(1). doi: 10.15252/embr.202154305.

Jung, T.M. and Dailey, M.O. 1990. Rapid modulation of homing receptors (gp90MEL-14) induced by activators of protein kinase C. Receptor shedding due to accelerated proteolytic cleavage at the cell surface. The Journal of Immunology 144(8), pp. 3130–3136.

Jutila, M.A., Kishimoto, T.K., Finken, M. 1991. Low-Dose Chymotrypsin Treatment Inhibits Neutrophil Migration into Sites of Inflammation in Viva: Effects on Mac-l and MEL-l 4 Adhesion Protein Expression and Function. Cellular Immunology 132(1), pp. 201-214. doi:10.1016/0008-8749(91)90019-8

Kansas, G.S., Ley, K., Munro, J.M. and Tedder, T.F. 1993. Regulation of leukocyte rolling and adhesion to high endothelial venules through the cytoplasmic domain of l-selectin. Journal of Experimental Medicine 177(3), pp. 833–838. doi: 10.1084/jem.177.3.833.

Kahn, J., Walcheck, B., Migaki, G. I., Jutila, M. A., & Kishimoto, T. K. 1998. Calmodulin regulates L-selectin adhesion molecule expression and function through a proteasedependent mechanism. *Cell* 92(6), pp.809-818.

Kiessling, R., Klein, E. and Wigzell, H. 1975. „Natural" killer cells in the mouse. I. Cytotoxic cells with specificity for mouse Moloney leukemia cells. Specificity and distribution according to genotype. European Journal of Immunology 5(2), pp. 112–117. doi: 10.1002/eji.1830050208.

Klinger, A., Gebert, A., Bieber, K., Kalies, K., Ager, A., Bel, E.B. and Westermann, J. 2009. Cyclical expression of L-selectin (CD62L) by recirculating T cells. International Immunology 21(4), pp. 443–455. doi: 10.1093/intimm/dxp012.

Kohn, L.A. et al. 2012. Lymphoid priming in human bone marrow begins before expression of CD10 with upregulation of L-selectin. Nature Immunology 13(10), pp. 963–971. doi: 10.1038/ni.2405.

Kraal, G. and Mebius, R.E. 1997. High Endothelial Venules: Lymphocyte Traffic Conhl and. Elsevier Masson SAS. Advances in Immunology 65, pp. 347-395, doi: 10.1016/S0065-2776(08)60746-4.

Kretowski, A., Gillespie, K.M., Bingley, P.J., Kinalska, I. 2000. Soluble L-selectin levels in type I diabetes mellitus: a surrogate marker for disease activity?. Immunology99(2), pp.320-325. doi: 10.1046/j.1365-2567.2000.00967.x.

Krętowski, A., Gillespie, K.M., Bingley, P.J. and Kinalska, I. 2000. Soluble L-selectin levels in type I diabetes mellitus: A surrogate marker for disease activity?. Immunology 99(2), pp. 320–325. doi: 10.1046/j.1365-2567.2000.00967.x.

Kuby, J. 2015. Kuby Immunology. 8th ed. New York: W.H. Freeman.

Kumari S, Arora M, Singh J, Chauhan SS, Kumar S, Chopra A. 2021. L-Selectin expression is associated with inflammatory microenvironment and favourable prognosis in breast cancer. 3 Biotech.11(2). doi: 10.1007/s13205-020-02549-y.

Lange C, Scholl M, Melms A, Bischof F. CD62L(high) Treg cells with superior immunosuppressive properties accumulate within the CNS during remissions of EAE. 2011. *Brain Behav Immun* 25 (1), pp.120–6. doi: 10.1016/j.bbi.2010.09.004

Lee, M.Y., Nam, K.H. and Choi, K.C. 2016. iRhoms; Its functions and essential roles. Biomolecules and Therapeutics 24(2), pp. 109–114. doi: 10.4062/biomolther.2015.149.

Lee, T.I. and Young, R.A. 2013. Transcriptional regulation and its misregulation in disease. Cell 152(6), pp. 1237–1251. doi: 10.1016/j.cell.2013.02.014.

Lemberg, M.K. and Freeman, M. 2007. Functional and evolutionary implications of enhanced genomic analysis of rhomboid intramembrane proteases. Genome Research 17(11), pp. 1634–1646. doi: 10.1101/gr.6425307.

Ley, K. 2003. The role of selectins in inflammation and disease. Trends in Molecular Medicine 9(6), pp. 263–268. doi: 10.1016/S1471-4914(03)00071-6.

Ley, K. 2008. The Microcirculation in Inflammation. Microcirculation, pp. 387–448. doi: 10.1016/B978-0-12-374530-9.00011-5.

Li, N. et al. 2007. Metalloproteases regulate T-cell proliferation and effector function via LAG-3. EMBO Journal 26(2), pp. 494–504. doi: 10.1038/sj.emboj.7601520.

Li, Y., Brazzell, J., Herrera, A. and Walcheck, B. 2006. ADAM17 deficiency by mature neutrophils has differential effects on L-selectin shedding. Blood 108(7), pp. 2275–2279. doi: 10.1182/blood-2006-02-005827.

Long, C., Wang, Y., Herrera, A.H., Horiuchi, K. and Walcheck, B. 2010. In vivo role of leukocyte ADAM17 in the inflammatory and host responses during E. coli -mediated peritonitis. Journal of Leukocyte Biology 87(6), pp. 1097–1101. doi: 10.1189/jlb.1109763.

Lorenzen, I., Trad, A. and Grötzinger, J. 2011. Multimerisation of A disintegrin and metalloprotease protein-17 (ADAM17) is mediated by its EGF-like domain. Biochemical and Biophysical Research Communications 415(2), pp. 330–336. doi: 10.1016/j.bbrc.2011.10.056.

Lou, Y., Lu, X. and Dang, X. 2012. FOXO1 up-regulates human L-selectin expression through binding to a consensus FOXO1 motif. Gene Regulation and Systems Biology 2012(6), pp. 139–149. doi: 10.4137/GRSB.S10343.

Lu, D., Scully, M., Kakkar, V. and Lu, X. 2010. ADAM-15 disintegrin-like domain structure and function. Toxins 2(10), pp. 2411–2427. doi: 10.3390/toxins2102411.

Maillard, I., Fang, T. and Pear, W.S. 2005. Regulation of lymphoid development, differentiation, and function by the Notch pathway. Annual Review of Immunology 23, pp. 945–974. doi: 10.1146/annurev.immunol.23.021704.115747.

Maretzky, T. et al. 2013. iRhom2 controls the substrate selectivity of stimulated ADAM17-dependent ectodomain shedding. Proceedings of the National Academy of Sciences of the United States of America 110(28), pp. 11433–11438. doi: 10.1073/pnas.1302553110.

Masayuki, M. 1998. Selectins (CD62-E/L/P). In: Encyclopedia of Immunology (Second Edition). Academic Press, pp. 2158–2161.

Mavilio, M. et al. 2016. Erratum: A Role for Timp3 in Microbiota-Driven Hepatic Steatosis and Metabolic Dysfunction. Cell Reports 16(8), p. 2269. doi: 10.1016/j.celrep.2016.07.078.

Mcever, R.P., Moore, K.L. and Cummings, R.D. 1995. Leukocyte trafficking mediated by selectin-carbohydrate interactions. The Journal of biological chemistry 270(19), pp.11025–11028.

Mionnet, C., Sanos, S.L., Mondor, I., Jorquera, A., Laugier, J.P., Germain, R.N. and Bajénoff, M. 2011. High endothelial venules as traffic control points maintaining lymphocyte population homeostasis in lymph nodes. Blood 118(23), pp. 6115–6122. doi: 10.1182/blood-2011-07-367409.

Mitoma, J. et al. 2007. Critical functions of N-glycans in L-selectin-mediated lymphocyte homing and recruitment. Nature Immunology 8(4), pp. 409–418. doi: 10.1038/ni1442.

Miyasaka, M. and Tanaka, T. 2004. Lymphocyte trafficking across high endothelial venules: Dogmas and enigmas. Nature Reviews Immunology 4(5), pp. 360–370. doi: 10.1038/nri1354.

Mohammed, R.N. 2016. The impact of L-selectin/CD62L on the co-stimulation and migration of CD8+ T cells during virus infection. PhD thesis, Cardiff University.

Mohammed, R.N. et al. 2019. ADAM17-dependent proteolysis of L-selectin promotes early clonal expansion of cytotoxic T cells. Scientific Reports 9(1). doi: 10.1038/s41598-019-41811-z.

Mohammed, R.N., Watson, H.A., Vigar, M., Ohme, J., Thomson, A., Humphreys, I.R. and Ager, A. 2016. L-selectin Is Essential for Delivery of Activated CD8+ T Cells to Virus-Infected Organs for Protective Immunity. Cell Reports 14(4), pp. 760–771. doi: 10.1016/j.celrep.2015.12.090.

Monks, C.R.F., Freiberg, B.A., Kupfer, H., Sciaky, N. and Kupfer, A. 1998. Three-dimensional segregation of supramolecular activation clusters in T cells. Nature 395, pp. 82–86.

Moon, O. R., 2021. Engineering homing properties of cancer-specific T lymphocytes in adoption cell therapy. PhD thesis, Cardiff University.

Moss, M.L. et al. 1997. Cloning of a disintegrin metalloproteinase that processes precursor tumour-necrosis factor-a. Natural 385(20), pp. 733–736.

Moussion, C., Girard, J.P. 2011. Dendritic cells control lymphocyte entry to lymph nodes through high endothelial venules. *Nature* 479(7374), pp. 542–6. doi:10.1038/nature10540

Murphy, K. (Kenneth M.), Weaver, C. and Janeway, C. 2022. Janeway's immunobiology.

Newe, A. et al. 2019. Serine Phosphorylation of L-Selectin Regulates ERM Binding, Clustering, and Monocyte Protrusion in Transendothelial Migration. Frontiers in Immunology 10. doi: 10.3389/fimmu.2019.02227.

Newman, A.C., 2017. The regulation of L-selectin activity by proteolys. PhD thesis, Cardiff University.

Nishijima, K.I., Ando, M., Sano, S., Hayashi-Ozawa, A., Kinoshita, Y. and Iijima, S. 2005. Costimulation of T-cell proliferation by anti-L-selectin antibody is associated with the reduction of a cdk inhibitor p27. Immunology 116(3), pp. 347–353. doi: 10.1111/j.1365-2567.2005.02234.x.

Nishiyama, M., Skoultchi, A.I. and Nakayama, K.I. 2012. Histone H1 Recruitment by CHD8 Is Essential for Suppression of the Wnt–β-Catenin Signaling Pathway. Molecular and Cellular Biology 32(2), pp. 501–512. doi: 10.1128/mcb.06409-11.

Nishizuka, Y., Sakakura, T. 1969.Thymus and reproduction: sex-linked dysgenesia of the gonad after neonatal thymectomy in mice. *Science* 166(3906), pp.753-5.

Oldefest, M. et al. 2015. Secreted Frizzled-related protein 3 (sFRP3)-mediated suppression of interleukin-6 receptor release by A disintegrin and metalloprotease 17 (ADAM17) is abrogated in the osteoarthritis-associated rare double variant of sFRP3. Biochemical Journal 468(3), pp. 507–518. doi: 10.1042/BJ20141231.

Onder, L., Danuser, R., Scandella, E., Firner, S., Chai, Q., Hehlgans, T., et al. 2013. Endothelial cell-specific lymphotoxin-beta receptor signaling is critical for lymph node and high endothelial venule formation. *J Exp Med* 210(3), pp. 465–73. doi:10.1084/jem.20121462.

Palframan, R.T. et al. 2001. Inflammatory Chemokine Transport and Presentation in HEV: A Remote Control Mechanism for Monocyte Recruitment to Lymph Nodes in Inflamed Tissues. Rockefeller University Press. J Exp Med 194 (9), pp.1361–1374. doi: https://doi.org/10.1084/jem.194.9.1361.

Park, J.J. et al. 2010. B7-H1/CD80 interaction is required for the induction and maintenance of peripheral T-cell tolerance. Blood 116(8), pp. 1291–1298. doi: 10.1182/blood-2010-01-265975.

Paul A., R. and Kazuyuki, F. 2015. The ins and outs of MHC class II-mediated antigen processing and presentation. Nature Reviews Immunology 15(4), pp. 203–216. doi: 10.1038/nri3818.

Pavalko, F.M., Walker, D.M., Graham, L., Goheen, M., Doerschuk, C.M., Kansas, G.S. and Pavalko, E.M. 1995. The Cytoplasmic Domain of L-Selectin Interacts with Cytoskeletal Proteins Via ct-Actinin: Receptor Positioning in Microvilli Does Not Require Interaction with et-Actinin. The Journal of Cell Biology 129(4), pp. 1155–1164.

Peschon, J.J. et al. 1998. An Essential Role for Ectodomain Shedding in Mammalian Development. CIENCE 282, pp. 1281–1284. Available at: https://www.science.org.
Pillay, J. et al. 2010. In vivo labeling with 2H2O reveals a human neutrophil lifespan of 5.4 days. Blood 116(4), pp. 625–627. doi: 10.1182/blood-2010-01-259028.

Pinazza, M. et al. 2018. Histone deacetylase 6 controls Notch3 trafficking and degradation in T-cell acute lymphoblastic leukemia cells. Oncogene 37(28), pp. 3839–3851. doi: 10.1038/s41388-018-0234-z.

Preston, G.C., Feijoo-Carnero, C., Schurch, N., Cowling, V.H. and Cantrell, D.A. 2013. The Impact of KLF2 Modulation on the Transcriptional Program and Function of CD8 T Cells. PLoS ONE 8(10). doi: 10.1371/journal.pone.0077537.

Rabi, L.T., Peres, K.C., Nascimento, M. et al. 2023. Investigation of the clinical utility of adhesion molecules in the management of thyroid nodules. *Sci Rep* 13(4069). Doi: 10.1038/s41598-023-31302-7.

Raffler, N.A., Rivera-Nieves, J. and Ley, K. 2005. L-selectin in inflammation, infection and immunity. Drug Discovery Today: Therapeutic Strategies 2(3), pp. 213–220. doi: 10.1016/j.ddstr.2005.08.012.

Rahman, I. et al. 2021. L-selectin regulates human neutrophil transendothelial migration. Journal of Cell Science 134(3). doi: 10.1242/jcs.250340.

Reed, S.G. and Ager, A. 2022. Immune Responses to IAV Infection and the Roles of L-Selectin and ADAM17 in Lymphocyte Homing. Pathogens 11(2). doi: 10.3390/pathogens11020150.

Richards, H., Longhi, M.P., Wright, K., Gallimore, A. and Ager, A. 2008. CD62L (L-Selectin) Down-Regulation Does Not Affect Memory T Cell Distribution but Failure to Shed Compromises Anti-Viral Immunity. The Journal of Immunology 180(1), pp. 198–206. doi: 10.4049/jimmunol.180.1.198.

von Rotz, R. C., Kohli, B. M., Bosset, J., Meier, M., Suzuki, T., Nitsch, R. M., & Konietzko, U. 2004. The APP intracellular domain forms nuclear multiprotein complexes and regulates the transcription of its own precursor. *Journal of cell science* 117(19), pp. 4435-4448.

Rutkowska, E., Kwiecień, I., Kłos, K., Rzepecki, P. and Chciałowski, A. 2022. Intermediate Monocytes with PD-L1 and CD62L Expression as a Possible Player in Active SARS-CoV-2 Infection. Viruses 14(4). doi: 10.3390/v14040819.

Rzeniewicz, K. et al. 2015. L-selectin shedding is activated specifically within transmigrating pseudopods of monocytes to regulate cell polarity in vitro. Proceedings of the National Academy of Sciences of the United States of America 112(12), pp. E1461–E1470. doi: 10.1073/pnas.1417100112.

Sakaguchi, S., Sakaguchi, N., Asano, M., Itoh, M., Toda, M. 1995. Immunologic self-tolerance maintained by activated T cells expressing IL-2 receptor alpha-chains (CD25). Breakdown of a single mechanism of self-tolerance causes various autoimmune diseases. *J Immunol* 155(3), pp.1151-64.

Sarin, R., Wu, X. and Abraham, C. 2011. Inflammatory disease protective R381Q IL23 receptor polymorphism results in decreased primary CD4+ and CD8+ human T-cell

functional responses. Proceedings of the National Academy of Sciences of the United States of America 108(23), pp. 9560–9565. doi: 10.1073/pnas.1017854108.

Schleiffenbaum, B., Spertini, O. and Tedder, T.E. 1992. Soluble L-selectin Is Present in Human Plasma at High Levels and Retains Functional Activity. The Journal of cell biology 119(1), pp. 229–238.

Schlondorff, J., David Becherer, J. and Blobel, C.P. 2000. Intracellular maturation and localization of the tumour necrosis factor α convertase (TACE). The Biochemical journal 347 (1), pp. 131–138.

Schroeter, E. H., Kisslinger, J. A., & Kopan, R. 1998. Notch-1 signalling requires ligand-induced proteolytic release of intracellular domain. *Nature* 393(6683), pp.382-386.

Schweisguth, F. 2004. Regulation of notch signaling activity. *Current biology* 14(3), pp.129- 138.

Selkoe, D., & Kopan, R. 2003. Notch and PS: regulated intramembrane proteolysis links development and degeneration. *Annual review of neuroscience* 26(1), pp.565-597.

Shamri, R. et al. 2005. Lymphocyte arrest requires instantaneous induction of an extended LFA-1 conformation mediated by endothelium-bound chemokines. Nature Immunology 6(5), pp. 497–506. doi: 10.1038/ni1194.

Shi, C. and Pamer, E.G. 2011. Monocyte recruitment during infection and inflammation. Nature Reviews Immunology 11(11), pp. 762–774. doi: 10.1038/nri3070.

Sinclair, L. v et al. 2008. Phosphatidylinositol-3-OH kinase and nutrient-sensing mTOR pathways control T lymphocyte trafficking. Nature Immunology 9(5), pp. 513–521. doi: 10.1038/ni.1603.

Smalley, D.M. and Ley, K. 2005. L-selectin: mechanisms and physiological significance of ectodomain cleavage. Journal of cellular and molecular medicine 9(2), pp. 255–266. doi: 10.1111/j.1582-4934.2005.tb00354.x.

Sobolev, O., Stern, P., Lacy-Hulbert, A. and Hynes, R.O. 2009. Natural killer cells require selectins for suppression of subcutaneous tumors. Cancer Research 69(6), pp. 2531–2539. doi: 10.1158/0008-5472.CAN-08-3126.

Sommer, T., Hoppe, T. and Rape, M. 2016. Stefan Jentsch (1955–2016). Cell 167(7), pp. 1667–1668. doi: 10.1016/j.cell.2016.11.057.

Spertini, O., Luscinskas, F.W., Gimbrone, M.A. and Tedder, T.F. 1992. Monocyte Attachment to Activated Human Vascular Endothelium In Vitro Is Mediated by Leukocyte Adhesion Molecule-1 (DSelectin) under Nonstatic Conditions. Experimental Medicine 175, pp. 1789–1792.

Stein, J. v, Cheng, G., Stockton, B.M., Fors, B.P., Butcher, E.C. and von Andrian, U.H. 1999. L-selectin-mediated Leukocyte Adhesion In Vivo: Microvillous Distribution Determines Tethering Efficiency, But Not Rolling Velocity. The Journal of Experimental Medicine 189(1), pp. 37–49.

Stolp, B. et al. 2012. HIV-1 Nef interferes with T-lymphocyte circulation through confined environments in vivo. Proceedings of the National Academy of Sciences of the United States of America 109(45), pp. 18541–18546. doi: 10.1073/pnas.1204322109.

Streeter, P.R., Rouse, T.N. and Butcher, E.C. 1988. Immunohistologic and Functional Characterization of a Vascular Addressin Involved in Lymphocyte Homing into Peripheral Lymph Nodes. The Journal of Cell Biology 107, pp. 1853–1862.

Szanya, V., Ermann, J., Taylor, C., Holness, C., Fathman, C. G. 2002. The subpopulation of CD4+ CD25+ splenocytes that delays adoptive transfer of diabetes expresses L-selectin and high levels of CCR7. *Journal of Immunology* 169 (5), pp.2461–2465.

Takada, A. and Kawaoka, Y. 2003. Antibody-dependent enhancement of viral infection: Molecular mechanisms and in vivo implications. Reviews in Medical Virology 13(6), pp. 387–398. doi: 10.1002/rmv.405.

Taguchi, O., Nishizuka, Y., Sakakura, T., Kojima, A. 1980. Autoimmune oophoritis in thymectomized mice: detection of circulating antibodies against oocytes. *Clinical and experimental immunology* 40(3), pp.540-53.

Tan, J.B., Visan, I., Yuan, J.S. and Guidos, C.J. 2005. Requirement for Notch1 signals at sequential early stages of intrathymic T cell development. Nature Immunology 6(7), pp. 671–679. doi: 10.1038/ni1217.

Tang, J. et al. 2011. Adam17-dependent shedding limits early neutrophil influx but does not alter early monocyte recruitment to inflammatory sites. Blood 118(3), pp. 786–794. doi: 10.1182/blood-2010-11-321406.

Tsou, C.L. et al. 2007. Critical roles for CCR2 and MCP-3 in monocyte mobilization from bone marrow and recruitment to inflammatory sites. Journal of Clinical Investigation 117(4), pp. 902–909. doi: 10.1172/JCI29919.

Tsukamoto, S. et al. 2014. Tetraspanin CD9 modulates ADAM17-mediated shedding of LR11 in leukocytes. Experimental and Molecular Medicine 46(4). doi: 10.1038/emm.2013.161.

Tucher, J. et al. 2014. LC-MS based cleavage site profiling of the proteases ADAM10 and ADAM17 using proteome-derived peptide libraries. Journal of Proteome Research 13(4), pp. 2205–2214. doi: 10.1021/pr401135u.

Ueha, S. et al. 2007. CCR7 mediates the migration of Foxp3 + regulatory T cells to the paracortical areas of peripheral lymph nodes through high endothelial venules. Journal of Leukocyte Biology 82(5), pp. 1230–1238. doi: 10.1189/jlb.0906574.

Urban, S., Lee, J.R. and Freeman, M. 2001. Drosophila Rhomboid-1 Defines a Family of Putative Intramembrane Serine Proteases. Cell107(2), pp.173-182.

Varela-Rohena, A. et al. 2008. Control of HIV-1 immune escape by CD8 T-cells expressing enhanced T-cell receptor. Nature medicine 14(12), pp. 1390–1395. doi: 10.1038/nm.1779.

Vassena, L., Giuliani, E., Koppensteiner, H., Bolduan, S., Schindler, M. and Doria, M. 2015. HIV-1 Nef and Vpu Interfere with L-Selectin (CD62L) Cell Surface Expression to Inhibit Adhesion and Signaling in Infected CD4 + T Lymphocytes. Journal of Virology 89(10), pp. 5687–5700. doi: 10.1128/jvi.00611-15.

Venturi, V., Kedzierska, K., Turner, S.J., Doherty, P.C. and Davenport, M.P. 2007. Methods for comparing the diversity of samples of the T cell receptor repertoire. Journal of Immunological Methods 321(1–2), pp. 182–195. doi: 10.1016/j.jim.2007.01.019.

Walcheck, B., Alexander, S.R., st. Hill, C.A. and Matala, E. 2003. ADAM-17-independent shedding of L-selectin. Journal of Leukocyte Biology 74(3), pp. 389–394. doi: 10.1189/jlb.0403141.

Watson, H.A. et al. 2019. L-selectin enhanced T cells improve the efficacy of cancer immunotherapy. Frontiers in Immunology 10(JUN). doi: 10.3389/fimmu.2019.01321.

Wedepohl, S., Kaup, M., Riese, S.B., Berger, M., Dernedde, J., Tauber, R. and Blanchard, V. 2010. N-glycan analysis of recombinant l-selectin reveals sulfated GalNAc

and GalNAc-GalNAc motifs. Journal of Proteome Research 9(7), pp. 3403–3411. doi: 10.1021/pr100170c.

Wong, K.H.K. et al. 2016. The Role of Physical Stabilization in Whole Blood Preservation. Scientific Reports 6. doi: 10.1038/srep21023.

Xu, J., Mukerjee, S., Silva-Alves, C.R.A., Carvalho-Galvão, A., Cruz, J.C., Balarini, C.M., Braga, V.A., Lazartigues, E. and França-Silva, M.S. 2016. A Disintegrin and Metalloprotease 17 in the Cardiovascular and Central Nervous Systems. *Frontiers in Physiology* 7(469). doi: 10.3389/fphys.2016.00469.

Xu, P. and Derynck, R. 2010. Direct Activation of TACE-Mediated Ectodomain Shedding by p38 MAP Kinase Regulates EGF Receptor-Dependent Cell Proliferation. Molecular Cell 37(4), pp. 551–566. doi: 10.1016/j.molcel.2010.01.034.

Xu, P., Liu, J., Sakaki-Yumoto, M. and Derynck, R. 2012. TACE Activation by MAPK-Mediated Regulation of Cell Surface Dimerization and TIMP3 Association. CELL BIOLOGY 5(22).

Yang, S., Liu, F., Wang, Q.J., Rosenberg, S.A. and Morgan, R.A. 2011. The shedding of CD62L (L-selectin) regulates the acquisition of lytic activity in human tumor reactive T lymphocytes. PLoS ONE 6(7). doi: 10.1371/journal.pone.0022560.

YOSHIDA, T., FENNIE, C., LASKY, L.A. and LEE, Y.C. 1994. A liquid-phase binding analysis for L-selectin A strong dependency on highly clustered sulfate groups. European Journal of Biochemistry 222(2), pp. 703–709. doi: 10.1111/j.1432-1033.1994.tb18915.x.

Zhang, D. et al. 2015. Neutrophil ageing is regulated by the microbiome. Nature 525(7570), pp. 528–532. doi: 10.1038/nature15367.

Zhang, Z., Li, J., Zheng, W., Zhao, G., Zhang, H., Wang, X., et al. 2016. Peripheral lymphoid volume expansion and maintenance are controlled by gut microbiota via RALDH+ dendritic cells. *Immunity* 44(2), pp.330–42.

Zunke, F. and Rose-John, S. 2017. The shedding protease ADAM17: Physiology and pathophysiology. Biochimica et Biophysica Acta - Molecular Cell Research 1864(11), pp. 2059–2070. doi: 10.1016/j.bbamcr.2017.07.001.